Macromodeling and Demonstration of the LT6600 Amplifier and Lowpass Filter

by

Cheng-Wei Pei

Submitted to the Department of Electrical Engineering and Computer Science

in partial fulfillment of the requirements for the degree of

Master of Engineering in Electrical Engineering and Computer Science

at the

MASSACHUSETTS INSTITUTE OF TECHNOLOGY

February 2004

Author .....
Department of Electrical Engineering and Computer Science
February 4, 2004

Certified by .....
Tim Regan
Linear Technology Applications Manager
VI-A Company Supervisor

Certified by .....
Charles G. Sodini
Professor EECS
M.I.T. Thesis Supervisor

Accepted by .....
Arthur C. Smith
Chairman, Department Committee on Graduate Students

Macromodeling and Demonstration of the LT6600 Amplifier and Lowpass Filter

by

Cheng-Wei Pei

Submitted to the Department of Electrical Engineering and Computer Science
on February 4, 2004, in partial fulfillment of the
requirements for the degree of
Master of Engineering in Electrical Engineering and Computer Science

Abstract

The goal of this thesis is to demonstrate the abilities of the Sevastopoulos-LaPorte active low-pass filter topology in Linear Technology Corporation's LT6600 integrated circuit (IC). The thesis is split into two parts, representing two facets of how engineers will evaluate the LT6600: by simulation and in the laboratory. The LT6600-10 macromodel and its design methodology is presented, as well as comparisons of macromodel characteristics with measured characteristics of the LT6600-10 IC. For the lab demonstration portion, the LT6600-2.5 was integrated into a digital code-division multiple access (CDMA) communications system, complete with transmit and receive sections. The performance of the LT6600 in this system was shown to be as good as or better than most conventional filtering approaches. When implemented in a communications system, the LT6600-10 required up to 13 less components than other reasonable filtering options and provided 4th-order signal attenuation with only 14 nV/$\sqrt{Hz}$ of voltage noise spectral density.

VI-A Company Supervisor: Tim Regan
Title: Linear Technology Applications Manager

M.I.T. Thesis Supervisor: Charles G. Sodini
Title: Professor EECS

Contents

Chapter 1

Introduction

The goal of this thesis is to demonstrate and model the capabilities and characteristics of the LT6600 amplifier and active lowpass filter. The LT6600, designed and manufactured by Linear Technology, is a monolithic IC active filter that employs patented technology [1] to implement a fourth-order Chebyshev lowpass filter with user-adjustable gain and low passband ripple. The research has two facets: computer simulation and lab demonstration. The combination represents two ways in which engineers will qualify and characterize the LT6600 for their designs.

The first part of the research was to macromodel the LT6600 for use in computer simulations, such as SPICE[1]. A good macromodel is a proverbial black box: from the outside, it looks exactly the same as the real component, but the insides can be vastly different. The LT6600 macromodel includes all of the important attributes for an active filter: low passband gain ripple, correct cutoff frequency, 4th-order Chebyshev rolloff, correct group delay over frequency, et cetera. Many operational amplifier characteristics have been modeled as carefully as possible, including Common-Mode Rejection Ratio (CMRR), Power Supply Rejection Ratio (PSRR), voltage limiting (both single-ended and differential), slew rate, offset, and others. These characteristics are discussed in Section 3.3. All of the characteristics of the LT6600 model have been taken from the datasheet [2], computer simulations, and observations in the lab.

For the second part of the research, the LT6600 was applied in a communications

[1]SPICE: Simulation Program With Integrated Circuit Emphasis

system. In the transmitter and receiver implementations, the LT6600 provides the Digital-Analog Converter (DAC) reconstruction and Analog-Digital Converter (ADC) anti-aliasing functions. Its performance was compared with that of other realistic filtering options, and this thesis presents the findings of those experiments. The various tradeoffs for choosing a filter solution will be presented, and the LT6600 will be shown to be a simple and robust overall filtering approach.

Chapter 2

Analog Filters: A Brief History

An analog filter is any filter that uses linear components such as resistors (R), capacitors (C), inductors (L), amplifiers, or any combination thereof to create a desired frequency response from its input to its output. A passive analog filter is simply made of discrete R's, C's, and L's. There is no way to provide low-frequency (DC) gain to a passive analog filter; that is where amplifiers come into play. An active analog filter uses amplifiers to provide, among other things, gain and signal buffering to the system. Additionally, active analog filters make it possible to integrate filters onto integrated circuits (ICs), since the nature of active analog filter topologies often allow designers to use smaller C's and L's than in discrete filter designs. Since the C's and L's are often the largest components in a discrete or IC filter, getting a good frequency response with smaller values is a good feature from a design standpoint.

Analog filters are not a new field of study; passive (using only R, L, and C) filters have been used since the 1910's[1], which means that filter theory and techniques have been studied for almost a century. Active analog filters, with the benefit of voltage and current gain, have been in existence since the 1930's, when vacuum tubes and feedback theory made their use possible [3]. Almost every analog circuit built has some sort of analog filtering, whether it be power supply bypassing or operational amplifier compensation.

[1] According to [3], the electric filter was invented by both Wagner (Germany) and Campbell (United States) independently in 1915.

Today's integrated circuit technology allows designers to trim capacitors and resistors to extremely tight tolerances (less than one percent), but inductors are much more difficult to integrate with good repeatability. Luckily, active filters have another bonus quality: using certain topologies, active filters can produce the same frequency response as discrete designs, but *without inductors*. This is another great feature from a design standpoint, and allows the mass-production of integrated active filters with good repeatable performance.

Chapter 3

Introduction to Macromodeling

The macromodeling of an integrated active RC filter[1] essentially comes down to the macromodeling of its component operational amplifiers (op amps). Besides the op amps, the filter consists only of resistors and capacitors connected in the proper configuration to create the response necessary. Therefore, this section will be dedicated to existing work on the topic of op amp modeling. Macromodeling of op amps is not a new concept: since the 1970's, op amp designers have been creating macromodels for their customers to use in computer simulations.

Macromodeling of amplifiers is useful for two reasons. The first reason is reduced computational complexity. In the early days of computer simulation, a full integrated circuit simulation in SPICE could take hours and even days, which is unacceptably slow. The circuit simulation time is proportional to the number of non-linear devices in the circuit, the most prominent of which are transistors and diodes. Since a larger IC could have hundreds and thousands of transistors, there needed to be a way to simulate faster. The second reason for macromodeling is the preservation of proprietary information: more often than not, transistor-level schematics for integrated circuits are not released to the customer. Therefore, if a customer wants to simulate a certain device for evaluation, there is no way for them to know for sure exactly what's in the circuit. However, the customer can often get a macromodel with many of the same

[1]There are other types of integrated filters, including switched-capacitor filters, that are not as simple to macromodel.

characteristics as the part itself. Then, with a good understanding of the limitations of the model, the customer can use the model for simulation of the part.

Today's computers are much more powerful than they were when macromodeling first became popular. However, simulation times for applications such as communications systems have increased as well. One example is a Bit-Error Rate simulation on a communications system. To simulate one error per one million data bits, the computer may need to simulate a few seconds of system operation. However, if the components of the system need to be simulated on the transistor level, the simulation resolution could be in the nanoseconds. The scale of such a simulation would encourage using macromodels to speed up the process. The accuracy of these macromodels could be less crucial than their decreased complexity for shorter simulation times.

An operational amplifier macromodeling technique, developed by Boyle et al in 1974 [4], consists of only two transistors and a few diodes. The rest of the circuit is made up of linear elements, including resistors, capacitors, inductors, and linear current/voltage sources. Over the years, many improvements to this original model have been made, to model the characteristics and operation of a real operational amplifier even more closely. The macromodeling technique to be used in this research project will be a combination of the methods presented in papers [4] [5].

For most simple circuit simulations, accuracy is more important than decreased simulation times. The recent trend of macromodels is to be more and more accurate in representing their counterparts, and when customers simulate a system using a filter or op amp macromodel, they expect it to perform in *exactly* the same way as the real circuit. Modern-day macromodels are getting more complex as they strive to model every single characteristic of a product, whether desirable or undesirable.

3.1 Boyle's Macromodel

Boyle's model for an operational amplifier is shown in Figure 3-1. The model consists of an input differential pair of transistors, followed by a gain/output stage which provides frequency compensation, output impedance, and current limiting. To reduce

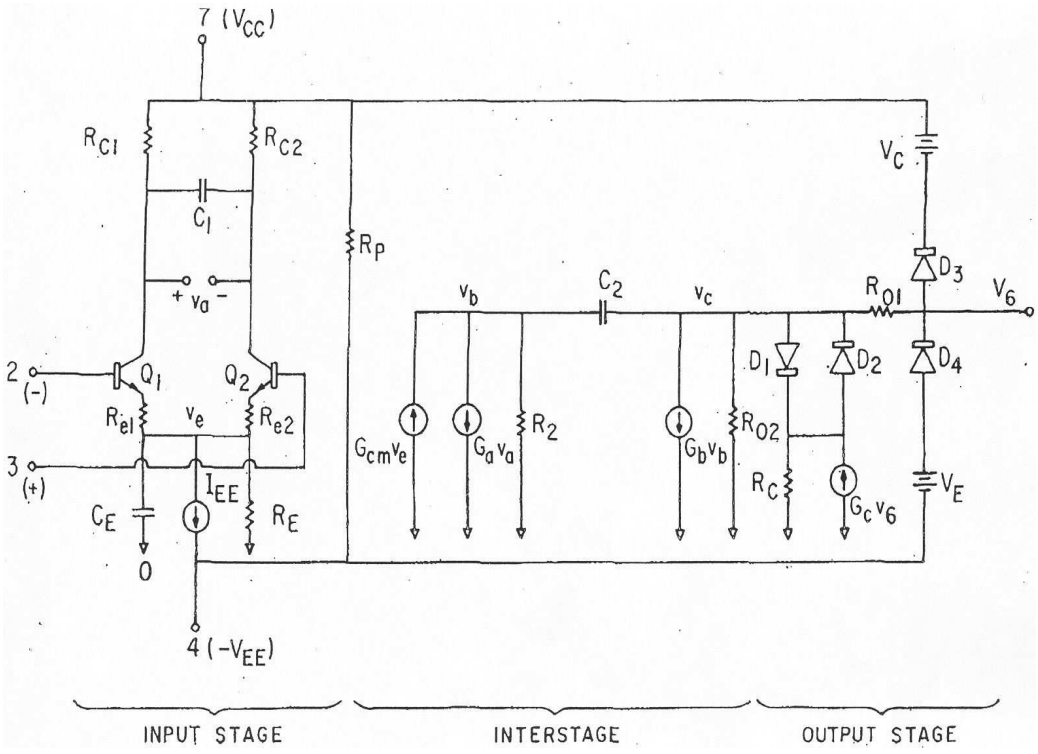

Figure 3-1: Boyle Model of the Operational Amplifier. Picture taken directly from the 1974 paper.

simulation time, the model consists mostly of linear elements, since SPICE spends the most time simulating non-linear elements such as transistors and diodes. The reason two transistors are used at the input is to provide the nonlinear large-signal characteristics that op-amps have, including bias current, saturation, distortion, and offset.

3.2 Analog Devices Macromodel

One limitation of the Boyle model is that it comes with a limited amount of frequency response modifiers (poles and zeros), which is insufficient to represent most modern amplifiers. In addition, the model gives the designer limited control over some of the more common amplifier characteristics, such as CMRR over frequency. A more flexible model, shown in Figure 3-2, was developed at Analog Devices (ADI) in 1990 by Alexander and Bowers [5]. The model consists of a very similar input differential

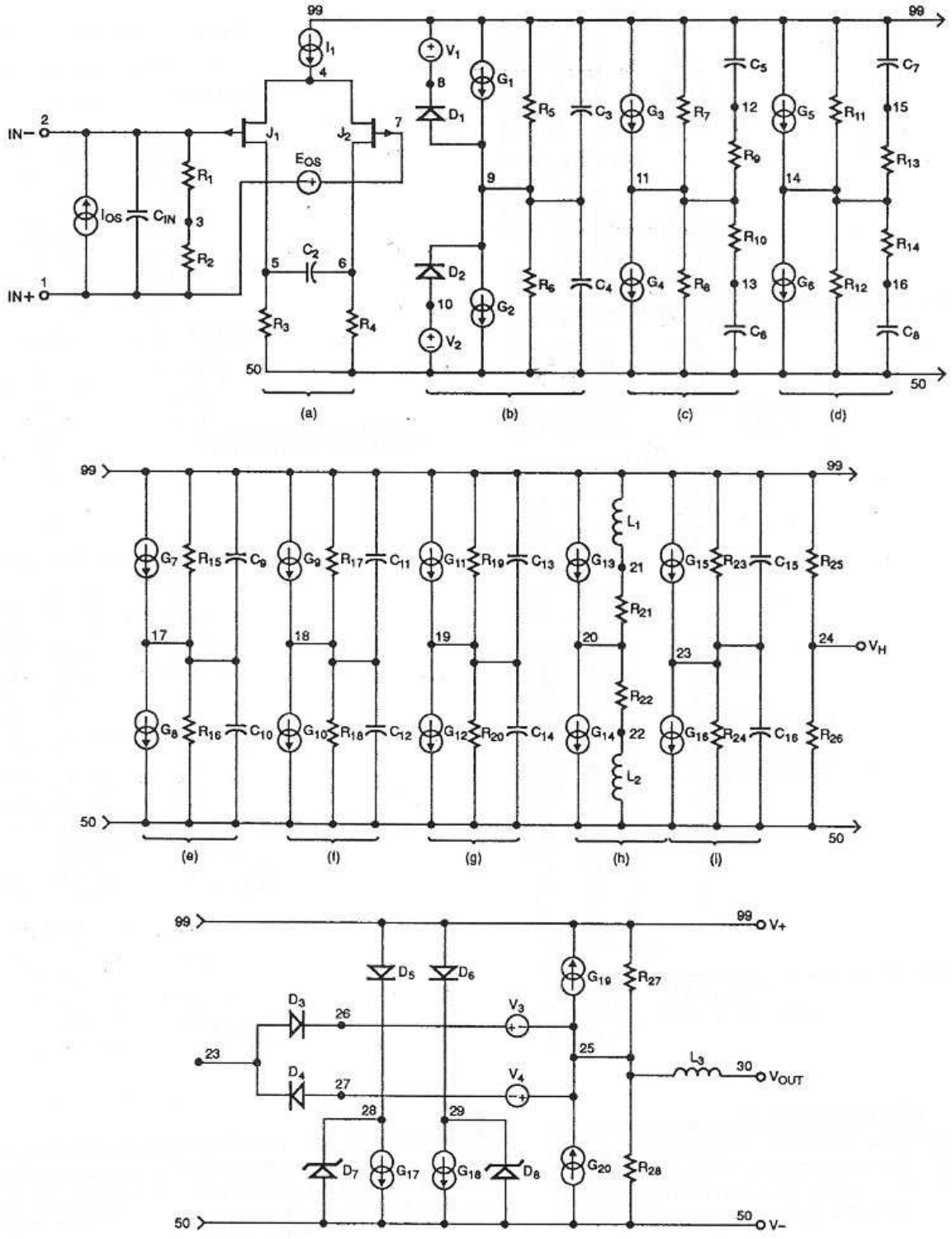

Figure 3-2: Alexander and Bowers' Model of a JFET-Input Op Amp. Picture taken directly from their 1990 paper.

pair, but very different gain and output stages. The ADI model is more modular than the Boyle model, with the flexibility of including as many poles and zeros as necessary. The model also has a common-mode gain stage for simulating CMRR, and simulates correctly the flow of power from the supplies instead of from ground. The modular nature of the ADI model allows the designer to add and remove components that directly affect the CMRR or PSRR, et cetera, without affecting all the other qualities of the macromodel.

3.3 Macromodeling Op Amp Characteristics

Op amps have dozens of characteristics that make each one unique, but it is impractical and very difficult to model them all with perfect precision in a macromodel. Since a macromodel replaces non-linear components with linear ones, there must be room left for error. For most simulations, it is adequate to pick some of the important qualities of amplifiers and focus on how to make the model reflect those attributes correctly. Which qualities are important is often application-specific, but there are a few universally important characteristics that can not be ignored in a model.

3.3.1 Analog Behavioral Modeling

Many modern-day macromodels include Analog Behavioral Modeling (ABM) blocks, whose transfer characteristics are defined using polynomial expressions in SPICE. Although these are non-linear elements, there is possibility for more accuracy in exchange for somewhat longer simulation times. However, the drawback to these blocks is that not all SPICE simulators accept ABM blocks, and each responds differently when they are used. ABM blocks cause some SPICE simulators to crash, while others will have no problem simulating with them. Since the LT6600 macromodel is not meant to be restricted it to one type of simulator, ABM blocks were not used in its design.

3.3.2 Open-Loop Gain and Phase

Although an op amp is usually operated in closed-loop conditions, the open-loop frequency response of an op amp is one of the most fundamental characteristics of an amplifier. According to feedback theory, an amplifier should have a very large open-loop gain and fast response so that the closed-loop response will be predictable and accurate. In addition, the phase of the amplifier response over frequency must be known so that the closed-loop system can be kept in a stable state. According to control theory [6], the open-loop transfer function of an op amp can be used to approximate both the closed-loop response and the transient response of an op amp. In short, we can understand an extraordinary amount about an op amp using its open-loop transfer characteristic.

The open-loop response of an operational amplifier is, in fact, one of the first considerations when building up the model from scratch. Referring to Figure 3-2, the input and gain stages are designed to implement the open-loop DC gain and the first two poles of the open-loop response. The remaining poles and zeros are implemented in later stages.

For filters especially, the phase of the amplifier matters because changes in phase introduce group delay. Filters are very versatile and universal devices, but for the majority of filter uses, the two main qualities by which a filter is judged are the gain response and group delay over frequency. The ideal filter changes the gain of a signal over frequency with flat group delay[2] , meaning it passes all frequencies of signal with a constant propagation delay. An example of non-linear phase is an op amp transient response to a fast-edge input step (voltage or current). Some frequencies are delayed more than others, resulting in the following common transient response properties: preshoot (undershoot), overshoot, and underdamped ringing.

[2]flat group delay $\Leftrightarrow$ linear phase over all frequencies

3.3.3 Measuring Open-Loop Response in Lab

Measuring the open-loop gain of an op amp does not necessarily mean that the op amp is set up in an open-loop configuration. The average op-amp can have an output voltage swing of up to tens of volts, and an open-loop gain of many thousands. Assuming a conservative op amp gain of 1000, producing a 1 V_{PP} at the output of an op amp would require a clean (low-noise) 1 mV_{PP} signal at its input. A good, clean 1 mV signal is not easy to produce from a lab signal generator. Additionally, setting up an op amp in an open-loop configuration will exaggerate the op amp's imperfect DC bias and amplify its offset voltage, which usually causes the op amp output to rail one way or the other. Therefore, an open-loop configuration is not the best way to measure open-loop gain.

A typical setup for measuring open-loop gain using a multiple-input network analyzer is shown in Figure 3-3. The op amp is set up in a closed-loop system, with the

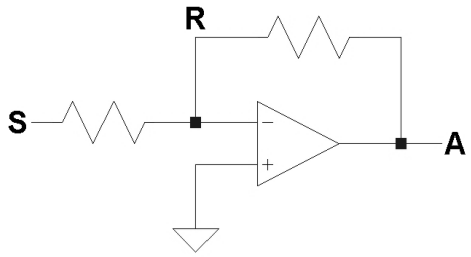

Figure 3-3: Open-Loop Gain Measurement With a Network Analyzer. Apply Input at 'S', Measure Gain at 'A' With Respect to 'R'

desired amount of closed-loop gain. A three-port network analyzer with at least two inputs is set up so that the source, S, drives the output, A. The network analyzer is set up to display the gain at point A with respect to point R, giving the output voltage swing in response to the corresponding voltage swing at the input of the amplifier. The op amp's phase and group delay characteristics can also be measured in this manner.

It is important to realize that there is a slight inaccuracy issue associated with the above measurement. There are two types of open-loop gain in an amplifier: voltage gain and current gain. The exact open-loop gain, T, is actually the parallel

combination of the open-loop voltage gain, T_v, and the open-loop current gain, T_i:[3]

$$T = (T_i + 1) \| (T_v + 1) - 1 = \frac{T_i \cdot T_v - 1}{T_i + T_v + 2} \tag{3.1}$$

Most operational amplifiers are built on a voltage feedback topology (the most common kind) in which the voltage gain is usually much smaller than the current gain. This is because the high input impedance of the voltage feedback amplifier topology makes current gain very large. In this case, the voltage measurement described above will be fairly accurate, since the voltage gain will dominate the parallel combination of the two types of gain. However, it can't be ignored that we are only measuring the gain to within a certain unknown percentage, depending on how much the voltage gain happens to dominate the overall gain. For maximum accuracy, it is necessary to have both. Unfortunately, there is no existing standard for measuring the current gain of an op amp in the lab.

3.3.4 Simulating Open-Loop Response in SPICE

Looking at Figure 3-3, it seems obvious that the open-loop gain of an amplifier is simply the output voltage divided by the voltage at the amplifier's input terminal (accounting for the amplifier's phase shift). However, consider the case of a "real" operational amplifier, which has a finite output impedance. Since output impedance can also be represented as a resistor in series with the output of the op amp (assuming the op amp has a mostly real output impedance), then the voltage seen at node 'A' in Figure 3-3 is attenuated by a resistive divider between the amplifier's output impedance and its load impedance. This results in a voltage error that can be significant if the amplifier's output impedance is large. However, the open-loop current gain of an amplifier does not change with series resistive dividers. Obtaining both open-loop current gain and voltage gain, as will be shown, can produce an accurate representation of the true open-loop gain of an amplifier.

In SPICE, we are able to simulate very accurately the exact open-loop gain and

[3]Equation 3.1's origin is explained in Section 3.3.4.

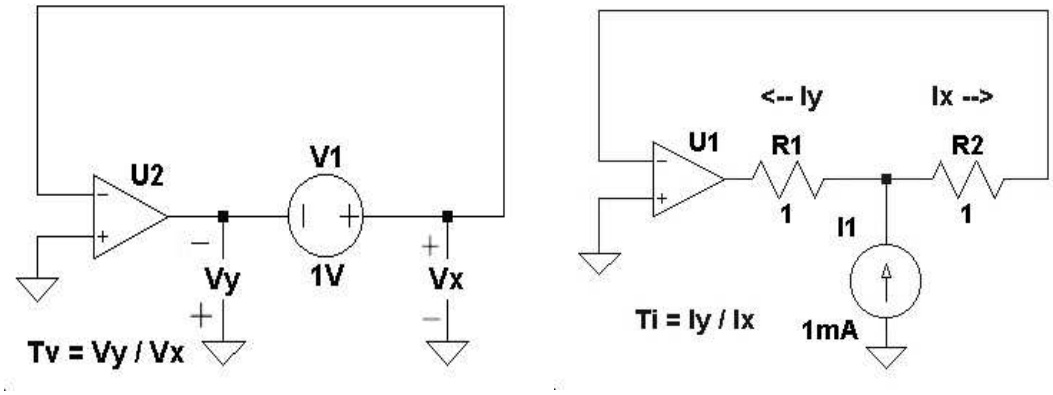

(a) (b)

Figure 3-4: Open-Loop Voltage Gain (a) and Current Gain (b) Measurement Techniques.

phase, using Equation 3.1 and the system known as Middlebrook analysis [7] [8]. The Middlebrook analysis technique involves measuring loop voltage gain and loop current gain using a null voltage and current injection in the feedback loop of the op-amp (see Figures 3-4(a) and 3-4(b)). The Middlebrook method requires the amplifier to be in a stable feedback loop, since an open-loop configuration tends to destroy the DC bias of the amplifier. Therefore, this method obtains the loop gain of the entire feedback loop, including the attenuation of any feedback network connected to the amplifier.

Middlebrook Analysis

The Middlebrook method of null current and voltage injection stems from the need to model "real" amplifiers with input and output impedances. The laboratory testing in Section 3.3.3 can be incomplete and inaccurate, although it works well if certain conditions are met. An understanding of the Middlebrook method begins with Figure 3-5, in which a null voltage is injected into the feedback loop of an operational amplifier. The circuit consists of a forced voltage in the feedback loop, with two impedances Z_1 and Z_2. In this case, the impedances in series make up the load of the amplifier, and there is additional attenuation in the feedback path due to the divider

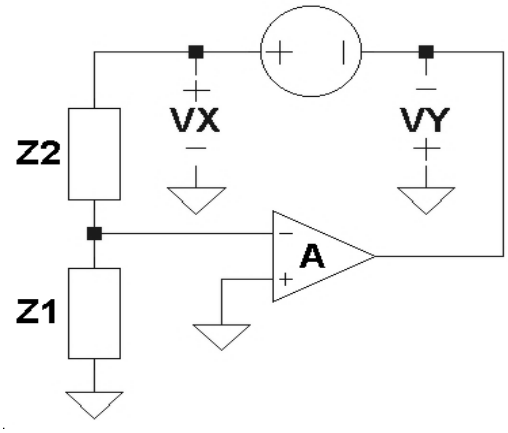

Figure 3-5: Null voltage injection into the feedback loop of an op amp.

created by the two. The op amp has an open-loop gain A. The voltages on either side of the voltage source are named V_x and $-V_y$. The negative sign in front of V_y exists so that the sum of V_x and V_y will equal the injected voltage. This way, the open-loop phase shift of the amplifier can also be established correctly.

By forcing a null voltage in the feedback loop, the op amp is forced to respond so that the system returns to a steady state. As long as the operational boundaries (saturation, et cetera) of the op amp are not violated, the following relation will be true:

$$-V_y = V_x A \left(\frac{Z_1}{Z_1 + Z_2} \right) \tag{3.2}$$

The sign of V_y is negative, although the amplifier is set up in an inverting gain configuration. This simply means that the phase shift of the amplifier is 180 degrees, and A will be a negative number. However, the amplifier's phase does not affect Equation 3.2. The loop gain T of the circuit, from Equation 3.2, can be written as:

$$T = \frac{V_y}{V_x} = -A \left(\frac{Z_1}{Z_1 + Z_2} \right) \tag{3.3}$$

Figure 3-5 shows an ideal circuit, where the amplifier has no output impedance to cause a resistive divider. The null voltage injected directly at the output gives an accurate indication of the amplifier's open-loop gain. However, a "real" amplifier has

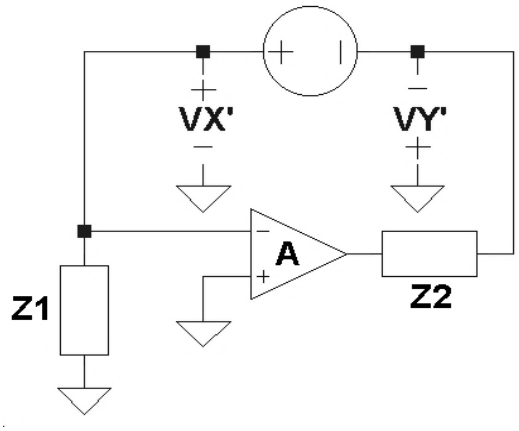

Figure 3-6: A more realistic circuit for null voltage injection of the op amp's feedback loop.

output impedance, and it is not possible to inject a voltage at its output. Figure 3-6 shows a more realistic setup, in which the null voltage is injected after the output impedance of the amplifier. The impedance Z_2 from Figure 3-5 has been moved to the output of the op amp, to represent its equivalent output impedance. The op amp's load impedance Z_1 is still in the same place, and can represent the op amp's load impedance in parallel with its own input impedance. The voltage injection into the feedback path now produces two voltages, V_x' and $-V_y'$. This circuit is more difficult to solve, but we can relate Figures 3-5 and 3-6 to find a common solution for the open-loop gain. The feedback resistor from Figure 3-5 was not replaced with another so that we can use the principles of superposition to relate the two circuits:

$$V_x' = \left(\frac{Z_1}{Z_1 + Z_2}\right) V_x \tag{3.4}$$

$$(-V_y') - V_x' = (-V_y) - V_x$$

$$V_y' = V_y + V_x - V_x' \tag{3.5}$$

Equation 3.4 comes from the resistive divider of Z_1 and Z_2, and Equation 3.5 comes from the fact that the null voltage is assumed to be the same in both circuits. Com-

bining Equations 3.2– 3.5, some algebraic manipulation will arrive at:

$$\begin{aligned}
V_y' &= (-V_x') + V_x + V_y \\
&= (-V_x') + V_x - A\left(\frac{Z_1}{Z_1+Z_2}\right)V_x \\
&= (-V_x') + V_x\left[1 - A\left(\frac{Z_1}{Z_1+Z_2}\right)\right] \\
&= (-V_x') + V_x'\left(\frac{Z_1+Z_2}{Z_1}\right)\left[1 - A\left(\frac{Z_1}{Z_1+Z_2}\right)\right] \\
&= (-V_x') + V_x'\left(1+\frac{Z_2}{Z_1}\right) - V_x'A \\
&= V_x'\left(\frac{Z_2}{Z_1}\right) - V_x'A \\
V_y' &= V_x'\left(\frac{Z_2}{Z_1} - A\right) \qquad (3.6)
\end{aligned}$$

From Equation 3.6, we can write down the equation for the voltage ratio across the injected voltage source:

$$T_v = \frac{V_y'}{V_x'} = \frac{Z_2}{Z_1} - A \qquad (3.7)$$

Equations 3.3 and 3.7 give us the overall loop gain and the voltage ratio in terms of the same elements, so the next step is to combine them together:

$$\begin{aligned}
T &= -\frac{Z_1}{Z_1+Z_2}A \\
&= \frac{-A}{1+\frac{Z_2}{Z_1}} \\
&= \frac{-A+\frac{Z_2}{Z_1}-\frac{Z_2}{Z_1}}{1+\frac{Z_2}{Z_1}} \\
T &= \frac{T_v - \frac{Z_2}{Z_1}}{1+\frac{Z_2}{Z_1}} \qquad (3.8)
\end{aligned}$$

Now, given a real op amp with an input and output impedance, we can figure out the actual open-loop gain of the op amp (assuming that we know the values of Z_1 and Z_2. By similarly analyzing the op amp circuit with an injected current source, as in Figure 3-4(b), we can come up with a very similar relationship between loop gain

and current ratio[4]:

$$T = \frac{T_i - \frac{Z_1}{Z_2}}{1 + \frac{Z_1}{Z_2}} \tag{3.9}$$

Under certain conditions, this Middlebrook analysis is not necessary, and simply knowing either the current or voltage ratio between the op amp input and output is enough to approximate its loop gain. Looking at Equations 3.8 and 3.9, these conditions are related to the ratio of impedances in the op amp circuit. Assuming that the loop gain of the op amp circuit will be much greater than 1, we can establish the following relations:

- if $\frac{Z_2}{Z_1} \ll 1$, $T \approx T_v$
- if $\frac{Z_2}{Z_1} \gg 1$, $T \approx T_i$

For most operational amplifiers, the first relation is true as the output impedance of the op amp is significantly smaller than the load impedance. In this case, knowing the voltage loop gain is sufficient to approximate the overall loop gain. However, knowing both the voltage and current loop gains can give us a better understanding of the overall loop gain:

$$\begin{aligned}
T_i &= \left(\frac{Z_1 + Z_2}{Z_2}\right) T + \frac{Z_1}{Z_2} \\
T_v &= \left(\frac{Z_1 + Z_2}{Z_1}\right) T + \frac{Z_2}{Z_1} \\
T_i + 1 &= \left(\frac{Z_1 + Z_2}{Z_2}\right) (T + 1) \\
T_v + 1 &= \left(\frac{Z_1 + Z_2}{Z_1}\right) (T + 1) \\
(T_i + 1) \parallel (T_v + 1) &= \frac{\frac{(Z_1+Z_2)^2}{Z_1 Z_2}(T+1)^2}{(T+1)\left(\frac{Z_1+Z_2}{Z_1} + \frac{Z_1+Z_2}{Z_2}\right)} \\
(T_i + 1) \parallel (T_v + 1) &= T + 1
\end{aligned} \tag{3.10}$$

Equation 3.10 is an identical form of Equation 3.1. By knowing both the voltage and current loop gains, which can simulated in SPICE, we can find the true loop gain of

[4]The analysis for Equation 3.9 is left out because it is nearly identical to that of Equation 3.8. It is also presented in [7].

an amplifier circuit (and thus, its open-loop gain) without knowing the exact input and output impedances of the op amp. When the values of circuit impedances are uncertain, the Middlebrook method will give a more accurate loop gain analysis than simply knowing the voltage or current loop gains individually.

3.3.5 Other Characteristics

This section briefly discusses some of the other important characteristics of filters and amplifiers that should be addressed here:

Input Bias Current The ideal op amp has zero input bias current, meaning that the bases of the transistors in no way affect the voltages applied to them. In a SPICE model, this can be influenced by either changing the current gain (for a bipolar transistor, the value of β_F), or by changing the operating current through the transistors.

Slew Rate Slew rate refers to the maximum rate at which the voltage at the output of the op amp can change. Normally, this value is limited by the dominant-pole capacitor in the op amp, and by the amount of bias current through the input transistors. However, in the case of an active filter, the cutoff frequency of the circuit will determine how fast the voltage at the output of the amplifier changes. Generally, in the case of an integrated low-pass filter, the cutoff frequency of the amplifier will exceed the cutoff frequency of the overall filter. Therefore, if the slew rate of the amplifier is faster than the rise time of the filter, the amplifier will generally not slew. For example, if the measured rise time of the filter is 1 microsecond for a 15 Volt step (15 V/μs), the amplifier should ideally have a slew rate of more than twice that (30 V/μs).

Voltage Offset Voltage offset[5] means that due to mismatches in the circuit, there is a DC output offset in the amplifier. This offset is divided by the gain of the circuit, and specified by an equivalent voltage source at the input of an ideal op amp.

[5]Voltage offset has been aptly referred to as DC noise. See [9]

AC Noise There are many different definitions of electrical 'noise', but the type described here is noise within the amplifier. There are 5 main types of internal noise: shot noise, thermal (Johnson) noise, flicker (1/f) noise, burst (popcorn) noise, and avalanche noise[6].

Noise is particularly important in a communications filtering application. The amount of stopband attenuation and SNR improvement a filter can provide is limited by its own noise floor. A filter with a high noise floor will limit or degrade the noise performance of the entire communications system.

Shot noise Shot noise is present in diodes and is associated with direct-current flow. Shot noise is white noise, meaning that it has equal energy over all frequencies.

Thermal noise Thermal noise is associated with resistors, and is caused by random thermal movement of electrons. It is present with or without direct current flow, and is also white noise.

Flicker noise Flicker noise is low-frequency noise found in active devices, and is caused mainly by traps in silicon due to contamination and crystal defects. Flicker noise energy decreases at higher frequencies, finally descending below the noise floor of shot and thermal noise.

Burst noise Burst noise (often called popcorn noise) is low-frequency noise that resembles low-level discrete signals. Played over a loudspeaker, it sounds like popcorn popping. Burst noise is not fully understood, and is speculated to be caused by heavy-metal ion contamination.

Avalanche noise Avalanche noise is caused by Zener or avalanche breakdown of pn junctions. Avalanche noise is associated with direct-current flow, and dominates shot noise when present.

In the context of macromodeling, burst and avalanche noise are usually ignored, unless there are Zener diodes present in the IC that can cause avalanche noise.

[6]for good discussion on noise, see [9] and [10]

Each of the amplifier noise types can be represented as an equivalent voltage noise source and equivalent current noise sources at the input of the amplifier. The effect of these noise sources on a system depends on the source impedance seen by the amplifier and the amplifier's closed-loop gain. For instance, if the amplifier's source impedance is large, current noise will become significant and dominate the voltage noise.

Common-Mode Range Amplifiers are always specified with a common-mode range specification, meaning that there is a common input voltage range inside of which the amplifier is guaranteed to perform properly. For differential amplifiers, such as the LT6600, there will also be a common mode range in which the output voltage is guaranteed to respond correctly.

Power-Supply Rejection All amplifiers need power to run, and in many cases, the power supplies feeding an amplifier will not be completely clean. The ideal power supply will handle any changes in load without any glitches or transients in its output voltage. In reality, as the load to an amplifier changes or the input varies, the load to its power supply will vary, and the resulting supply voltage transients can affect the amplifier's output (a sort of feedback condition). The better the amplifier design, the less a signal on the power supply will appear at the output of the amplifer.

Common-Mode Rejection Observing that an op amp has two inputs, it follows that there are two types of signals that can be given to it: a differential signal, in which the voltages at the inputs move separately, and a common-mode signal, in which the voltages at the inputs move together. The ideal op amp is designed to respond only to differential inputs, but mismatches in the circuit will cause the output to respond to common-mode signals as well. The common-mode rejection is usually specified as a ratio of differential-mode gain to common-mode gain of the amplifier, termed Common Mode Rejection Ratio (CMRR).

Chapter 4

Macromodeling the LT6600

After having read the various papers available on the subject of op amp macromodeling, it was obvious that the Boyle model was insufficient for macromodeling the LT6600. The LT6600's transfer function and overall characteristics were more complex than the Boyle model could represent, and so therefore a form of the Alexander and Bowers model was used. The modular concept was favorable because of its versatility, in that a designer can add and remove modules at will with minimal effect on the rest of the system. Though that is not the way a real amplifier is built, it was suitable for a simulation model.

Linear Technology currently manufactures three versions of the LT6600 low-pass filter: a 2.5 MHz version, a 10 MHz version, and a 20 MHz version. In the laboratory portion of the thesis, the LT6600-2.5 is used to simulate one CDMA channel. However, the 2.5 MHz version has less voltage limiting than the other two versions, so the more-sophisticated LT6600-10 macromodel is presented here. Figure 4-1 shows the LT6600-10 macromodel. The model consists of two separate internal amplifiers, with the first amplifier providing a few poles to the transfer function, and the second amplifier providing the bulk of the filtering. Staying true to the original design, there are protection diodes on all of the input and output pins to protect them from high voltage transients that might otherwise destroy the IC. The topology of the amplifier itself consists of two lowpass RC filters, one active and one passive, as well as an additional second-order active Sevastopoulos-LaPorte (SLP) filter (see

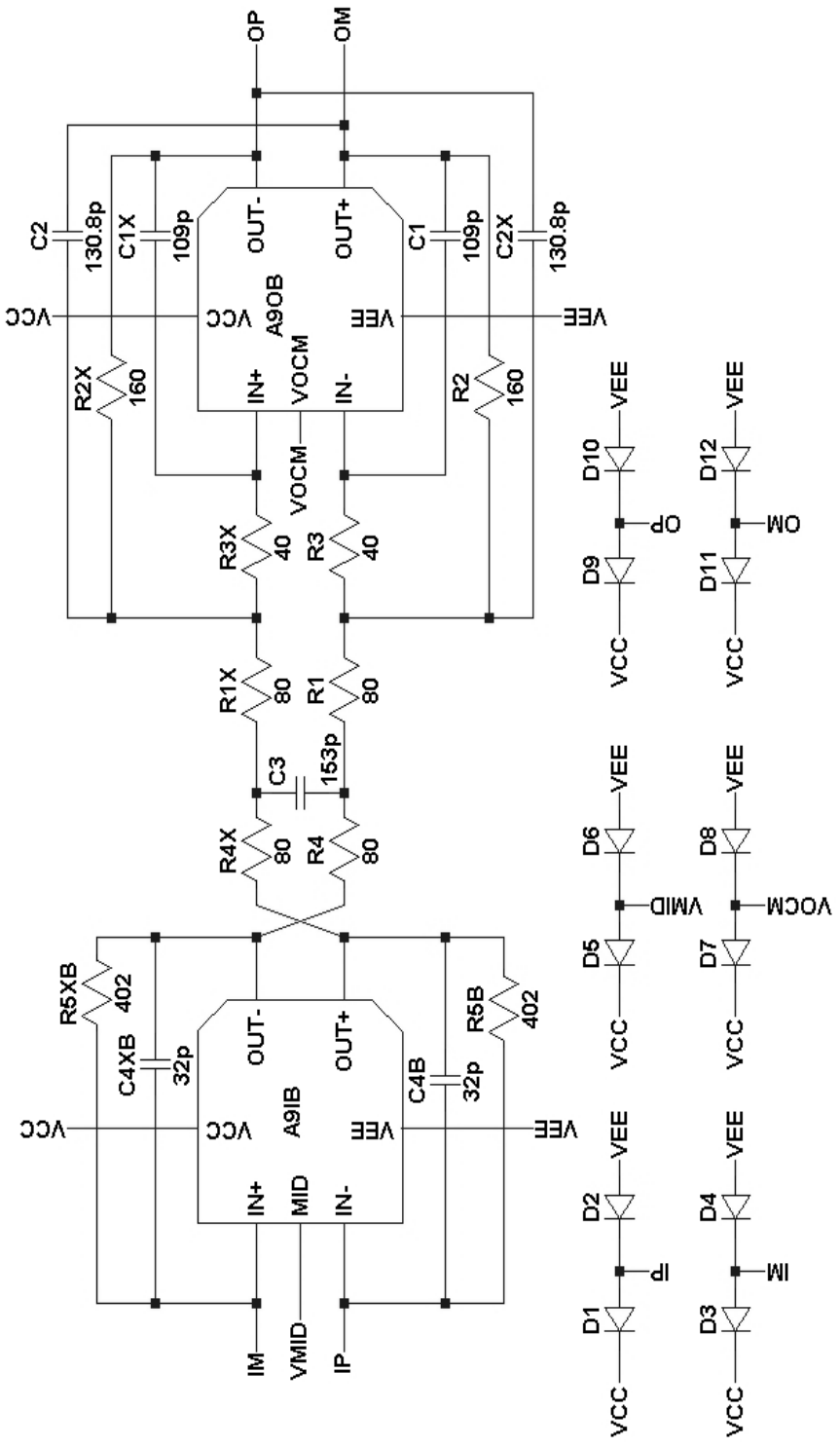

Figure 4-1: LT6600-10 Macromodel (10 MHz cutoff frequency) shown. Internal amplifiers are shown as amplifier blocks.

Appendix A). The topology used in the LT6600 is the differential SLP topology examined in Appendix A.

The input amplifier in the LT6600, A9IB, serves two functions: a pole in the transfer function and DC gain setting. The LT6600-10 has resistor-adjustable DC gain, and therefore requires two matched resistors at the inputs (IP and IM) of A9IB. The DC gain will then be $\frac{402}{R_{IN}}$. The capacitor in parallel with A9IB's feedback resistor creates an active pole in the transfer function. At the output of A9IB is a differential passive RC circuit. These two poles help to sharpen the transition from passband to stopband, as well as increasing the signal attenuation in the stopband of the filter.

4.1 A9IB: Input Amplifier

The macromodel of A9IB is shown in Figure 4-2. The influence of the modular Alexander and Bowers approach is clear. A9IB consists of a two-transistor input stage and a gain stage. The common-mode rejection is reduced by a common-mode gain stage, to match the performance of the LT6600. In addition, there is a common-mode feedback stage that controls the level of A9IB's common-mode output to match the level set by the pin V_{MID} on the LT6600. Normally this pin is set to the internally-biased mid-supply potential to allow for maximum output signal swing. The LT6600's output common-mode voltage is independent of V_{MID}, and is set by the V_{OCM} pin.

Compared to the output amplifier, the input amplifier of the LT6600 is much less critical in determining key amplifier output characteristics, such as output impedance and current sourcing or sinking. The input amplifier only needs to correctly model the amplifier input characteristics, such as input-referred noise, voltage offset, and common-mode rejection. This gives much more flexibility to the A9IB amplifier model, which is much simpler in comparison to the output amplifier A9OB.

The input of A9IB consists of a voltage noise source, E_1, to model the noise voltage of the real amplifier. This noise source adds to the noise already present in the amplifier. Normally, a current noise source would also be present, but the A9IB model already simulated with the correct current noise. The current source

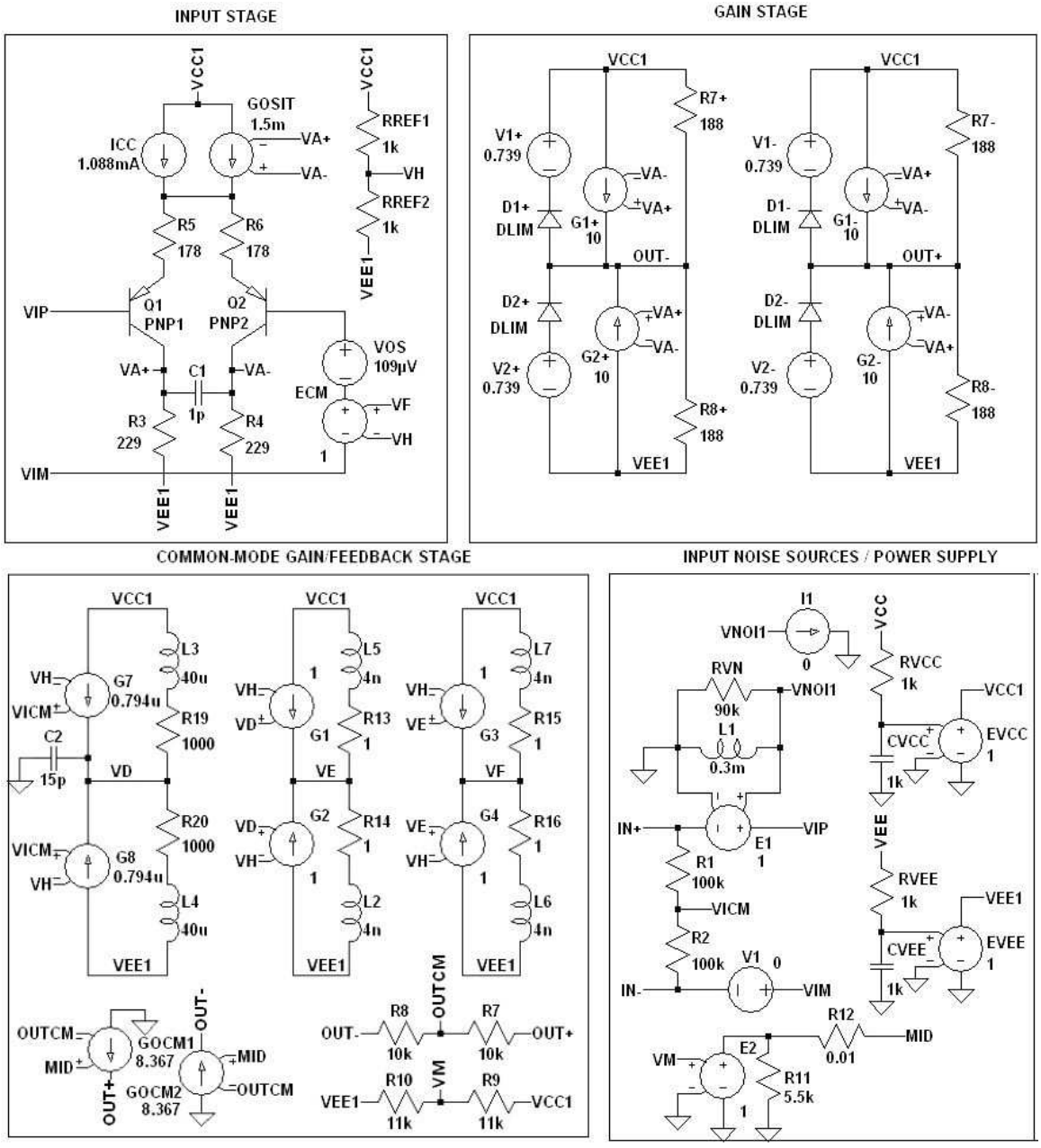

Figure 4-2: Input amplifier macromodel of the LT6600-10.

I_1, connected to the voltage noise source, acts only to satisfy the SPICE engine's netlist reader. The two power supplies for A9IB, VCC1 and VEE1, are not tied to the LT6600's main supplies. This is to control the amount of current that flows from VCC to VEE, and to control the model's power supply rejection.

The input stage of A9IB contains two emitter-coupled transistors (Q_1 and Q_2) with emitter degeneration, reminiscent of the Boyle macromodel. There is a compensation capacitor C_1 between the two collectors to add a high-frequency pole to the transfer function. The DC gain of the input stage is approximately the collector resistance divided by the emitter degeneration resistance, 1.3 in this case. In addition to the DC current source, there is a voltage controlled current source, G_{OSIT} [11]. This current source varies with the voltage across the differential outputs of the input stage, and creates asymmetrical slew rates for positive and negative output transitions (at the cost of slightly increased distortion).

The two voltage sources at the negative input, V_{OS} and E_{CM}, are the offset and common-mode voltages. V_{OS} represents the average input-referred offset voltage of the LT6600, and E_{CM} represents the common-mode-to-differential-mode gain of the circuit. E_{CM} is driven by a common-mode stage that adds poles and zeros to the CMRR transfer function (and is discussed below).

The gain/output stage of A9IB consists of simple dependent current sources ($G_{1\pm}$ and $G_{2\pm}$) with current-sinking resistors ($R_{7\pm}$ and $R_{8\pm}$), and a voltage-limiting circuit consisting of voltage sources and diodes ($V_{1\pm}$, $V_{2\pm}$, $D_{1\pm}$, and $D_{2\pm}$). $R_{7\pm}$ and $R_{8\pm}$ sink the current from the sources, and the parallel combination of $R_{7\pm}$ and $R_{8\pm}$ match the output impedance of A9IB. The diodes $D_{1\pm}$ and $D_{2\pm}$ are normally reverse-biased, but will limit the output voltages of A9IB when they approach either supply voltage. There is no output current limit in A9IB, because current limiting is done in the output amplifier.

The common-mode stage of A9IB, shown in Figure 4-3, plays an important role and is worth a closer look. There are two parts to this stage: the common-mode gain stage and the output common-mode feedback stage. The common-mode gain stage, consisting of three similar modular blocks, shapes the common-mode voltage rejection

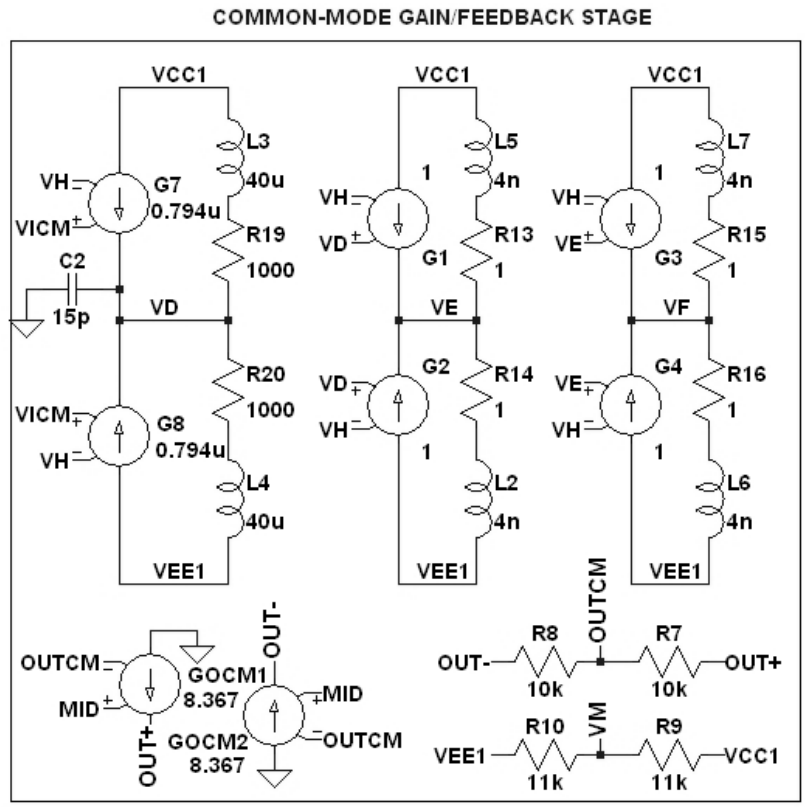

Figure 4-3: Input amplifier common-mode stage.

of the model. In the first block, C_2 and L_3/L_4 shape the frequency response of the common-mode gain. The latter two blocks use L_5/L_2 and L_6/L_7 to add zeros to the common-mode gain. A scaled-down, frequency-shaped version of the common-mode input is then applied back to the input through voltage source E_{CM}, in the input stage.

The internal common-mode voltage of the part, which is set either internally or via V_{MID} on the LT6600 [2], determines the output common-mode voltage of A9IB. If no external voltage is applied to the LT6600-10's output common-mode pin, voltage source E_2 sets this level to half-supply. This level is then compared dynamically to the output common-mode level, and any errors are corrected via negative feedback by current sources G_{OCM1} and G_{OCM2}. R_{11}, a 5.5 kilohm resistor to ground, matches the impedance of the V_{MID} pin on the actual LT6600.

4.2 A9OB: Output Amplifier

Figure 4-4 shows the complete output amplifier macromodel, which is much more complex than the input amplifier macromodel. The A9OB model incorporates more control over output impedance, current and voltage limiting, and other considerations to match the real amplifier. The input stage of the A9OB model is very similar to that of the A9IB model. It contains two transistors, an offset voltage source, slew rate improvement, and power dissipation sources.

Unlike the A9IB model, the A9OB model includes the effects of current noise, to more accurately model that of the LT6600. The A9OB noise stage is shown in Figure 4-5. There are identical current noise sources at both inputs, and one voltage noise source to the negative input of the amplifier. As was the case with the input amplifier, the noise sources are resistors, with added capacitors and inductors for noise shaping with frequency. As in the A9IB model, there are dummy current sources and dummy inductors to satisfy the SPICE netlist reader.

The gain stage of the A9OB model is shown in Figure 4-6. Contrary to the A9IB model, the gain stage does not also serve as the output stage, mainly for out-

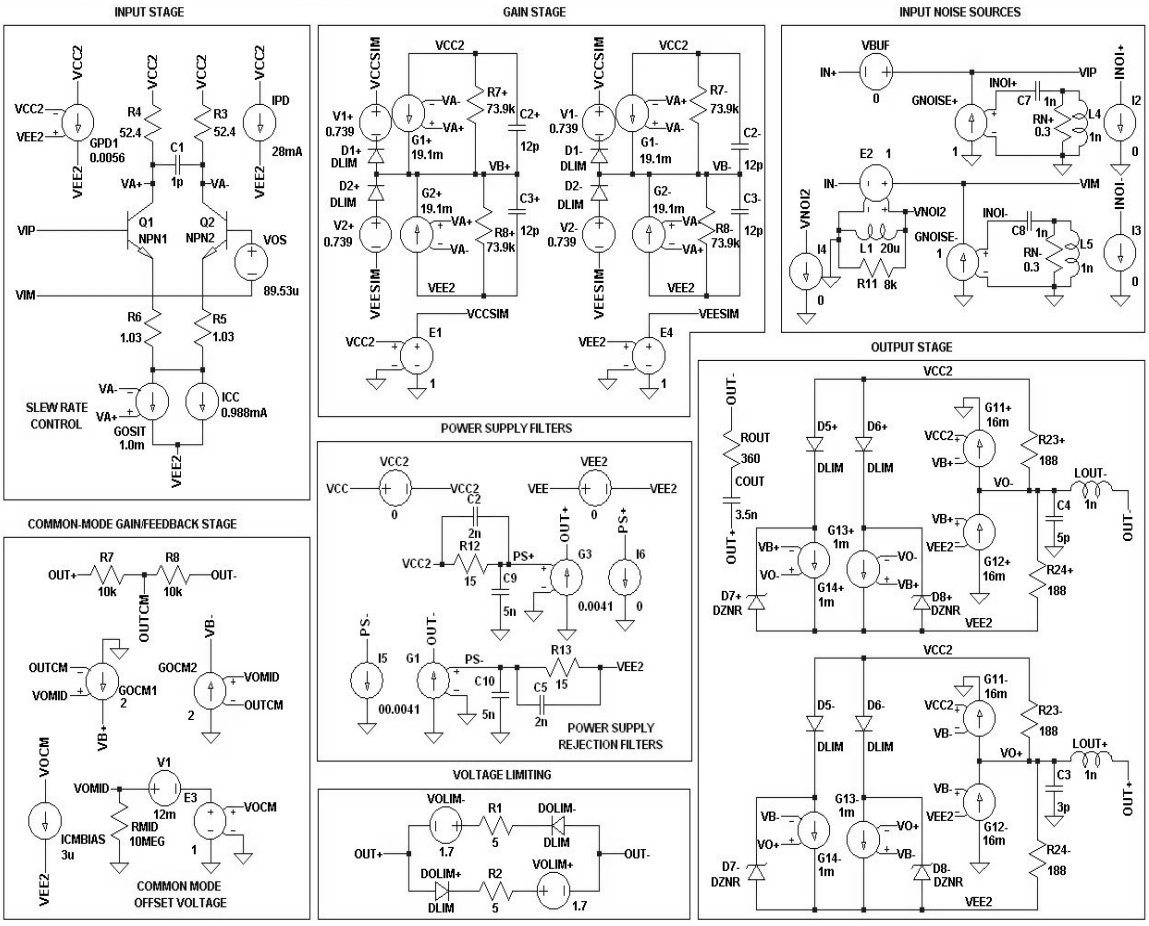

Figure 4-4: Output amplifier macromodel of the LT6600-10.

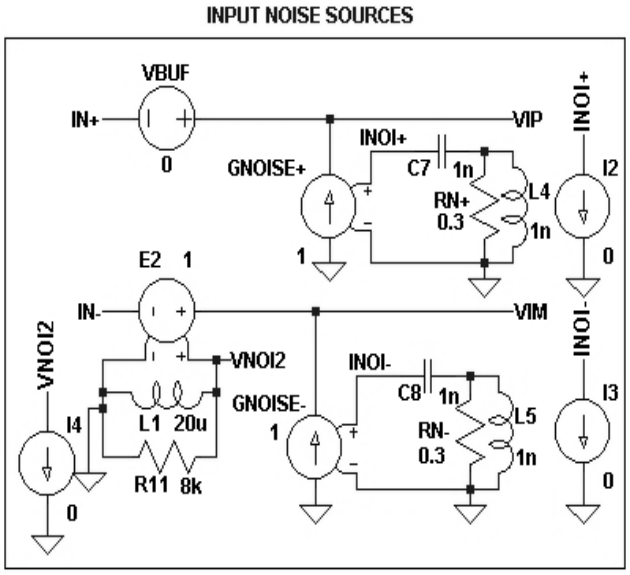

Figure 4-5: Output amplifier noise sources.

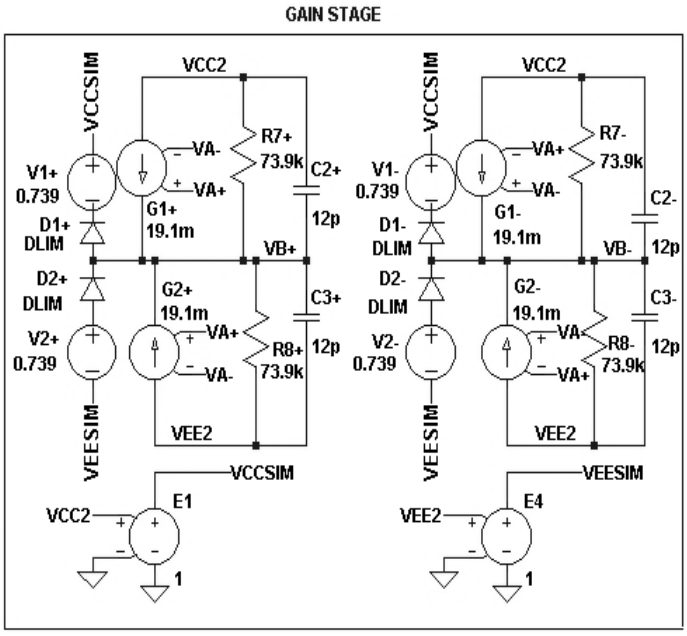

Figure 4-6: Output amplifier model gain stage.

put impedance and current limiting reasons. Capacitors $C_{2\pm}$ and $C_{3\pm}$ add a high-frequency pole to the transfer function. The rest of the gain stage functions the same way as in the A9IB model.

4.2.1 Output Stage

The output stage of the A9OB model is shown in Figure 4-7. An output stage is necessary for A9OB, unlike for A9IB, because output impedance and current/voltage limiting are easier to incorporate with two separate stages. The output impedance is set by the inductor L_{OUT}, the capacitors C_3-C_4, the resistors $R_{23\pm}$-$R_{24\pm}$, and the additional zero consisting of R_{OUT} and C_{OUT}. R_{OUT} and C_{OUT} simulate the crosstalk that occurs between the outputs in the real component. The current limiting is naturally achieved through the values of $G_{11\pm}$ and $G_{12\pm}$. Due to the nature of the voltage limiting in the gain stage, the maximum current provided by the output stage when the output is short-circuited will match that of the LT6600.

The output stage includes current equalizing networks consisting of $D_{5\pm}$, $D_{6\pm}$, and everything connected to them. These networks ensure that the correct current flows

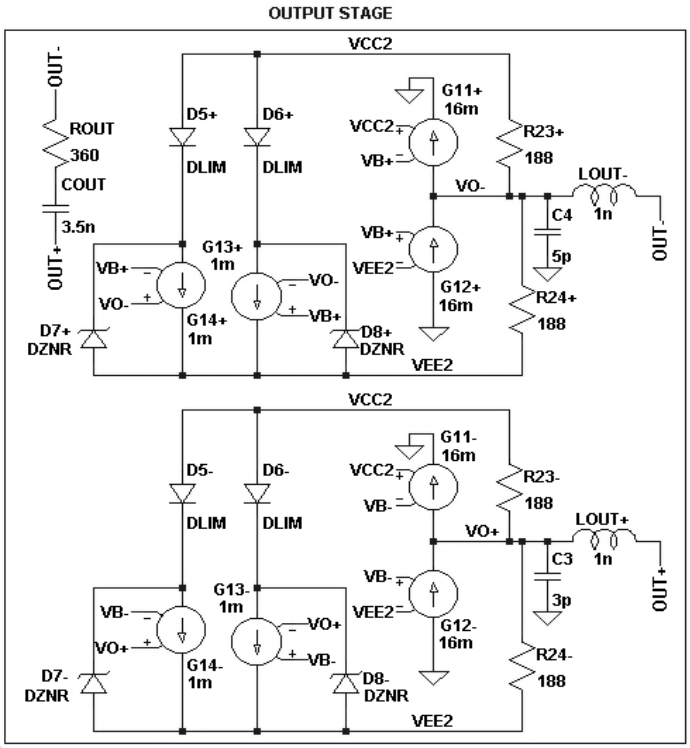

Figure 4-7: Output amplifier model output stage.

from V_{CC} to V_{EE} when the output changes dynamically. The zener diodes ensure that the current sources always have current sink devices, since current only flows through $D_{5\pm}$ and $D_{6\pm}$ in one direction.

The gain stage takes care of the single-ended voltage limiting, but the differential voltage limiting is implemented separately and affects the output stage. Referring to Figure 4-4, the differential voltage limiting stage consists of diodes $D_{OLIM\pm}$, voltage sources $V_{OLIM\pm}$, and some parasitic resistors R_1 and R_2. These devices limit the peak-to-peak differential voltage at the outputs to match the LT6600-10.

4.2.2 Other Characteristics

Other characteristics modeled by the A9OB model include output common-mode voltage setting and power supply rejection. There is no common-mode-to-differential-mode gain in the A9OB amplifier, since it has been modeled in the A9IB amplifier. However, the LT6600 has the feature that the output common-mode voltage is pin-

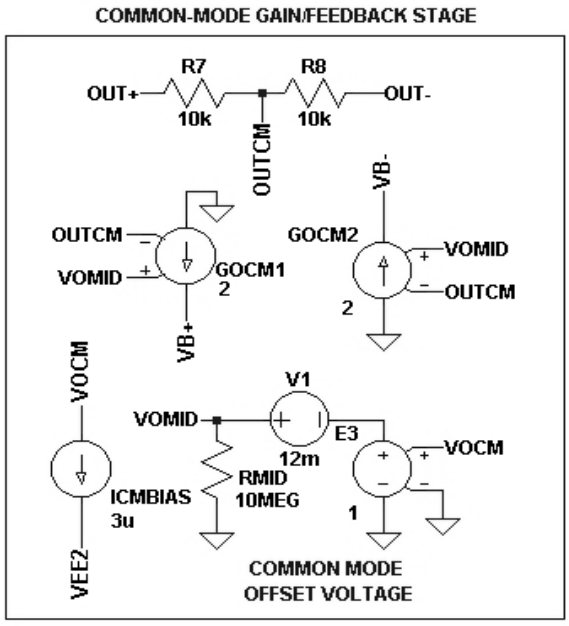

Figure 4-8: Output amplifier model common-mode feedback stage.

settable; therefore, the common-mode feedback stage ensures that the common-mode level of the two outputs match that of the LT6600. The common-mode feedback stage is shown in Figure 4-8. As in A9IB, the resistors R_7 and R_8 are connected to the outputs, causing the voltage at their midpoint to be the average of the outputs, also known as the common-mode voltage level. This voltage is compared to the desired voltage, and current is fed to the gain stage accordingly to ensure that the output common-mode voltage remains at the proper level. The voltage source V_1 gives the output common-mode voltage a 12 mV offset that exists in the LT6600, due to internal mismatches. Also notable in Figure 4-8 is the current source I_{CMBIAS}, which represents the bias current in the output common-mode pin of the LT6600.

Power supply rejection refers to the amplifier's ability to ignore AC variations in the power supply rail voltages. The power supply voltage filtering is shown in Figure 4-9. Simple first-order RC filters are used for the power-supply filtering, with small bypass capacitors C_2 and C_5 to increase the high-frequency supply rejection. Two dummy current sources are included to satisfy the SPICE netlist reader.

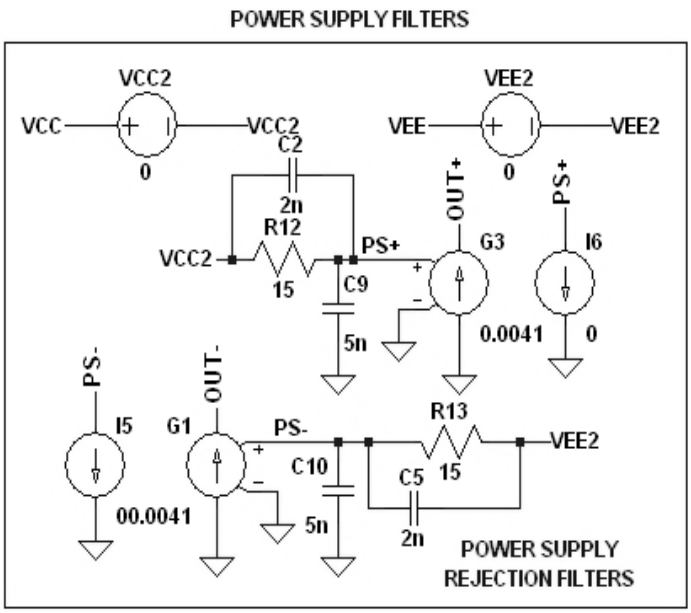

Figure 4-9: Output amplifier model power supply filters.

4.3 Verifying the LT6600-10 Macromodel

In order to be an effective representation of the LT6600-10 for use in simulation, the most important characteristics of the LT6600-10 must be matched by the macromodel. Since the focus of the LT6600-10's applications are in communications filtering, the macromodel will be judged by communications criteria as well as by the criteria of a normal operational amplifier. The LT6600-10 macromodel will be compared to the real part, and should closely match datasheet specifications as well as computer simulations of the transistor-level IC. The results are presented in this section, and the following characteristics will be compared:

- Differential AC Gain and Group Delay
- Transient Response
- Common-Mode Rejection
- Power-Supply Rejection
- Voltage Noise

- Output Impedance
- Power Consumption

The macromodels are based on a combination of ideal performance, typical datasheet specifications, laboratory results, and computer simulations of the transistor-level IC.

4.3.1 Gain and Group Delay

Since the primary function of the LT6600-10 is as a 10-MHz differential low-pass filter, it was important to match the AC frequency response and group delay of the IC as closely as possible. The Middlebrook analysis technique of measuring differential gain (very similar to that of Section 3.3.4) was used to compare the response of both the macromodel and the device datasheet. The analysis schematic is shown in Figure 4-10. The mathematics behind a differential-mode measurement is fundamentally the same as for a single-ended measurement [7] [8]. The gain and delay over frequency of the macromodel is compared with the datasheet specifications in Figure 4-11. Figure 4-11 shows that the gain and group delay characteristics for the LT6600-10 model are extremely close to that of the real IC. The gain response and group delay are important because these are two of the major ways that filters are compared with each other. A flat group delay means that the phase of the filter is linear, and this can be advantageous for many reasons (an example is phase modulation, where a non-linear-phase filter would have to be accounted for in the system design). The gain of the filter and its frequency response is used to determine if the filter is suitable for the filtering needs of the application.

4.3.2 Transient Response

With the gain response and group delay of the model matching the real part so well, there is no reason to expect that their transient responses would vary. Shown in Figure 4-12 is the laboratory setup used to measure the transient response of the LT6600-10. The simulation schematics are identical to the laboratory schematic. The

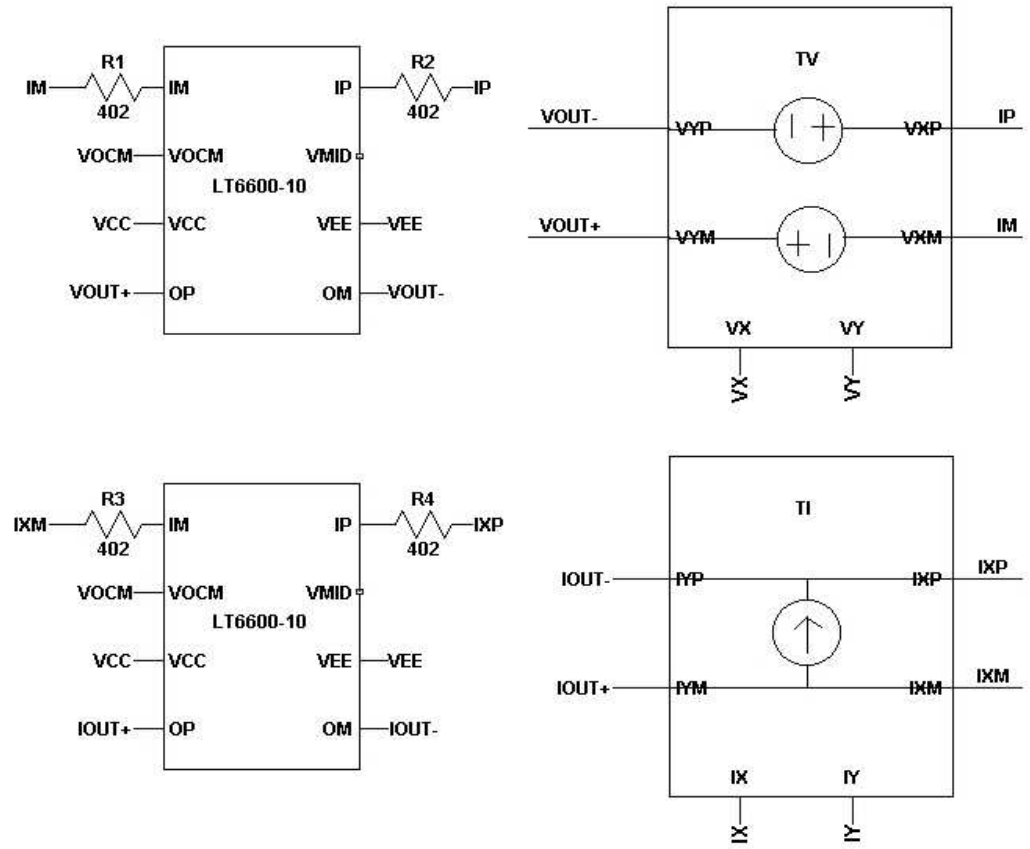

Figure 4-10: Method of measuring differential open-loop gain.

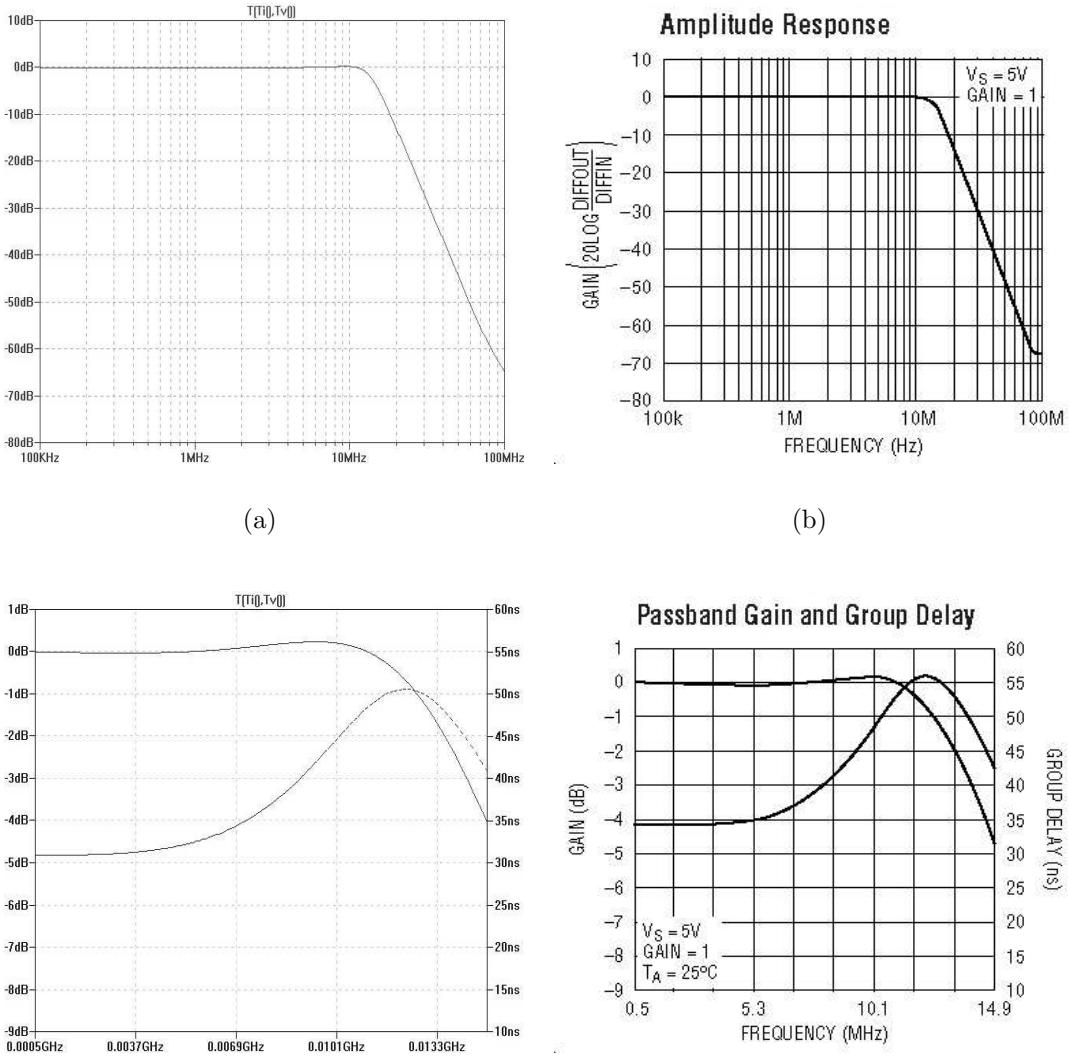

Figure 4-11: Comparisons of the LT6600-10 macromodel's amplitude response (a) with the datasheet (b). Also, a zoomed-in version of the macromodel's amplitude response with group delay (c) is compared with that of the datasheet (d).

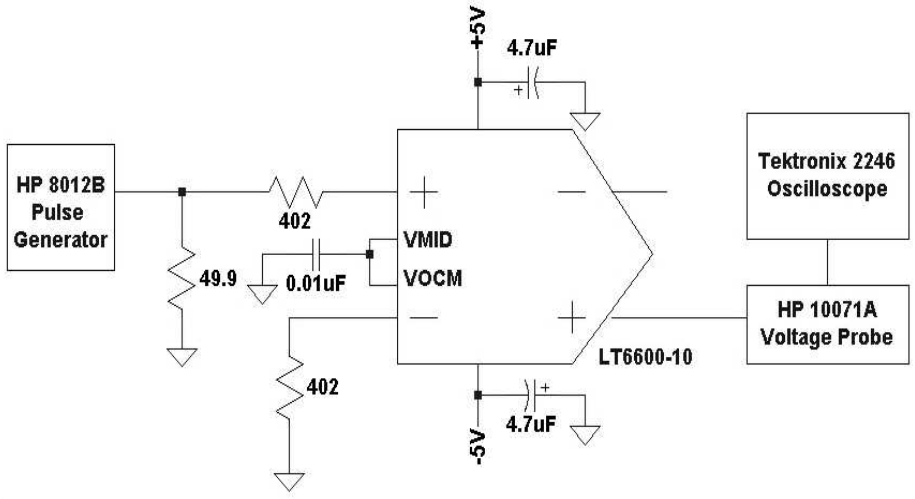

Figure 4-12: Method of measuring transient response in the laboratory.

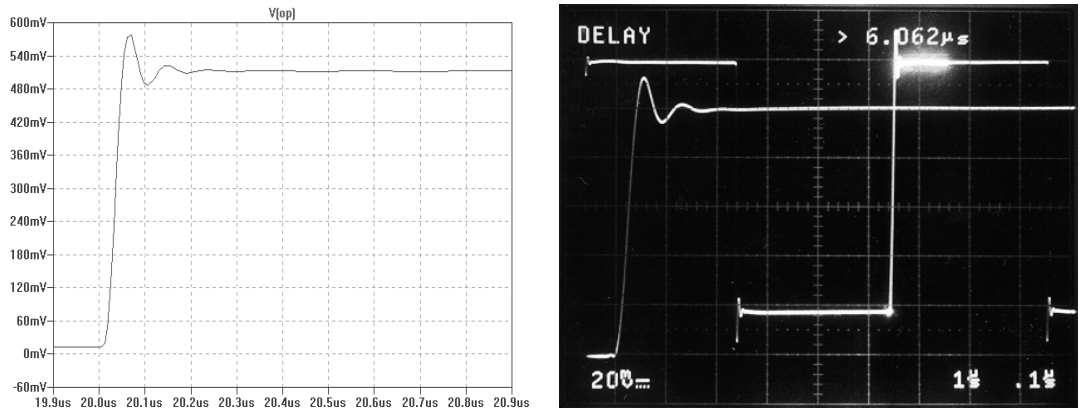

(a) (b)

Figure 4-13: Comparison of the transient responses of the LT6600-10 model (a) and the LT6600-10 in the laboratory (b). Laboratory picture shows the Tektronix 2246 oscilloscope in intensified (zoom) mode, displaying both the square wave and the zoomed-in positive transition.

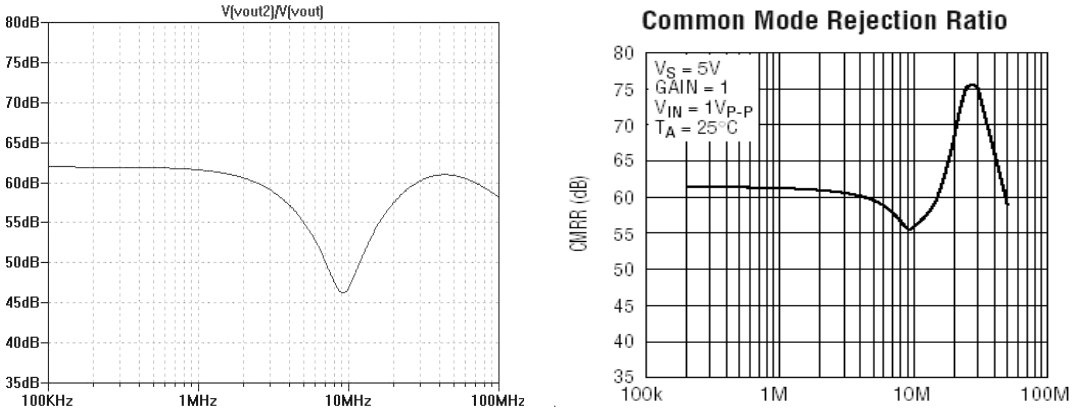

(a) (b)

Figure 4-14: Common-Mode Rejection Ratio comparison between the LT6600-10 model (a) and the datasheet specification (b).

results are presented in Figure 4-13. From the figure, the transient responses of the model and the real IC are well-matched. The underdamped ringing frequencies are approximately 11 MHz for both, and the overshoot is around 14%. The 2% settling time comes out to 140 nanoseconds for both.

4.3.3 Common-Mode Rejection Ratio (CMRR)

Designers are often interested in the common-mode rejection of a differential circuit. An ideal fully-differential circuit does not react to common voltages applied to its input pins, but in reality, differential ICs will have slight internal mis-matches, with attenuated versions of the common-mode input voltage appearing at the output. CMRR is the ratio of the LT6600's differential-mode gain to its common-mode gain, and is usually presented in decibels. Figure 4-14 shows the comparison of the LT6600-10 model CMRR with the datasheet specification for the IC.

The CMRR of the macromodel matches at of the IC well until after the 10MHz cutoff frequency of the filter. At this point, the CMRR of the LT6600 experiences a dip and a sharp rise, then drops steadily above 25MHz. The CMRR of the macromodel contains a similar dip at 10MHz, peaks softly at 30MHz, and then drops steadily above a few tens of MegaHertz. The unusual CMRR of the LT6600 is due to the

fact that it has two separate amplifiers. The input amplifier's input stage contains a zero in its common-mode gain response, which is included in the Alexander and Bowers model. However, the input amplifier also has a pole in the feedback loop and a passive pole at its output, which helps to explain the dip and rise in the CMRR (the pole frequencies are higher than the zero frequency). The SLP filter at the output amplifier causes the steadily decreasing CMRR above 25MHz.

The CMRR of the LT6600-10 rises and falls quickly, which requires many poles and zeroes to model correctly. Since most of the activity mentioned above occurs above the cutoff frequency of the filter, replicating the CMRR with exact precision is not necessary. The LT6600-10 macromodel does not contain the number of common-mode poles and zeros necessary to replicate the function exactly, but is precise below the cutoff frequency of the filter. Above the cutoff frequency, the CMRR of the macromodel drops off after a few tens of MHz, which reflects the characteristic of the LT6600-10 IC.

4.3.4 Power Supply Rejection Ratio (PSRR)

Power supply rejection pertains to voltage variations in the power supply, which may be caused by a variety of reasons. Since power supplies do not have zero output impedance, there will be variations of their output voltage with changing currents, and these changes will show up as minor disturbances in the output of the amplifier. Other devices connected to the same power supplies may also cause voltage transients on the supplies. PSRR is a ratio of the power supply voltage disturbance to the disturbance at the output of the differential amplifier, and is usually presented in decibels. Figure 4-15 shows the comparison of the LT6600-10 model's PSRR with the datasheet specification for the IC. The PSRR of the macromodel is very close to that of the LT6600-10. Both start at around 80dB of rejection, which rolls off after 100kHz and stops around 40dB at the cutoff frequency of the filter. Above the cutoff frequency of the filter, the power supply noise increase has many different potential sources on the LT6600-10 IC. However, as PSRR at high frequencies is not one of the more critical characteristics of a macromodel, a more complex PSRR stage was not

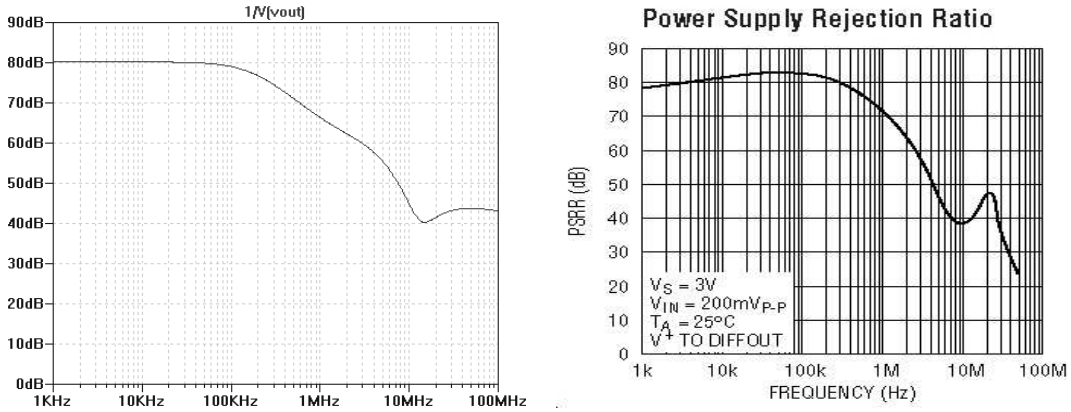

(a) (b)

Figure 4-15: Power Supply Rejection Ratio comparison between the LT6600-10 model (a) and the datasheet specification (b).

pursued for this model.

4.3.5 Voltage Noise

In a communications system, signal-to-noise ratio is important. The amount of noise added to a signal helps to determine how well that signal can be reconstructed, and how much will be misinterpreted. Therefore, every component in the system (including the analog filter) must be as low-noise as possible. This holds for a macromodel, since SPICE is capable of calculating the noise in a circuit or system. Figure 4-16 shows the voltage noise calculated in the LT6600-10 model versus what the datasheet specifies for the part. The voltage noise of the LT6600-10 model does not match the voltage noise of the real LT6600 exactly, but the shape of the voltage noise is correct over frequency.

4.3.6 Output Impedance

The output impedance of the LT6600-10 is effectively the same as a resistor connected in series with the output. As a load changes dynamically, and the currents out of the LT6600-10 change accordingly, a series resistor would cause voltage variations that

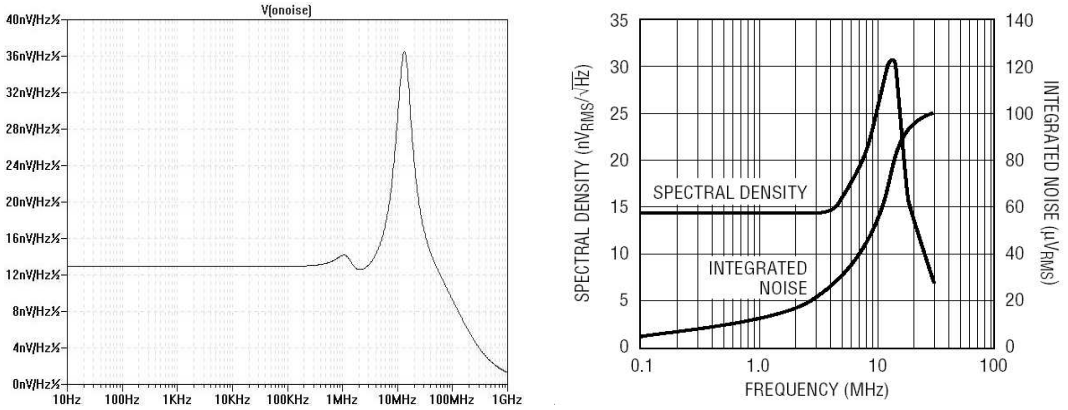

(a) (b)

Figure 4-16: Voltage noise comparison between the LT6600-10 model (a) and the datasheet specification (b).

in turn would cause errors in the output. The lower the output impedance, the more the load tends to see what the amplifier wants it to see.

The output impedance of the LT6600-10 is shown in Figure 4-17, along with the output impedance of the LT6600-10 model. The output impedance of the LT6600-10 model is fairly close to the actual performance of the part, and follows the same impedance changes over frequency. Note that the output impedance does not rise gradually, as it does in an operational amplifier. Since the LT6600-10 has filtering components in the IC, the output impedance will look more like that of an active filter. This explains the sharp sudden rise in output impedance at a few MegaHertz.

4.3.7 Power Consumption

According to the LT6600-10 datasheet, the power supply current draw of the LT6600 will stay between 35 mA and 46 mA. Even though the AC current of the LT6600-10 model varies according to load and input signal, as the real part would do, the average power supply current draw stays within that range over the entire range of power supply voltages.

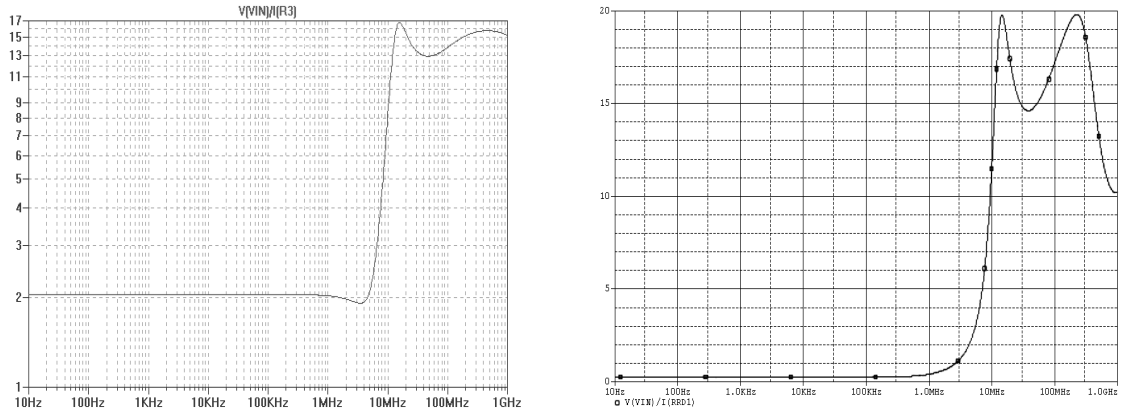

(a) (b)

Figure 4-17: Output impedance comparison between the LT6600-10 model (a) and the LT6600-10 transistor-level simulation (b).

4.4 Limitations of the LT6600-10 Model

Besides those limitations already discussed above, the LT6600-10 model was not designed to model the real IC over temperature or for distortion. The LT6600-10 model's characteristics do not change appreciably over temperature (except for the natural increase in noise), while the actual LT6600 may suffer more severe effects as the temperature changes. It is difficult to model what happens to a real IC as temperature changes, especially if different parts of the IC heat up faster than others. For now, it is sufficient that the LT6600-10 model stays within datasheet specifications over the entire temperature range. More specific modeling can be classified under possible future work.

The distortion performance of the LT6600-10 is also difficult to model accurately. Except for the predictable distortion caused by voltage limiting and current starving at higher amplitudes, the distortion that the part experiences over frequency is not due to any one factor alone. To correctly model the datasheet distortion of the LT6600-10 would have been very time-consuming, and not worth the effort. Most macromodel users won't require accurate distortion performance, and therefore it is enough that the LT6600-10 macromodel's distortion is better than reality. However, modeling amplifier distortion is an interesting area for future study.

Chapter 5

Introduction to Modern Communications Systems

All communications systems can be simplified down to a transmitter, a transmission medium (i.e. channel), and a receiver. Having a good understanding of all three is the key to good system design. The medium over which information is transmitted can be air, water, electrical wire, optical fiber, etc. Each transmission medium dictates a different set of requirements for the transmitter and the receiver. There are some standard metrics for determining the performance of a communications system, and some of them are discussed in this section.

Bit Rate vs. Symbol Rate These two metrics apply only to digital systems. A bit refers to a one or a zero, or one unit of digital information. A symbol refers to one unit of transmitted information. The difference is easy to see in example: Take a 2-bit digital-to-analog converter (DAC), whose output voltage levels are at 0V, 1V, 2V, and 3V. In one unit of time (one DAC clock cycle), the DAC will output one symbol, at one of the four output voltage levels. However, since there are four total levels represented in that one symbol, then one symbol contains two bits of information[1]. As a result, the bit rate of the 2-bit DAC is exactly twice its symbol rate.

[1] In bits, the four voltage levels can be represented digitally as 00, 01, 10, and 11

Increasing the bit rate to symbol rate ratio is an important way to improve the amount of information that we can transfer in a given period of time. Using digital modulation schemes such as Quadrature Amplitude Modulation (QAM) allows for a greater bit rate to symbol rate ratio.

Signal-to-Noise Ratio Signal-to-Noise Ratio (SNR) is a measure of the signal level in a system compared to the amount of noise that system adds. A low SNR limits the ability of a digital receiver to distinguish different symbols from one another, and so limits the amount of information that can be sent. In the analog world, an example of poor SNR would be a cell phone call where a voice is barely distinguishable from the noise that the cell phone receives. If the SNR is 1 (0 dB), then the desired signal has exactly the same energy as the noise in the system.

Although a high SNR is always more desirable, some systems can tolerate much more noise than others. For instance, analog telephones can tolerate tens of decibels more noise than an analog video signal, since a slightly fuzzy audio voice signal is more tolerable than a slightly fuzzy video screen. Also, many digital modulation schemes have ways of decoding information even in very noisy channels.

Bit Error Rate Bit Error Rate is a digital-domain metric of how many bits of information are interpreted incorrectly by the receiver, and is directly related to the SNR. If the noise level in a given signal is high, then there will be statistically more incorrect symbols received, and BER will be higher. For example, if a system interprets 1 in every one thousand symbols incorrectly, then the BER is 0.001 (assuming one bit per symbol). Receiving too many incorrect symbols requires overhead bits (i.e. error-correction codes or information retransmission), which lowers the overall data rate of the system.

For sake of consistency, speaking in terms of incorrect symbols requires the clarification that BER is also a function of the modulation scheme used. If the bit rate is much higher than the symbol rate, then one incorrect symbol will

cause many bits to be incorrect. For a given SNR, some modulation protocols will have a higher BER than others.

Channel Capacity Claude Shannon, widely considered as the founder of information technology as we know it today, spent some time writing about the theoretical capacity of an information channel [12]. According to Shannon, each information system has a maximum rate of information that can be transmitted and received with small probability of error in the presence of noise. Shannon set a theoretical limit for this channel capacity, with consideration of the channel's bandwidth, and SNR. Assuming a Gaussian channel with an additive white (Gaussian) noise, the Shannon-Hartley Theorem states that the channel capacity will be:

$$C = BW \cdot \ log_2(1 + SNR)$$

where C is the channel capacity in bits per second (bps), BW is the bandwidth of the channel in Hertz, and SNR is the signal-to-noise ratio (*not* in decibels). A proof of the Shannon-Hartley theorem lies beyond the scope of this thesis.

Spectral Efficiency Spectral efficiency is a measure of how much information is transmitted in a system versus how much bandwidth is required to transmit that information. Spectral efficiency is mainly determined by the system communications protocol. Analog modulation, in which an analog signal is directly modulated up to RF frequencies, is a very simple protocol. The bandwidth that the system requires is exactly the bandwidth that the baseband signal requires. CDMA, on the other hand, uses digital coding to transmit over ten times the amount of information that analog modulation can transmit in the same amount of bandwidth. Therefore, CDMA has much greater spectral efficiency than analog modulation.

Spectral efficiency is important because more and more electronics devices are becoming wireless, and ever faster data rates are demanded for each device. Therefore, the airwaves are getting very congested, and more information trans-

mitted over a smaller bandwidth means less congestion. This is analogous to 5 people carpooling together to work, which requires one-fifth the amount of cars on the road as each person driving separately. If everyone did this, the roads would be less congested, and everyone would get to work much faster.

Power Efficiency Power efficiency is a measure of the power wasted by a communications system. In mobile applications, since batteries have limited power, we want the device to use as little power as possible while still maintaining long range and high data transfer rates. A Digital Signal Processor (DSP) uses a majority of its power just to keep itself running, since it is a general-purpose processor. An Application-Specific Integrated Circuit (ASIC), on the other hand, is specifically designed for a certain task, and therefore uses less power for that task. However, an ASIC is difficult to reprogram once it is manufactured, and thus an important tradeoff exists between ease of development and power efficiency. Many cell phones today contain DSP chips due to their shorter development time and faster time-to-market.

The power efficiency of a system is also dependent on the communications protocol used. In mobile applications, there has been a push to send the most data in the smallest bandwidth (see above, Spectral Efficiency). However, this also corresponds to sending the most data using the smallest amount of *power* in the system. With mobile applications like cell phones, power efficiency is just as important an issue as spectral efficiency, so the selection of protocol is essential to good system performance.

5.1 Transmitter

The transmitter in a digital communications system will no-doubt contain some digital components, but most of its design considerations are strictly analog. Its purpose is to convert a digital signal to a form that can be transmitted over the desired transmission medium, and to do so without adding noise and distortion. A typical transmitter

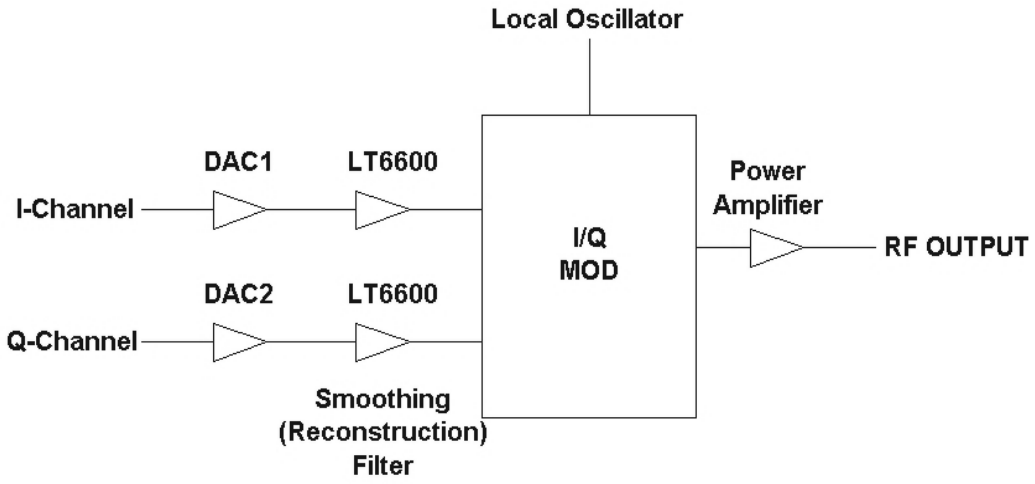

Figure 5-1: Simplified Communications Transmitter. RF Output goes to a transmission channel.

block diagram is shown in Figure 5-1. The system shown in Figure 5-1 contains an I/Q Modulator[2], which is used in many types of communications protocols. The data coming out of the digital-to-analog converter (DAC) will be digitized and coded versions of the data that needs to be transmitted, e.g. a voice signal. On each of the channels, the signal is then low-pass filtered and passed to the modulator. The modulator mixes the signals with a local oscillator at the RF frequency, and the resulting signal is amplified and fed to the transmission channel. The power amplifier exists to boost the signal power and increase the range of the signal.

The power level of the I/Q modulator without an amplifier will be sufficient for the analysis in this thesis, and so the power amplifier will be left out of the communications system. However, in implementations where the signal needs to propagate significant distances (as in cell phones), power amplifiers become useful to improve the signal range and the SNR of the received signal.

5.2 Receiver

A digital communications receiver is shown in Figure 5-2. The RF input is demod-

[2]I/Q Modulation is explained in Section 5.5

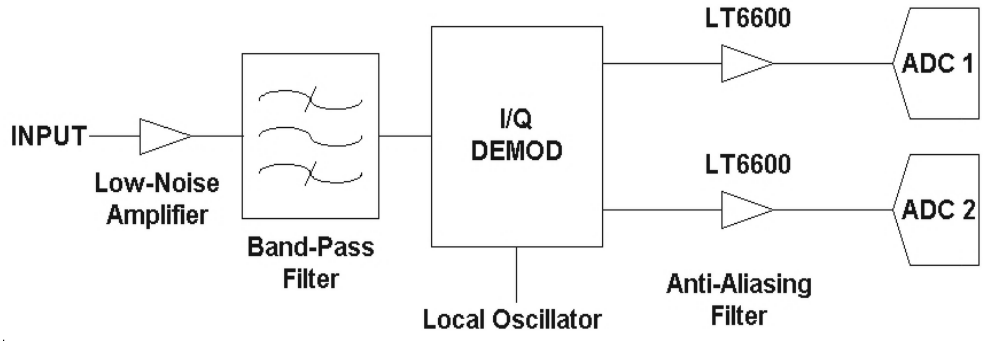

Figure 5-2: Simplified Communications Receiver. RF Input comes from a transmission channel.

ulated and filtered, then digitized by two analog-to-digital converters (ADC). The low-noise amplifier and RF band-pass filter are typical components used to boost the level of a low-noise RF signal before demodulation. The transmitted binary data sequence can then be interpreted and used in the digital domain.

Since the power level of the received signal will be sufficient to demodulate, and the RF noise will be well-controlled, the low-noise amplifier and band-pass filter will be left out of the communications system in this thesis.

5.3 Frequency Domain Analysis of Filtering

For sake of simplicity, the examples shown in this section will involve a simple square wave, or binary data, coming from the output of a DAC. From Fourier theory, the magnitude of the frequency spectrum of a simple square wave looks like a sinc function, or $\frac{\sin(x)}{x}$. The nulls of the sinc function fall at multiples of the DAC clock frequency, which in this case is 5 MHz[3]. A pseudo-random binary sequence (PRBS) is just a random digital binary signal, and has the spectrum shown in Figure 5-3. A long PRBS will contain all of the possible binary sequences and transitions, so that the performance of a system is evident under all data conditions. However, a PRBS can also be seen as a square wave with varying phase, so the spectrum shown in Figure 5-3 is the same as for a square wave at the same frequency. The output spectrum

[3]The use of a 5 MHz DAC clock frequency is arbitrary at this point, and will be explained in Chapter 6.

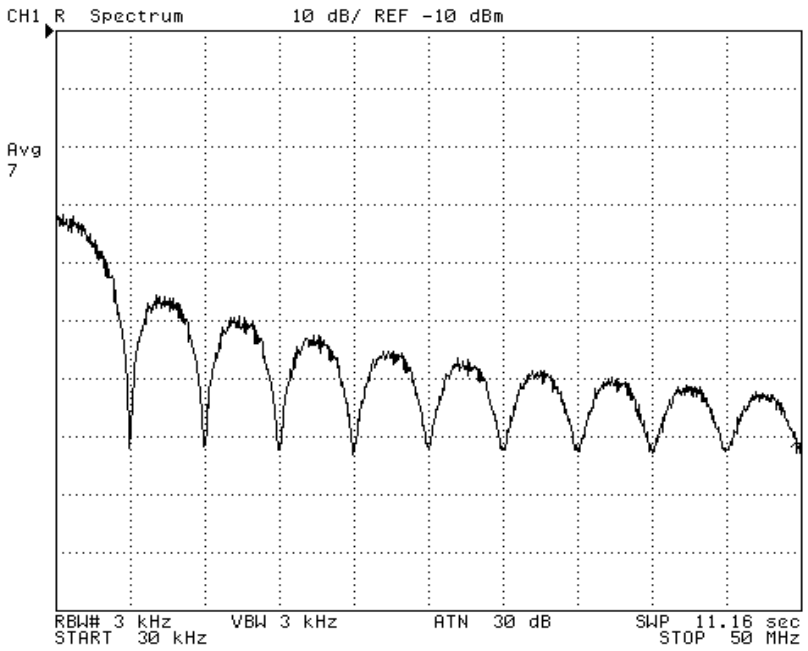

Figure 5-3: Frequency Spectrum of a Pseudo-Random Binary Sequence. Horizontal divisions are 5 MHz, vertical divisions are 10 dB.

of the DAC (a PRBS) represents the magnitude of a sinc function in frequency. True to a sinc function, the magnitude of the side lobes will drop off as frequency increases. However, it is clear from the figure that a binary sequence with sharp transition edges will have infinite frequency content, which can't be tolerated in a congested communications channel. Ideally, the same information must be transmitted in a much smaller bandwidth, with very little signal energy outside of that bandwidth. That is where the low-pass filter in Figure 5-1 comes in: the function of the filter is to attenuate any and all signals at frequencies outside the passband of the filter. For example, one channel in the CDMA (Code-Division Multiple Access) communications protocol is 5 MHz wide in the RF spectrum, and 2.5 MHz wide in the baseband. This is because an up-converted baseband signal is symmetrical around the center frequency. Any signal energy outside of that band will corrupt and interfere with other signals in the transmission medium. A perfect 'brick-wall' filter would allow zero energy to pass outside of that 2.5 MHz band. However, filters are not perfect, and some small attenuated signal will pass through. A filter is judged by how much it attenuates

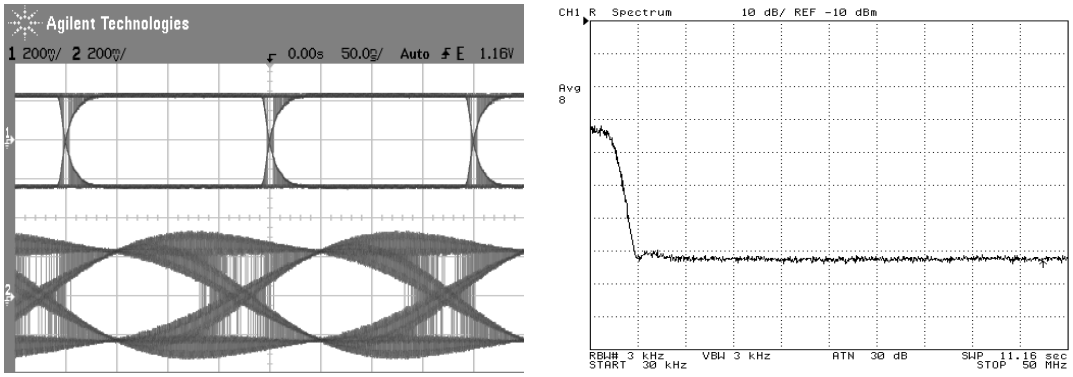

(a) (b)

Figure 5-4: Effect of low-pass filtering the binary signal. Shown in 5-4(a) are the original binary signal (top) and the filtered binary signal (bottom). Shown in 5-4(b) is the frequency spectrum of the filtered signal.

signals in the stopband, how sharp the transition is from passband to stopband, and how well the desired signal passes through the filter undistorted.

In the time domain, the binary signal output of the DAC will clearly not look the same after much of the signal energy is filtered. The more high-frequency content is chopped away, the more the square wave looks like a sine wave. Figure 5-4 shows the binary signal's eye diagram[4] before and after being filtered by the LT6600-2.5, which is made for one CDMA channel. In the figure, the effect of low-pass filtering is to close the digital eye, and therefore slightly reduce the likelihood of the original data being reconstructed at the output. However, this filtering is a necessary step for bandlimiting the signal (see 5-4(b)). The challenge for designers is to bandlimit the signal enough for good spectral efficiency while minimizing the negative effects on the data itself.

The I/Q modulation of a filtered baseband signal ideally just reproduces the same frequency spectrum as in the baseband, but up at a much higher frequency. The mathematics of modulation require that an up-converted analog signal is symmetric

[4]An eye diagram shows all the possible transitions in a digital signal superimposed on the same graph. As the "eye" closes, the transitions of the digital signal exhibit more timing variation, causing errors in the received signal.

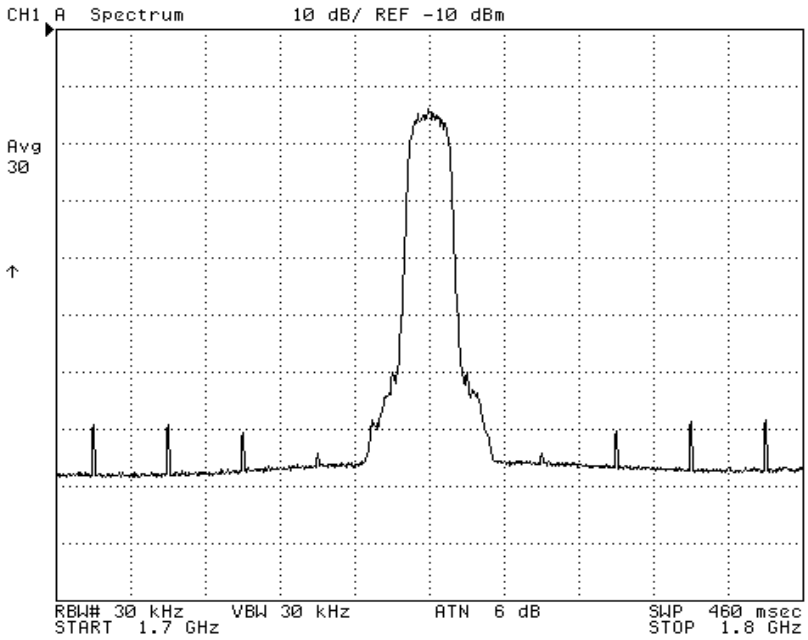

Figure 5-5: Up-Converted Frequency Spectrum of a PRBS. Horizontal divisions are 100 MHz, vertical divisions are 10 dB.

and has double the frequency content of the baseband signal [13]. The up-converted spectrum from the previous example is shown in Figure 5-5. Notice that the LO in this case was set at 1.75 GHz, so the signal energy is centered around that frequency. The asymmetries of the signal content and the harmonic content spikes at higher and lower frequencies are due to non-idealities of the modulator, and can be further attenuated by an RF-frequency bandpass filter.

On the receive side, filtering the baseband signal does the job of anti-aliasing before the ADC. Although the transmitted signal is bandlimited, the transmission medium will probably have all sorts of unwanted signals. In the RF spectrum, there will be microwave ovens, other cell phones, GPS devices, cordless phones, and other items interfering with the signal that was transmitted. When the receiver demodulates an RF input, the signal will appear to no longer be bandlimited. However, since the receiver knows that the useful information is within the first 2.5 MHz of bandwidth (for one CDMA channel), the rest of the information can be attenuated by the filter. Otherwise, aliasing will occur at the analog-to-digital conversion.

Aliasing is a phenomenon that comes from sampling an analog signal. In the

frequency spectrum, it causes high-frequency noise to be folded down into the base-band, where the useful information lies. From there, it is impossible to distinguish that noise from useful signal. In the digital domain, aliasing may cause useful data to become unrecoverable.

5.4 Pulse Shaping

Pulse shaping is a term that refers to the digital filtering of a binary signal before it is converted to analog by a DAC. The Nyquist Criterion[5] for no inter-symbol interference (ISI) [13] states that for a DAC with an update frequency of ω, the highest frequency that can be cleanly reconstructed is $\frac{\omega}{2}$. Therefore, for a single CDMA channel of 2.5 MHz in the baseband, we want the DAC clock to run at 5 MHz. However, referring to Figure 5-3, we see that the shape of the output spectrum for a binary signal is such that the nulls are at 5 MHz intervals, and that there is significant signal content from 2.5 MHz to 5 MHz. In order for the CDMA spectrum to remain within its one-channel limit, that content must be significantly attenuated before the I/Q modulator.

In order to make this filtering job simpler, digital filtering is often employed to help the analog filter with the baseband signal. Since the analog filter's main job is reconstruction of the DAC output, the pulse-shaping (limiting the useful information to a 2.5 MHz bandwidth) should be done mostly in the digital domain. This requires oversampling and Finite-Impulse Response (FIR) filtering. Figure 5-6 shows the conceptual block diagram: first, the data is band-limited in the digital domain, then converted by a DAC, and then finally reconstructed by an analog filter.

In the communications system built for this thesis, the DAC output employed an oversampling rate of 4x, and the FIR filtering was done in MATLAB. Oversampling by 4 means that the DAC clock is actually run at 20 MHz, and each data point lasts for four clock cycles instead of one. At the transitions, the signal is smoothed so that the transition is gradual instead of abrupt. The more gradual a transition is, the less

[5]Harry Nyquist worked for AT&T and Bell Labs. His signal transmission work led to numerous patents and laid the foundation for modern communications systems.

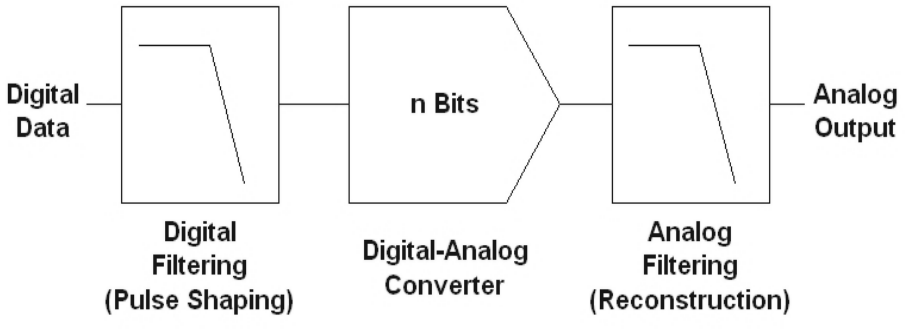

Figure 5-6: Block diagram of filtering steps (first digital, then analog).

high-frequency content it contains.

The FIR filter is a digital filter used to do the smoothing of the data transitions. For a discrete filter to correctly simulate a continuous-time filter, there must be an infinite number of samples of that filter's impulse response with which to filter the digital data. A FIR filter has a finite number of taps (data points), but is no less useful for filtering data. FIR filter design is beyond the scope of this thesis, however, and is discussed in [13] and other texts. The convolution of a FIR filter with a set of digital data is analogous to filtering a continuous-time signal with an analog filter.

Using a continuous-time lowpass filter like the LT6600 with a pulse-shaped digital signal can limit the CDMA output signal to 2.5 MHz, and can provide significant attenuation at frequencies beyond 2.5 MHz in the baseband. This will limit the cross-channel interference and potentially improve the SNR of all the adjacent CDMA channels, since uncorrelated signal energy from an adjacent channel in the frequency spectrum is very similar to random noise. The performance and usefulness of lowpass filters like the LT6600 will be demonstrated in Chapter 6.

5.5 I/Q Modulation

After being low-pass-filtered, the two digital information data streams are fed into an I/Q modulator. The modulator then mixes the two data streams with a local oscillator (LO), which is a sine wave at a RF frequency, adds the two together, and sends the resulting signal to the transmission channel (usually via an antenna and

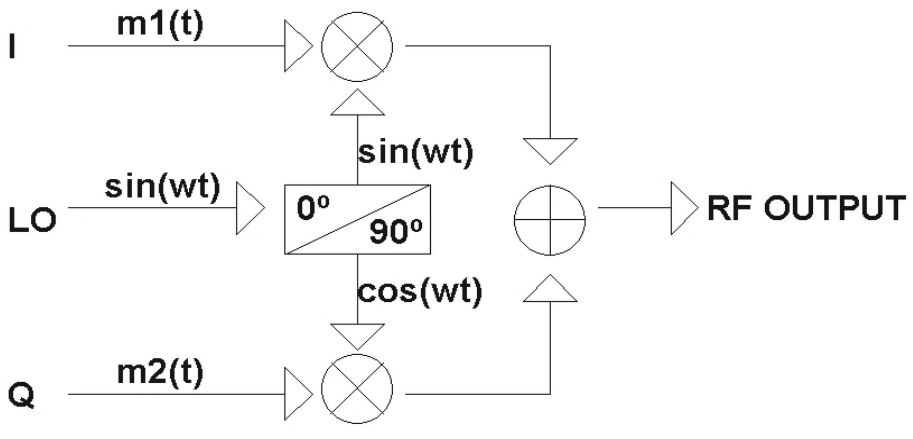

Figure 5-7: Diagram of a basic I/Q modulator.

sometimes a power amplifier). A basic explanation of I/Q modulation is presented here.

I/Q modulation packs more data into a given bandwidth, improving spectral efficiency and data transfer rates. In order to use this type of modulation, we must first ensure that the two independent data streams can be reproduced at the receiver. The basic block diagram of an I/Q modulator are shown in Figure 5-7. The I (in-phase) signal will be referred to as $m_1(t)$ and the Q (quadrature) signal will be referred to as $m_2(t)$. The phase-shifter inside the modulator separates the local oscillator (LO) signal into two signals with the same frequency and different phases, 90 degrees apart. Since sine and cosine are 90 degrees out of phase from each other, we will represent these two signals as $\sin(\omega t)$ and $\cos(\omega t)$. The sine wave LO is called *in-phase* (I), and the cosine LO is called *quadrature* (Q), meaning shifted by one quadrant (i.e. 90 degrees). That is where the term I/Q modulation comes from.

$$RF_{OUT} = m_1(t)\sin(\omega t) + m_2(t)\cos(\omega t) \tag{5.1}$$

An I/Q demodulator does essentially the opposite function of an I/Q modulator: it takes the received RF signal and multiplies it by two quadrature phase-shifted LO signals to reproduce the same original signals. A sample I/Q demodulator is shown in Figure 5-8. The basic insides of a demodulator are very similar to a modulator. The

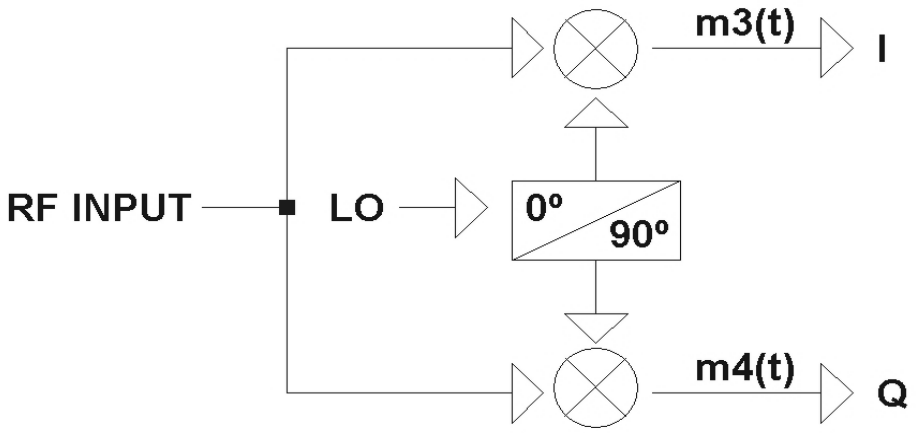

Figure 5-8: Diagram of a basic I/Q demodulator.

demodulator LO should be at the same frequency as the modulator's LO[6], and it will be similarly phase-shifted by 90 degrees for the quadrature channel. For the analysis, a phase term ϕ will be included to represent the difference in phase between the modulator's LO and the demodulator's LO. Let the demodulated I and Q channels be represented as $m_3(t)$ and $m_4(t)$, respectively.

$$\begin{aligned} m_3(t) &= RF_{INPUT} \cdot \sin(\omega t - \phi) && (5.2) \\ &= m_1(t)\sin(\omega t)\sin(\omega t - \phi) + m_2(t)\cos(\omega t)\sin(\omega t - \phi) && (5.3) \end{aligned}$$

The following sine and cosine trigonometric identities allow us to substitute in for the sine and cosine products:

$$\begin{aligned} \sin(\alpha)\cos(\beta) &= \frac{1}{2}\sin(\alpha+\beta) + \frac{1}{2}\sin(\alpha-\beta) && (5.4) \\ \sin(\alpha-\beta) &= \sin(\alpha)\cos(\beta) - \cos(\alpha)\sin(\beta) && (5.5) \\ \cos(\alpha-\beta) &= \cos(\alpha)cos(\beta) + \sin(\alpha)\sin(\beta) && (5.6) \\ \frac{1}{2}\sin(2\alpha) &= 2\sin(\alpha)\cos(\alpha) && (5.7) \\ \sin^2(t) &= \frac{1-\cos(2\,t)}{2} && (5.8) \\ \cos^2(t) &= \frac{1+\cos(2\,t)}{2} && (5.9) \end{aligned}$$

[6]In a real application, there are many ways to encode the local oscillator in a transmit signal so that the receiver can use it. However, these methods are not discussed in this thesis.

Substituting 5.5 and 5.4 into 5.3, we get

$$
\begin{aligned}
m_3(t) &= m_1(t)\sin(\omega t)\sin(\omega t-\phi) + m_2(t)\cos(\omega t)\sin(\omega t-\phi) && (5.10)\\
m_3(t) &= m_1(t)sin^2(\omega t)\cos(\phi) - m_1(t)\sin(\omega t)\cos(\omega t)\cos(\omega t)\sin(\phi) \\
&\quad + m_2(t)\cos(\omega t)\sin(\omega t)\cos(\phi) - m_2(t)\cos^2(\omega t)\sin(\phi) && (5.11)\\
m_3(t) &= m_1\left(\frac{1-\cos(2t)}{2}\right) - \frac{m_1(t)}{2}\sin(2\omega t)\sin(\phi) \\
&\quad + \frac{m_2(t)}{2}\sin(2\omega t)\cos(\phi) - m_2(t)\left(\frac{1+\cos(2t)}{2}\right)\sin(\phi) && (5.12)\\
m_3(t) &= \frac{1}{2}m_1(t)\cos(\phi) - \frac{1}{2}m_2(t)\sin(\phi) + [\cdots]\cos(2\omega t) + [\cdots]\sin(2\omega t) && (5.13)
\end{aligned}
$$

Similarly, it can be shown that

$$
m_4(t) = \frac{1}{2}m_2(t)\cos(\phi) - \frac{1}{2}m_1(t)\sin(\phi) + [\cdots]\cos(2\omega t) + [\cdots]\sin(2\omega t) \qquad (5.14)
$$

The I/Q demodulator creates four terms: two are multiplied by twice the LO frequency, and two are multiplied by a DC term depending on the phase relationship between the modulator and demodulator oscillators. If they are exactly in phase, i.e. $\phi = 0$, then the I and Q channels will be reproduced exactly. If they are not in phase, there will be two effects, visible in Eqs. 5.13 and 5.14—the desired channel will be attenuated by the cosine of the phase, and there will be cross-channel interference from the other channel multiplied by the sine of the phase. Therefore, it is important to keep the phase differential of the local oscillators well-controlled. In a typical digital communications system, there is a Phase-Locked Loop (PLL) in the receiver to detect and track the phase of the modulator's local oscillator.

The two terms that are multiplied by twice the LO frequency will be at very high RF frequencies. Signal energy at those frequencies will be attenuated by the receiver's RF bandpass and anti-alias filters to very low levels, and won't affect the useful signals at the receiver.

Chapter 6

A CDMA Communications System For Filtering Comparisons

This chapter presents the communications system that was built for comparing the LT6600-2.5 with other types of filters. The system was built based on the basic system presented in Figures 5-1 and 5-2. It consists of a DAC, reconstruction filtering, I/Q modulation, I/Q demodulation, and anti-alias filtering. The information is then fed into an ADC, and analyzed in the frequency domain.

The frequency at which the baseband data is modulated for transmission is 1.75GHz, which comes about for two reasons: first, that is very close to the 1.8GHz PCS band. Secondly, the spectrum analyzer used for this research has a limited frequency range of 1.8GHz, and therefore set the upper limit of the frequency range available.

The basic function of the filters in a transmitter system is to limit the amount of signal energy present in the frequency spectrum to a narrow frequency band (for one CDMA channel, the band is 5 MHz wide). This is to prevent interference with other devices trying to communicate in nearby frequency bands. At the receiver, the function of the filters is to limit the amount of high-frequency spurious information seen by the receiver, since the useful information is limited to a narrow frequency band. Spurious information at high frequencies tend to make their way into useful information and reduce its Signal-to-Noise Ratio.

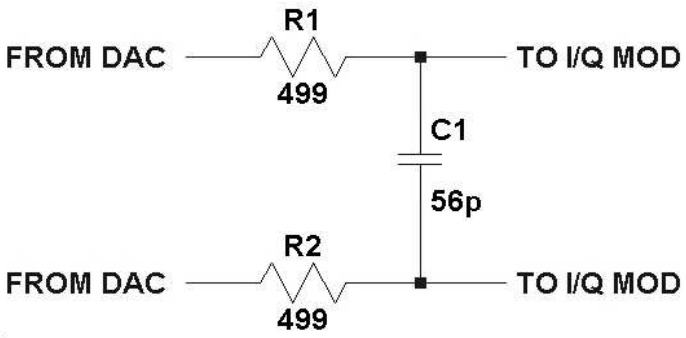

Figure 6-1: Differential RC Lowpass Filter.

6.1 Filter Types Used

Four different filters were evaluated in the communications system, including the LT6600. In order to level the playing field for evaluation, the filters were all fully-differential (both input and output), and all are set up for unity gain (or, in the case of the passive filters, as close to unity gain as possible). The filters used are: a first-order passive RC filter, a fourth-order passive LC filter, a second-order Sallen-Key active filter, and the LT6600 fourth-order integrated filter. The order of the filters are not the same, so attenuation will not be one of the main considerations of the filter comparison. The reason for using different-ordered filters is that in practice all of these filters are used in system designs. The comparisons that will be made will be for the purpose of highlighting the pros and cons of using each filter in the system.

6.1.1 RC Filter

The RC filter is just about the most basic low-pass filter that can be employed in a communications system. Although the rolloff of a first-order RC filter is not very sharp (-20dB/decade gain rolloff), a well-designed electronics board with some digital pulse shaping may not need much analog filtering. Therefore, the differential first-order RC filter shown in Figure 6-1 was chosen for evaluation. The differential nature of the RC filter is beneficial because the designer does not need to worry about the matching of the capacitor for each input—because the capacitor is shared, the matching is automatic. However, the use of two such RC filters means that the matching between

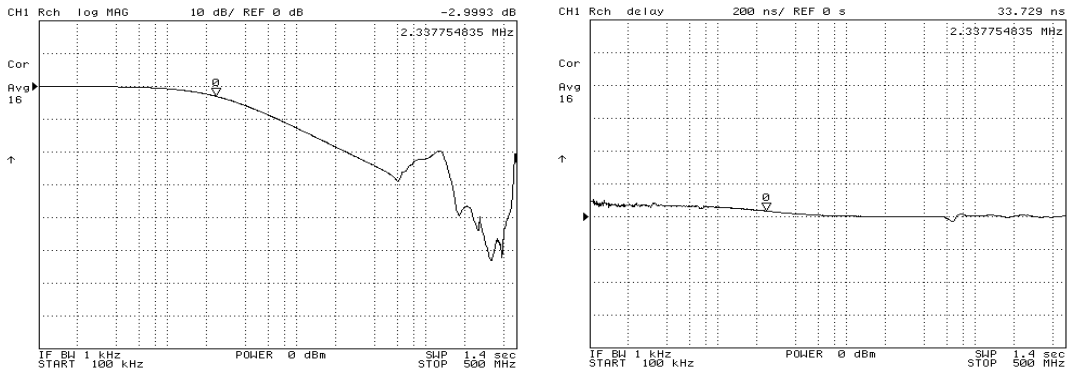

(a) (b)

Figure 6-2: RC differential filter gain (a) and group delay (b). Cutoff frequency $f_{-3dB} \approx 2.33$ MHz.

the I and Q channels will still depend on the tolerances of the capacitors (normally 5% or less).

The gain and delay of the RC filter are shown in Figure 6-2. Note that although the RC filter does not have such a sharp transition from passband to stopband, its group delay is relatively flat. This means that in the passband, the filter will preserve the fidelity of the signal very well, with minimal overshoot and ringing. Additionally, this filter requires no power consumption to operate.

6.1.2 LC Filter

LC filters and their design is a subject of study too advanced for the scope of this thesis; however, the most popular LC filter for use in communications systems seems to be the 4th-order Butterworth filter with a double-terminated resistor network, so that is what has been demonstrated. The reason for the double-terminated resistor ladder with this type of topology is that it decreases the sensisitivity of the filter to the wide tolerances of inductor and capacitor values. The 6dB voltage attenuation that the resistor termination adds is acceptable, given this tremendous benefit. The circuit is shown in Figure 6-3. The differential capacitors are shared between the I and Q channels, as was the case for the RC filter. The inductors must be chosen

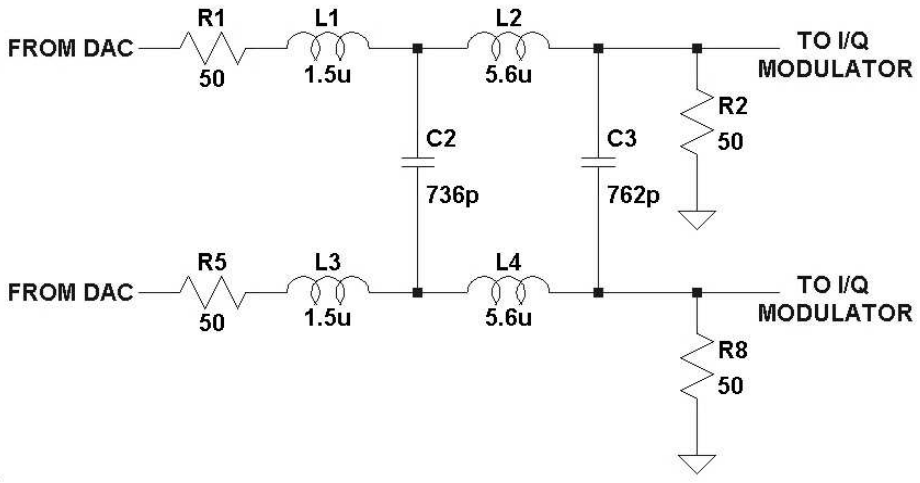

Figure 6-3: Differential 4th-order LC Lowpass Filter.

with consideration of internal resistance and Q value[1]. Since inductors tend to have higher tolerances than resistors (10% or more, compared to 1% or 0.1% for resistors), the inductors will be the primary limiting factors in the repeatability of filter characteristics.

The gain and delay of the LC filter are shown in Figure 6-4. Since the LC filter is 4th-order, the group delay will be significantly higher than for the RC filter. There are methods to smooth the group delay, but at the expense of more components and complexity. The filter presented is the most common LC filter topology.

6.1.3 Sallen-Key Filter

Second-order active filter topologies come in many shapes and sizes. Shown in Figure 6-5 is the popular second-order unity-gain Sallen-Key configuration. The Sallen-Key filter was built with a very-low-noise LT6203 100 MHz op-amp. The filter shown is a unity-gain filter, but different gains are possible with a small modification. The mathematical analysis of the two topologies are presented in Appendices A.2 and A.3. The gain and group delay of the Sallen-Key filter is shown in Figure 6-6. Since the filters used in this system are differential, two identical filters were built and used for

[1]Inductor Q is defined as $\frac{\omega L}{R}$, which is different than the overall filter's Q, and is a measure of an inductor's impedance over frequency.

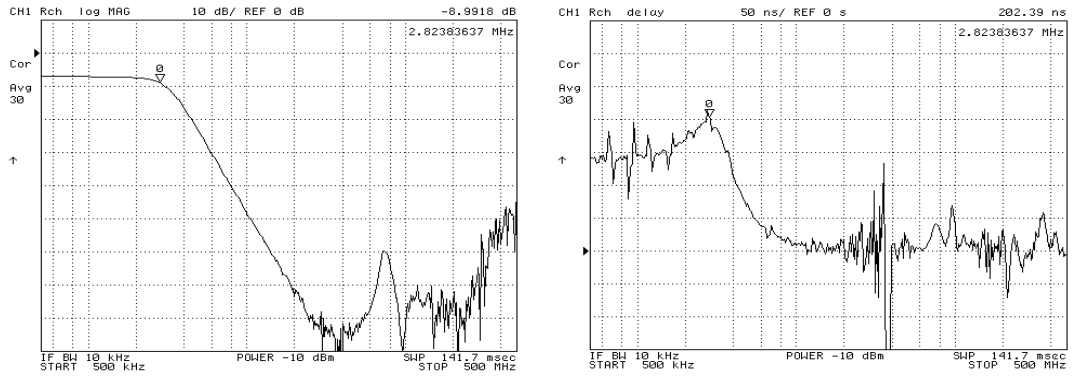

(a) (b)

Figure 6-4: LC differential filter gain (a) and group delay (b). Cutoff frequency $f_{-3dB} \approx 2.8$ MHz, taking into account the low-frequency gain of -6dB.

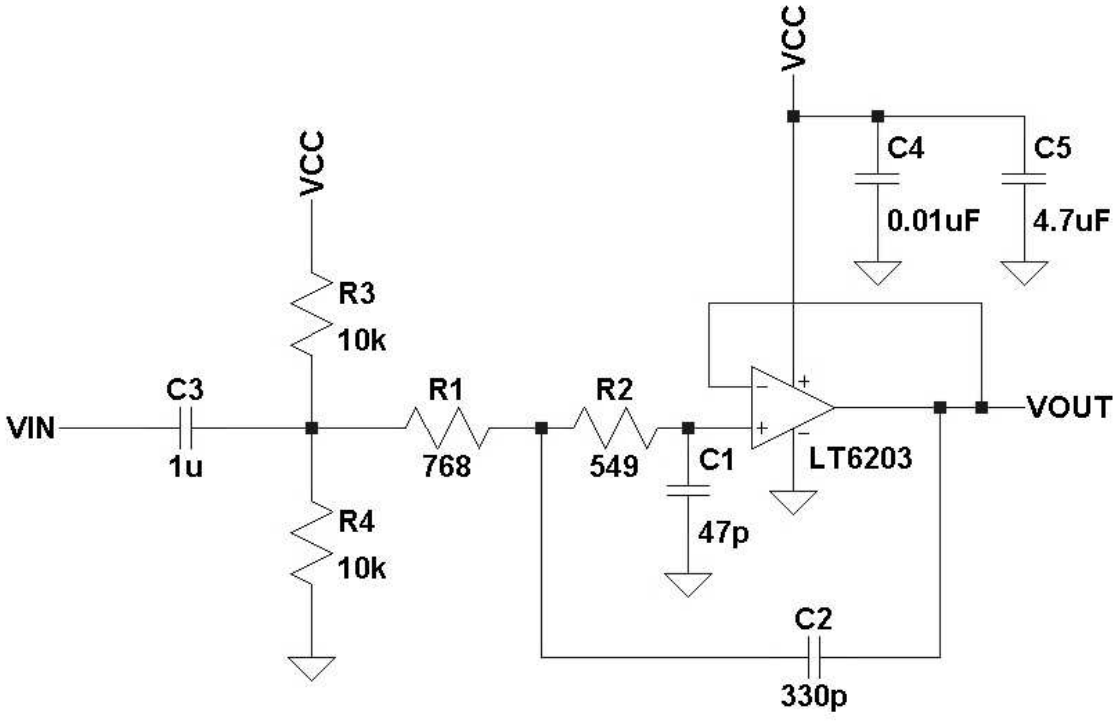

Figure 6-5: Differential Sallen-Key Lowpass Filter.

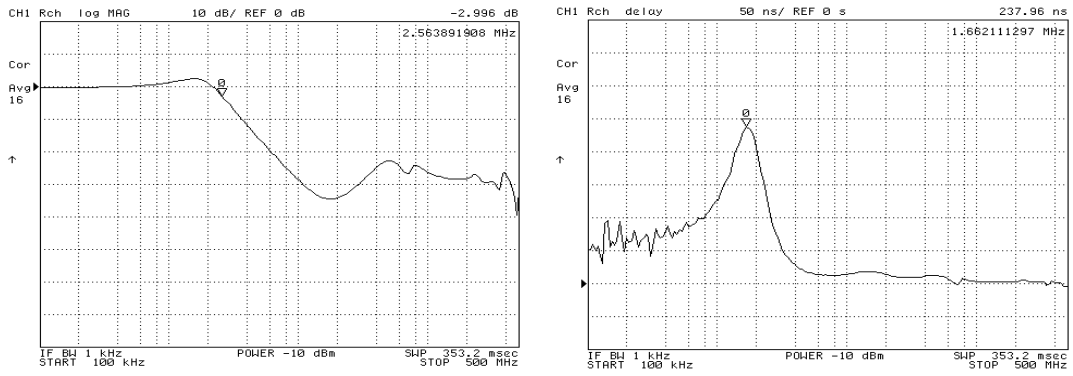

(a) (b)

Figure 6-6: Sallen-Key filter gain (a) and group delay (b). Cutoff frequency $f_{-3dB} \approx$ 2.5 MHz.

the I and Q channels. The Sallen-Key filter has the gain and group delay expected. The filter was designed to have a slight amount of gain peaking, since the transition from passband to stopband would be sharper. The group delay is not very flat, but is somewhat better than in the case of the LC filter.

6.1.4 LT6600-2.5 Integrated Low-Pass Filter

The LT6600-2.5 is an integrated fourth-order low-pass filter employing the Sevastopoulos-LaPorte filter topology. The rolloff of the LT6600-2.5 is a Chebyshev-type rolloff with less than 0.5 dB of passband ripple. The filter and its associated components are shown in Figure 6-7. The LT6600-2.5 has a fourth-order rolloff, meaning the group delay will have a bump near the cutoff frequency. There are techniques to smooth the group delay and make the phase more linear, but the original LT6600-2.5 has the gain and delay shown in Figure 6-8. The -3 dB frequency in Figure 6-8 is shown at 2.7 MHz because a Chebyshev filter's cutoff frequency is defined as the frequency where the passband ripple specification is violated, and in this case it is 2.5 MHz. The group delay looks fairly similar to that of the LC filter, and so the transient responses can be expected to be similar.

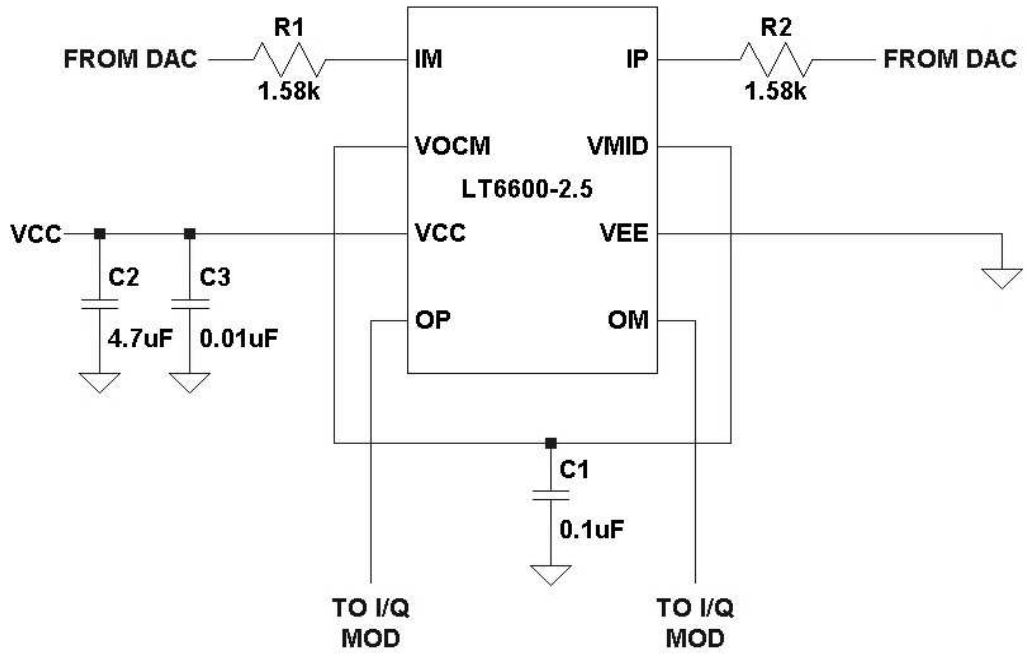

Figure 6-7: LT6600-2.5 Integrated Differential Lowpass Filter.

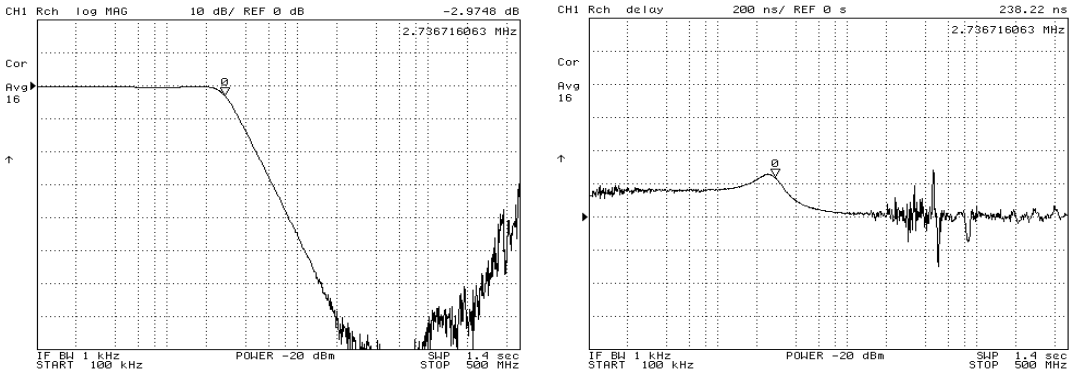

(a) (b)

Figure 6-8: LT6600-2.5 filter gain (a) and group delay (b). Cutoff frequency $f_{-3dB} \approx$ 2.5 MHz.

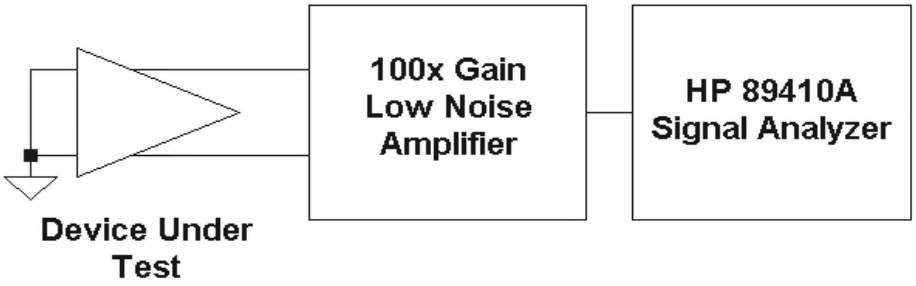

Figure 6-9: Filter Noise Measurement Setup.

6.2 System Noise

One of the most crucial considerations in whether to implement a component in a communications system is noise. A high level of noise in a system directly limits a system's signal-to-noise ratio, and thus increases its bit-error rate. In this section, the absolute noise performance of each filter type will be compared. The setup used to measure noise is shown in Figure 6-9. The low noise amplifier (LNA) shown has a measured gain of 100 over the frequency range of interest (30 kHz to 2.5 MHz), and is used here to bring the noise up to a level much greater than the input noise of the signal analyzer. An HP 89410A signal analyzer was used to measure the power spectral density (PSD) of each noisy output signal and measure the integrated noise.

The results of the noise measurements are presented in Table 6.1, along with the noise performance of all of the other components in the system. The noise of the I/Q modulator and demodulator are taken from the datasheets; everything else is measured using the setup of Figure 6-9. The role of the active buffers is to drive the ADC with the output of the I/Q demodulator, since ADC driving is not a trivial task. The signal analyzer used in these measurements will have some intrinsic noise at its input as well, but the LNA overwhelms that input noise, so that it is irrelevant in these calculations. Since noise adds in a RMS fashion (square-root of the sum of the squares), the LNA noise dominates the noise of the signal analyzer front end.

The noise of the demodulator is somewhat less important than the noise of the transmit-side components, since a noisy channel will easily overwhelm any noise added by the demodulator. The job of the filters at the receive end will then be to prevent

Device	Noise $\left(\frac{nV_{RMS}}{\sqrt{Hz}}\right)$	Noise $\left(\frac{dBm}{Hz}\right)$	Integrated Noise (μV_{RMS})
100x Noise Box	0.7	-170	1.1
LTC1668 DAC	1.1	-166	1.7
RC Filter	0.8	-169	1.3
LC Filter	1.6	-163	26
Sallen-Key Filter	22	-140	35
LT6600-2.5 Filter	25	-139	40
LT5518 Modulator	3.2	-156.8	5
LT5515 Demodulator	3.15	-157	5
Active 1x Buffer	22	-140	35
Active 2x Buffer	28	-138	44

Table 6.1: Output noise performance of each component of the communications system. Integrated noise is measured in a 30kHz to 2.5MHz spectrum.

extra channel noise from being aliased and further interfering with the signal.

The relative noise of each filter shown in Table 6.1 allows the designer to carefully budget the noise of the system. If the active Sallen-Key or LT6600-2.5 are used in the transmit system, the noise of these active filters will likely dominate the noise of the transmit system. If the lowest possible noise configuration is absolutely necessary in a system, then a passive filter may be the best choice.

6.3 Communications Transmitter

The communications transmitter used to evaluate the different filter types is shown in Figure 5-1. It consists of the LTC1668 16-bit differential-output DAC, two low-pass filters, and the LT5518 I/Q Modulator. The circuit for the LT5518 is shown in Figure 6-10. The LT5518's RF output has a 50 ohm impedance, so no impedance-matching network is necessary. Similarly, the LT5518's LO input does not require impedance matching with a 50 ohm source.

6.4 Communications Receiver

The communications receiver used to evaluate the different filter types is shown in Figure 5-2. It consists of the LT1746 14-bit differential ADC, two low-pass filters, and

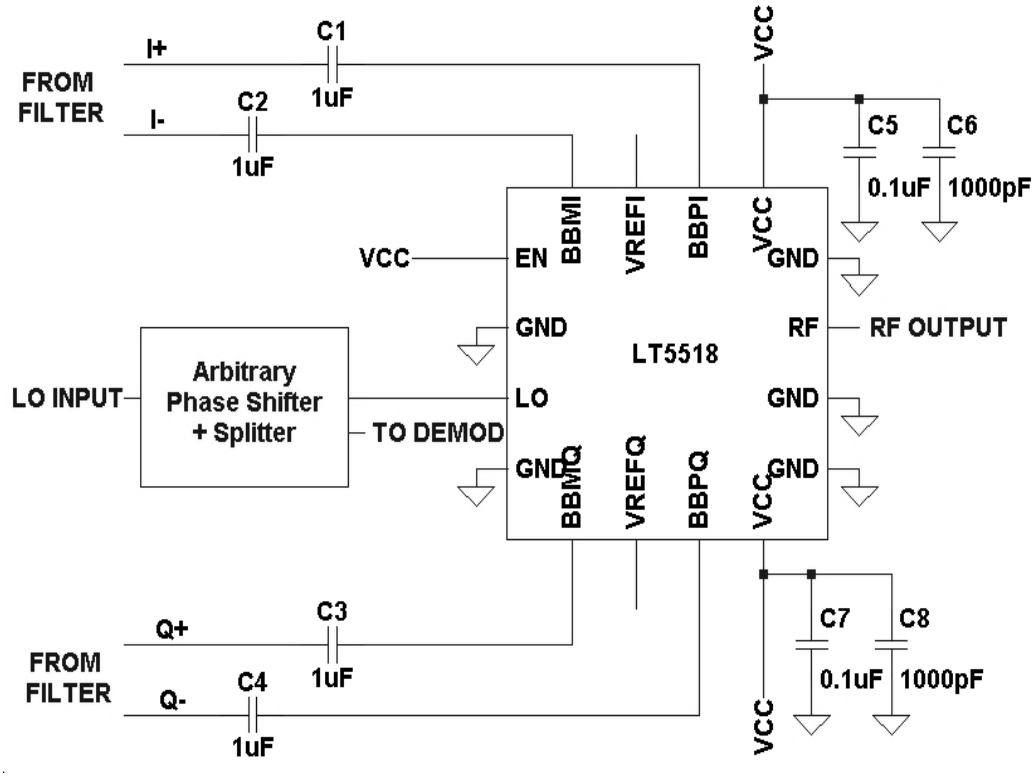

Figure 6-10: LT5518 I/Q Modulator. No impedance-matching network is necessary.

the LT5515 I/Q Demodulator. The circuit for the LT5515, along with impedance-matching networks, is shown in Figure 6-11. The RF and LO inputs to the LT5515 must be converted to differential signals and impedance-matched by the inductors to 50 ohms at 1.75GHz, which is the RF modulation frequency used by the transmission system. After low-pass filtering, the signal is digitized by the ADC. The ADC circuit is shown in Figure 6-12. The true schematic of the LTC1746 converter setup is much more complicated, but the most important portions are shown in the figure. The input network consists of AC-coupling the output of the filters and resistors to set the DC level at the required input common-mode level for the ADC. The low-pass filter network is designed not to filter the input signal, but to help provide the input charge required when the ADC switches its sampling capacitors on and off. Without this network, driving the ADC would require more output drive than most amplifiers could produce.

The difficulty of driving an ADC is the reason for the 1x and 2x active buffers. Al-

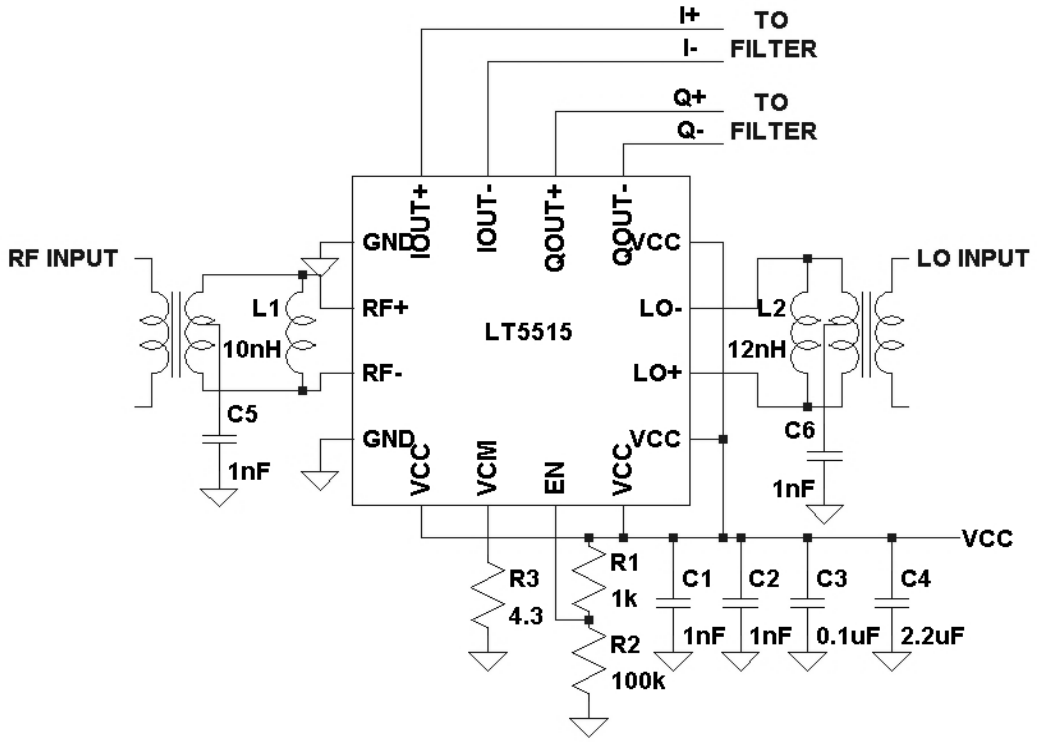

Figure 6-11: LT5515 I/Q Demodulator, shown with balun and matching networks.

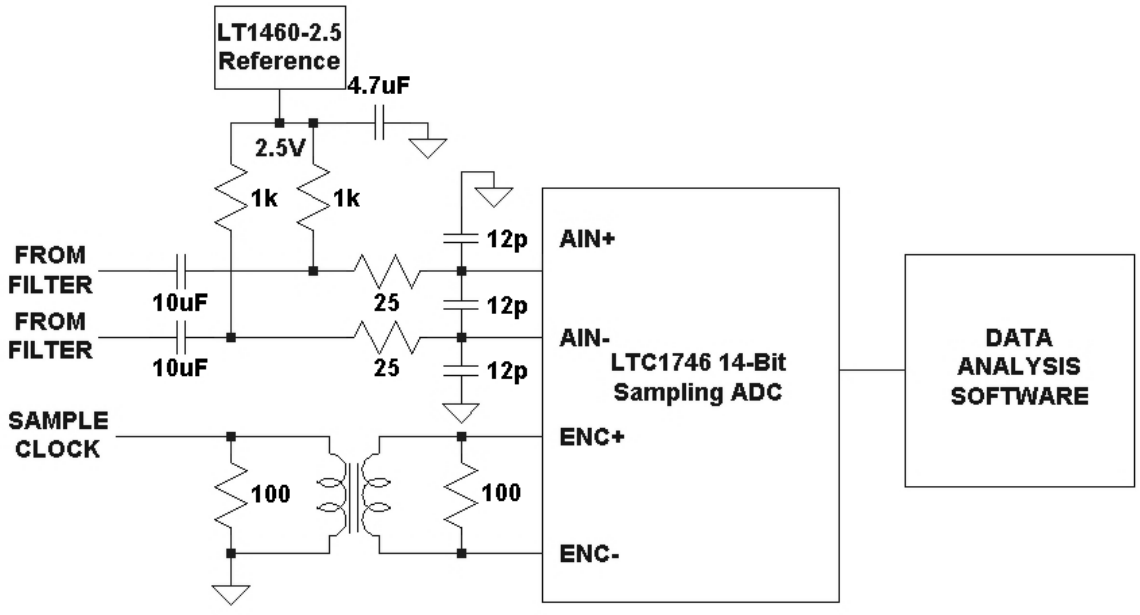

Figure 6-12: LTC1746 Analog-Digital Converter, Simplified Schematic.

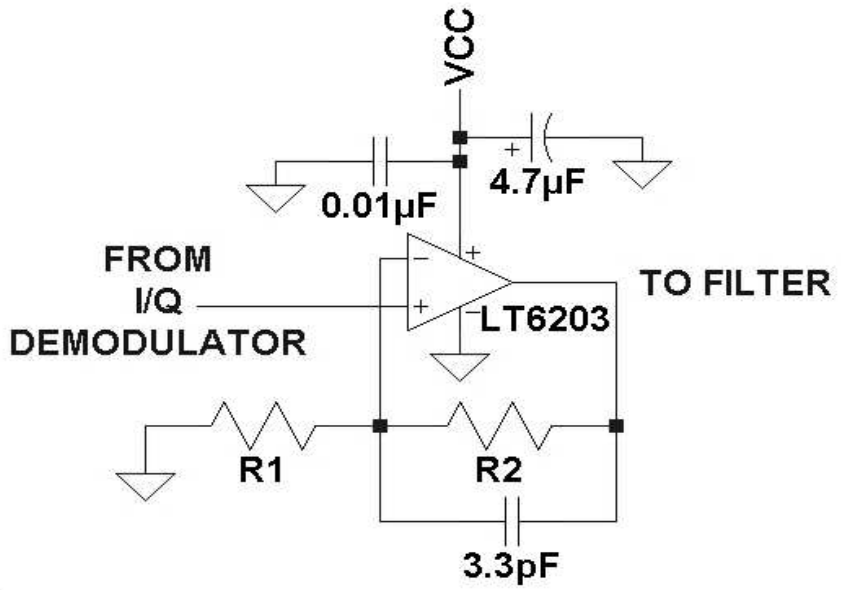

Figure 6-13: I/Q Demodulator Buffer. For Gain of 1, $R_1 = \infty$, $R_2 = 0$ (no need for 3.3pF). For Gain of 2, $R_1 = 1k$, $R_2 = 1k$.

though the active filters (Sallen-Key and LT6600-2.5) don't require additional buffering to drive the ADC, the I/Q demodulator can't drive the ADC by itself. Therefore, in order to use the passive RC and LC filters as anti-alias filters, the output of the demodulator must first be buffered. The buffers are constructed with low-noise LT6203 operational amplifiers, and are shown in Figure 6-13.

The block marked "Data Analysis Software" in Figure 6-12 refers to data processing hardware and software that takes samples of the ADC's digital output and performs FFT analysis, displaying the results on the computer screen. This data will be presented in Section 6.8.

6.5 Transmit Signals

The communications transmission system was built to emulate a CDMA system. The CDMA pulse was a digitally-pulse-shaped pseudo-random binary signal. The pulse-shaping was accomplished using 4x oversampling on the DAC (i.e. the DAC was outputting at 20MHz for a 5MHz digital signal). The entire signal was created and pulse-shaped in MATLAB, and output to the DAC via a PC driven DAC out-

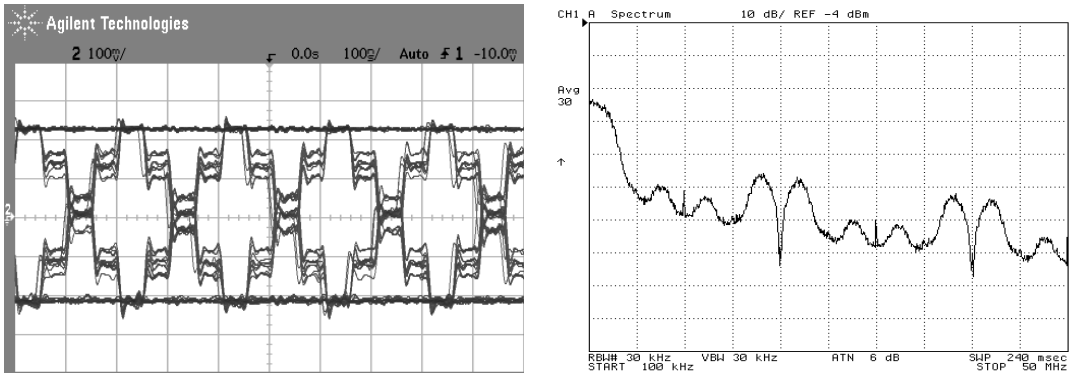

(a) (b)

Figure 6-14: (a) DAC Output Eye Diagram. (b) DAC Output Baseband Spectrum. Horizontal divisions are 5 MHz, and vertical divisions are 10 dB.

put board. Without filtering, the pseudo-random signal is shown in Figure 6-14. As shown, the pulse-shaped CDMA spectrum has frequency content far beyond the 2.5MHz bandwidth that one CDMA channel uses. Analog filtering is necessary. Figure 6-15 shows the effect of the various filters on the CDMA signal, and their resulting frequency spectra.

Eye diagrams can be judged by how vertically open the eye is at its widest point (eye closure), as well as how wide the eye remains. Higher-order filters will tend to inherently cause more horizontal closure of the eye, although horizontal eye closure doesn't affect system performance unless it is severe. Since the ADC will only sample at the eye's most vertically-open point, horizontal closure does not usually translate directly to more bit errors. Therefore, unless the timing jitter of the sampling device is significant (causing it to sample at a point when the eye is not maximally open), which usually is not an issue, the horizontal eye closure is not significant. Therefore, the horizontal eye closure will be ignored, and this analysis will focus on the vertical closure of the eye.

From the eye diagram, the RC filter looks to have pretty good performance. However, a look at the frequency spectrum plot (Figure 6-15(b)) reveals that the attenuation of the RC filter may not be enough to suit the needs of the system. The

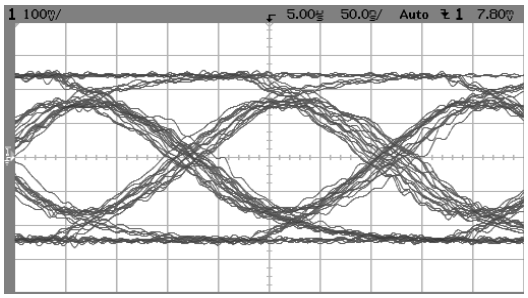

(a) RC Filter

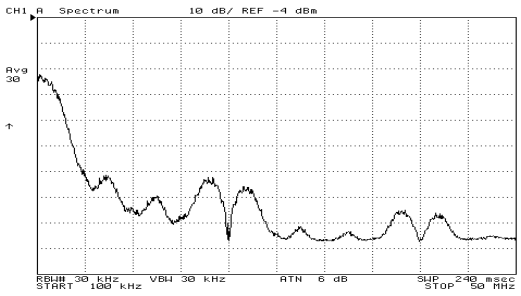

(b) RC Filter Spectrum

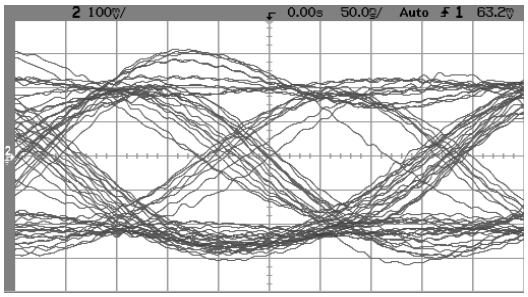

(c) LC Filter

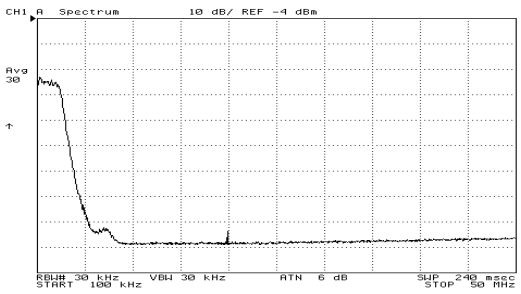

(d) LC Filter Spectrum

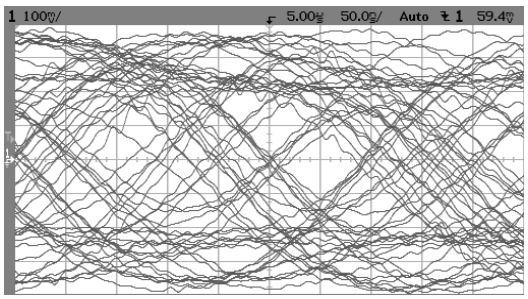

(e) Sallen-Key Filter

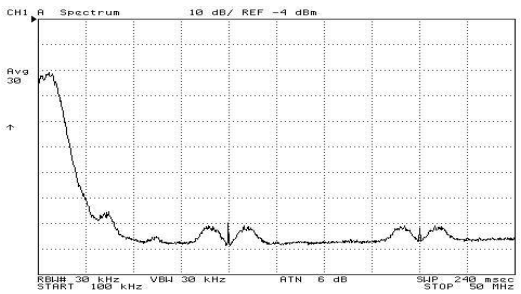

(f) Sallen-Key Filter Spectrum

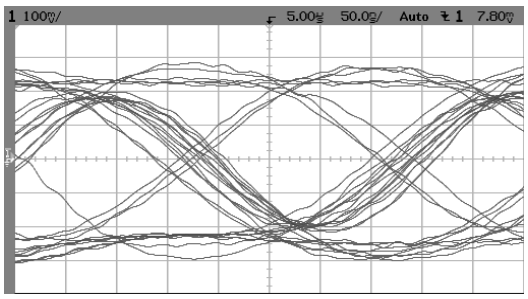

(g) LT6600-2.5 Filter

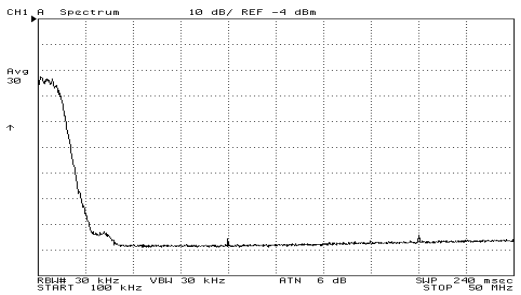

(h) LT6600-2.5 Filter Spectrum

Figure 6-15: Eye diagrams and baseband spectra of filtered CDMA signals.

Filter Type	Eye Closure Vertical	Signal Energy >5 MHz (dB)
RC	40%	38
LC	45%	50
Sallen-Key	75%	47
LT6600-2.5	30%	48

Table 6.2: Comparisons of each filter in terms of eye diagram closure and remaining signal energy above 5 MHz. Eye closure is defined as the vertical closure at the maximally-open point of the eye, as compared with an unfiltered (fully-open) eye.

Sallen-Key filter's transient response[2] significantly closes its eye diagram, but its spectrum looks better than that of the RC filter. The LC and LT6600-2.5 filters do not significantly close the signal eye, and both have excellent stopband attenuation. Table 6.2 compares each filter in terms of eye closure (in percentage) and amount of stopband attenuation.

6.5.1 RF Spectra

The next step in the signal chain, after the baseband filtering, is the I/Q modulator. This step takes the baseband signals and modulates them with a high-frequency oscillator, creating the frequency spectra shown in Figure 6-16. The local oscillator is at 1.75 GHz, so the signal energy will be centered around that frequency. Since the baseband spectrum of one CDMA channel is 2.5 MHz, the same CDMA channel will occupy 5 MHz in the RF spectrum (the signal energy is symmetrical). As mentioned before, one of the main functions of the transmit filter is to attenuate any signal energy outside of this 5 MHz band.

6.6 Noisy Communications Channel

To simulate a noisy communications channel, a wideband RF noise generator was used to add noise to the transmitted RF signal. A sophisticated receiver can correctly interpret digital transmitted signals even if the noise level is extremely high, so -15

[2]Poor transient response is not necessarily a trait of all Sallen-Key filters.

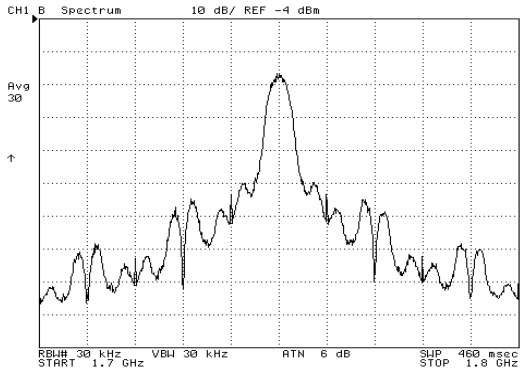

(a) RC Filter

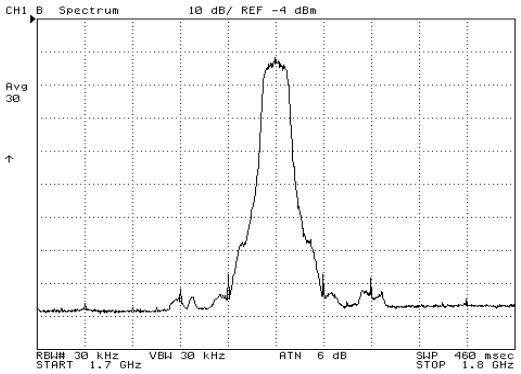

(b) LC Filter

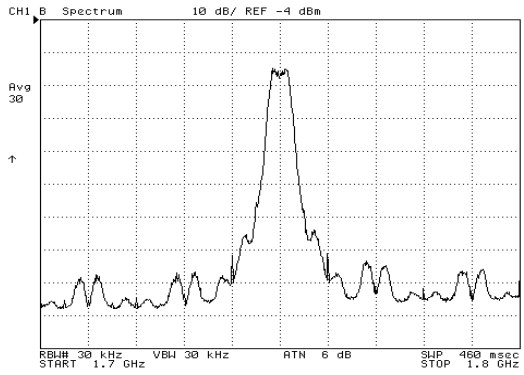

(c) Sallen-Key Filter

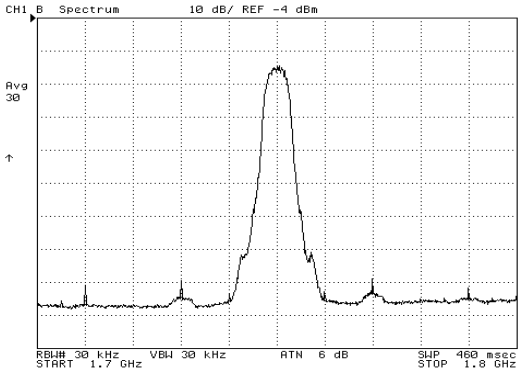

(d) LT6600-2.5 Filter

Figure 6-16: RF spectra of filtered CDMA signals.

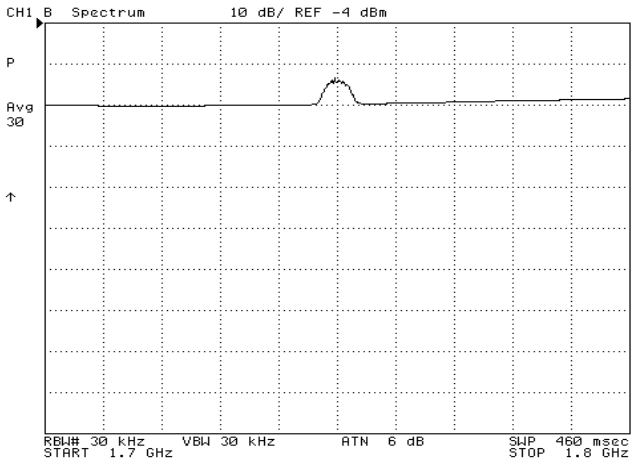

Figure 6-17: Transmitted CDMA Signal With Channel Noise Added.

dBm of noise was added to the signal. This drops the SNR of the signal to around 10dB. The new noisy CDMA spectrum is shown in Figure 6-17.

6.7 Receive Signals

With the channel noise added, the quality of the received signals is degraded. Figure 6-18 shows the impact of the filters on the noisy signals. The 'before' eye diagrams in Figure 6-18 represent the noisy received signal that was filtered by each corresponding filter. That is, the RC transmit filter was matched with the RC receive filter, and so on. Each of the four filters seems to do a decent job filtering out the noisy signals that were picked up in the communications channel. The eye diagrams of the signals will not look as open as they did on the transmit side, because the broadband noise also affects the 5MHz bandwidth of interest, distorting in-band information signals.

The SNR of the transmitted information is further degraded by the fact that the signal loses energy in the modulation and demodulation. Referring to Equations 5.13 and 5.14, there is a 6 dB attenuation of the signal in addition to the loss associated with the ϕ term from the LO phase error.

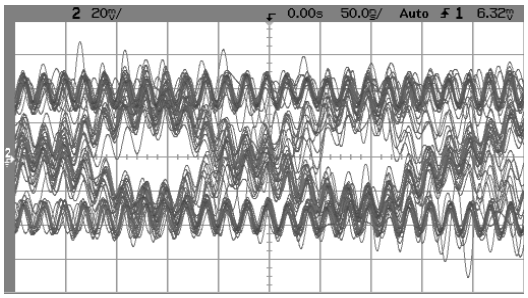

(a) RC Filter (before)

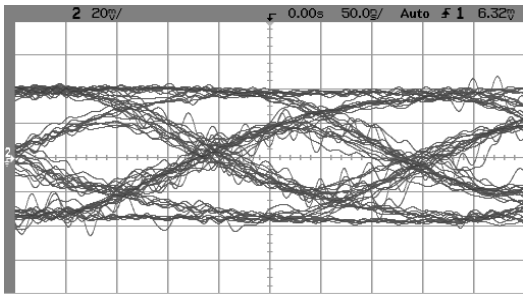

(b) RC Filter (after)

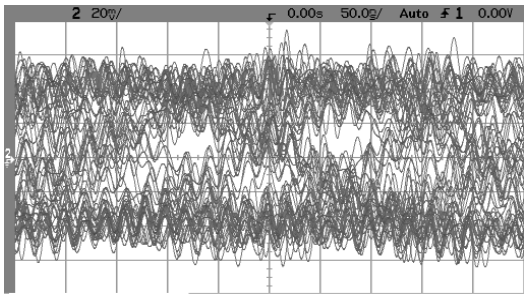

(c) LC Filter (before)

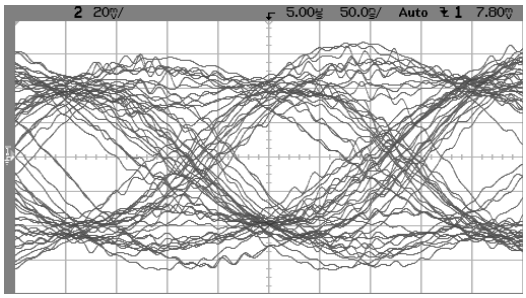

(d) LC Filter (after)

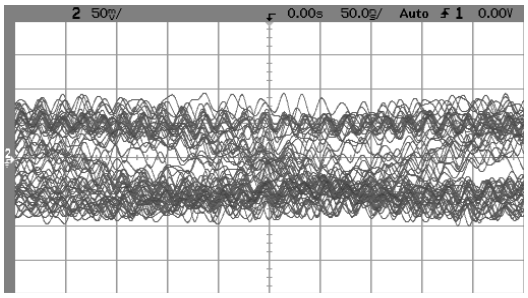

(e) Sallen-Key Filter (before)

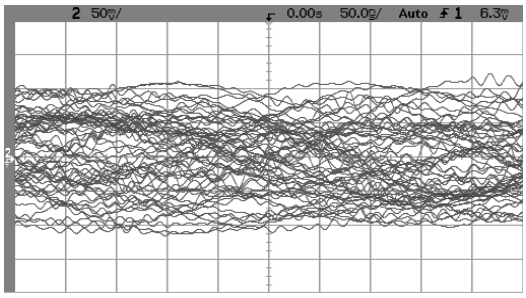

(f) Sallen-Key Filter (after)

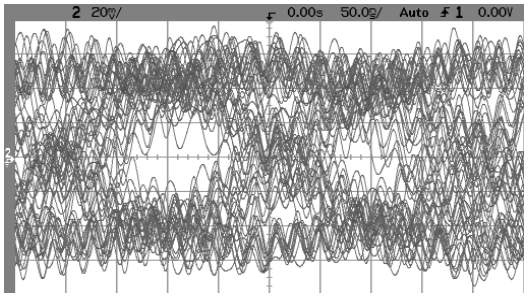

(g) LT6600-2.5 Filter (before)

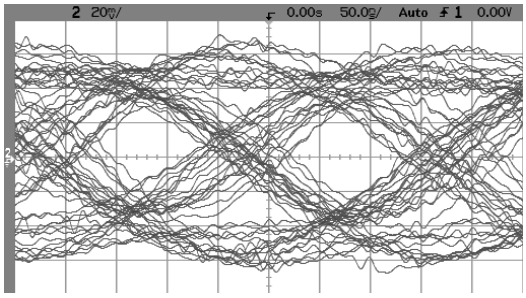

(h) LT6600-2.5 Filter (after)

Figure 6-18: Receiver eye diagrams before filtering (left) and after filtering (right). Like filters were grouped together (e.g. RC filter transmitter was matched with RC filter receiver, etc.).

6.8 Analog to Digital Conversion

The last hardware step in the communications link is the analog-to-digital converter, which digitizes the received signals for further signal processing in the digital domain. For this thesis, FFT analysis was performed on the resulting signals, to see the effect of aliasing when insufficient anti-alias filtering is used. If insufficient filtering is employed in the receiver, any wideband noise above the Nyquist frequency (half of the ADC sampling frequency) will be aliased back into the baseband (for further explanation, see [13]). This will distort the signal, as well as add additional noise.

The FFTs of each filtered signal are shown in Figure 6-19. Although Nyquist's theorem states that a 2.5MHz-bandwidth signal can be sampled at 5MHz, oversampling is beneficial when possible, to reduce the effects of aliasing and to preserve as much of the signal as possible. If a signal is oversampled by 2 (twice the minimum sampling frequency), then the analog filter has more room to filter out potentially-aliased noise, since the Nyquist frequency moves up to twice what it was before. Therefore, the signals were sampled at 12.5MHz (5 times oversampling). Since the FFT is symmetrical, the graphs of Figure 6-19 show only up to the Nyquist frequency, which is 6.25MHz. Therefore, the highest FFT bin (Bin 4096) corresponds to approximately 6.25 MHz.

The only spectrum in which significant aliasing can be seen is the RC filter spectrum. The first-order filter rolloff of the RC filter is not sufficient to prevent aliasing with 5 times oversampling.

It is important to note something that was mentioned before: in order to drive the ADC with the filtered outputs of the RC and LC filters, it was necessary to include a buffer after the I/Q demodulator. Although the buffer does not filter the signal, it does add noise and complexity to the system. The RC filter used a 1x buffer, and the LC filter used a 2x buffer to compensate for the -6dB loss suffered in the filter's resistive divider. The buffer circuits are shown in Section 6.4.

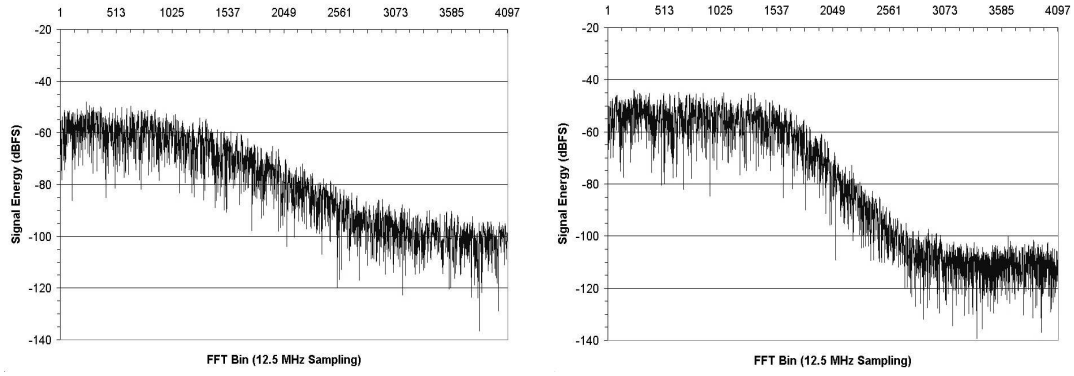

(a) RC Filter

(b) LC Filter

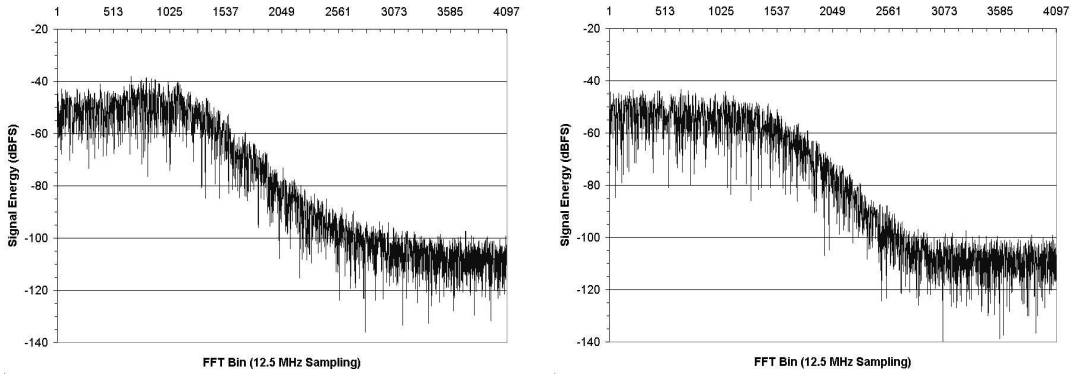

(c) Sallen-Key Filter

(d) LT6600-2.5 Filter

Figure 6-19: FFT spectra of digitized receive signals.

Filter	Order	Noise	Transient Response	Power Consumption	Parts Count	Requires Buffer?
RC	1	very low	acceptable	none	3	yes
LC	4	low	good	none	10	yes
Sallen-Key	2	medium	poor	30 mW	19	no
LT6600-2.5	4	medium	good	175 mW	6	no
1x Gain	N/A	medium	good	30 mW	3	N/A
2x Gain	N/A	medium	good	30 mW	9	N/A

Table 6.3: Comparison of the different filters and their characteristics. Parts count refers to the approximate number of components necessary to implement a fully-differential filter, including recommended power-supply bypassing needs.

6.9 Conclusions

The above experiments have shown and compared the various filters and their design tradeoffs. There are many considerations a designer must consider when designing a filter circuit for communications: noise, parts count, filter order, repeatability (for mass production), and others. Table 6.3 compares the different filters and summarizes the above findings. Although the noise of the RC and LC filters are low, it is important to remember that when used as anti-alias filters, the RC and LC filters require additional buffer stages, which raise their noise level to equal those of the active filters. However, there is no such requirement on the transmit side.

From Table 6.3 and the findings in this chapter, one can conclude that the clear choice of filter to use depends on the application. For mass-production systems, good repeatability of filter characteristics is important. The 10% tolerance of the inductors and 5% tolerance of the capacitors can cause significant variation in filter characteristics, while the integrated LT6600-2.5 is trimmed for repeatable performance. The LT6600-2.5 also lowers the overall parts count of the filter, which decreases the circuit board area that the filter requires.

On the transmit end of a communications system, the RC and LC filters do not require a buffer, so their low-noise characteristics may give them a benefit over the active filters. Additionally, they do not require the additional power that the active filters require, giving them an edge in power efficiency. However, the RC filter may not provide enough attenuation for the application. The LC filter provides more

attenuation, but has a high parts count and may suffer from poor repeatability, due to the high tolerances of the inductors and capacitors. Precision components can be used, but they come at a price premium. On the receive end of a communications system, additional buffering (i.e. increased noise, circuit area, power consumption, and cost) is required to use a passive filter. However, the combined power consumption of the passive filter and buffer is still less than that of the LT6600-2.5.

The only filter that seems inferior to the others, due to its high parts count, and poor transient response, is the Sallen-Key filter. In addition, the Sallen-Key requires many high-precision components to maintain good repeatability of the filter response. A re-design of this filter, requiring more complexity and higher parts count, can yield better transient performance. However, there is no clear advantage to this route over using one of the other filtering approaches.

Chapter 7

Future Work

This section describes research and experiments that were outside of the scope of this thesis, due to time constraints, equipment constraints, or both. Although the author feels that the current thesis achieves its goals, having the time and resources to complete the things listed below would have contributed to a broader and more comprehensive thesis.

7.1 Macromodeling

The macromodel of the LT6600 presented in this thesis uses robust macromodeling techniques, with as many linear SPICE elements as possible. Over the years, SPICE has increased in capabilities, including the ability to handle Analog Behavioral Model (ABM) blocks. The main reason these were not used in the LT6600 macromodel was broad portability between systems–every SPICE simulator handles the same linear elements in similar ways. An interesting topic of research would be to research the portability of ABM models between SPICE systems, and why some are not compatible with ABM elements. A thorough understanding of how to make models work in all systems would allow macromodel designers to potentially model ICs as true black boxes with equations to describe each input's affect on the output (including power supplies, common-mode inputs, et cetera).

7.2 Communications System

Although digital communications contains many different disciplines in one, and there is no way that any thesis on digital communications could give them all due justice, one important aspect that was outside of the reach of this thesis is Bit Error Rate (BER) analysis. From both the lack of equipment and time, measuring the BER of the system with different filtering methods was not possible. For digital communications system designers, however, BER is the bottom line (given the same communications protocol and data transfer rate). Although the noise of a system essentially determines BER, actual measurements would have been helpful in supporting the conclusions drawn in this thesis.

Appendix A

Analysis of the Sevastopoulos-LaPorte (SLP) filter topology

The patented [1] Sevastopoulos-LaPorte filter topology is shown in Figure A-1. For easy reference, the component numbering of the figure matches that of the patent. The SLP topology is very similar to the popular and widely-published Multiple Feedback topology, except for the fact that in the SLP topology, C_3 is connected to nodes E_1 and E_2 instead of E_1 and ground. The topology includes an op amp with DC gain A, assumed ideal, and a buffer with gain K. K is usually a negative number, and the reason will become apparent later.

For the purposes of analyzing the ideal filter characteristics, we will assume that $A \rightarrow \infty$, so that $E_3 \rightarrow 0$. We will begin with the simple Kirchoff's Current Law (KCL) and Kirchoff's Voltage Law (KVL) relationships, and then simplify.

$$\frac{E_1}{R_6} = \frac{-V_{OUT}}{1/sC_4}$$

$$V_{OUT} = -\frac{E_1}{sC_4R_6}$$

$$\frac{E_1 - V_{IN}}{R_4} + \frac{E_1 - V_{OUT}}{R_5} + \frac{E_1}{R_6} + sC_3(E_1 - KV_{OUT}) = 0$$

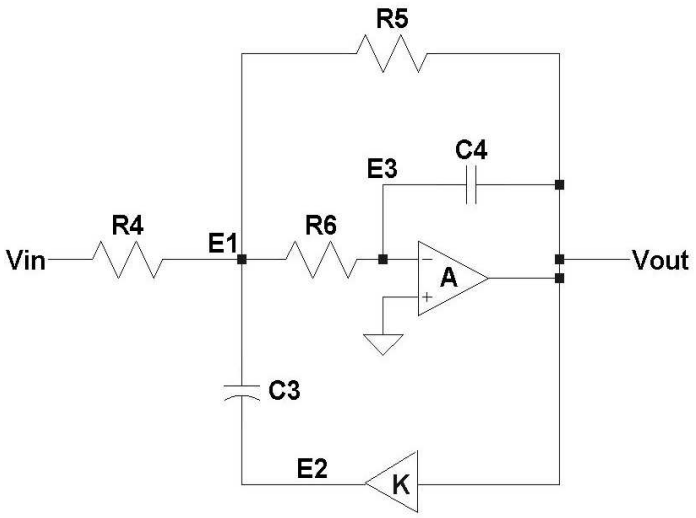

Figure A-1: Patented 4th Order Chebyshev Lowpass Filter Topology.

Substituting in for V_{OUT},

$$E_1\left[\frac{1}{R_4}+\frac{1}{R_5}+\frac{1}{sC_4R_5R_6}+\frac{1}{R_6}+sC_3+\frac{KC_3}{C_4R_6}\right]=\frac{V_{IN}}{R_4}$$

Substituting V_{OUT} back into the formula,

$$-V_{OUT}\left[sC_4R_6+\frac{sC_4R_4R_6}{R_5}+\frac{R_4}{R_5}+sC_4R_4+s^2C_3C_4R_4R_6+sKC_3R_4\right]=V_{IN}$$

$$-\frac{V_{OUT}}{V_{IN}}=\frac{1}{s^2C_3C_4R_4R_6+s\left[C_4R_6+\frac{C_4R_4R_6}{R_5}+C_4R_4+KC_3R_4\right]+\frac{R_4}{R_5}}$$

After some algebra,

$$\frac{V_{OUT}}{V_{IN}}=-\frac{R_5}{R_4}\cdot\frac{\frac{1}{C_3C_4R_5R_6}}{s^2+s\left[\frac{C_4R_5R_6+C_4R_4R_6+C_4R_4R_5+KC_3R_4R_5}{C_3C_4R_4R_5R_6}\right]+\frac{1}{C_3C_4R_5R_6}}$$

This looks very much like the equation of a second-order filter, with the filter characteristics

$$H_o=-\frac{R_5}{R_4} \tag{A.1}$$

$$\omega_o=\frac{1}{\sqrt{C_3C_4R_5R_6}} \tag{A.2}$$

$$Q = \frac{R_4\sqrt{C_3C_4R_5R_6}}{C_4(R_5R_6 + R_4R_6 + R_4R_5) + KC_3R_4R_5} \tag{A.3}$$

With a little bit of algebraic manipulation, the Q expression becomes:

$$Q = \sqrt{\frac{C_3}{C_4}}\frac{R_4\sqrt{R_5R_6}}{R_5R_6 + R_4R_6 + R_4R_5\left(1 + \frac{C_3}{C_4}K\right)} \tag{A.4}$$

The beauty of the SLP topology lies in the above equations: Notice that by making K a negative number, an arbitrarily high Q can be obtained in Equation A.3 without affecting the values of ω_o and H_o. Looking at Equation A.4, with certain values of capacitors C_3 and C_4, the value of Q can be further increased by increasing K (remember that K is negative). Therefore, the capacitor ratio does not need to be quite so large to achieve the same high Q, and the overall capacitor values can decrease[1]. Since capacitors take up massive amounts of area on an IC, this feature allows significantly smaller die sizes, which makes the SLP topology very easy to integrate when compared to other topologies.

The SLP topology, though elegant, is not without drawbacks. As presented in Figure , the SLP requires an additional amplifier for the K gain block. On an IC, this means greater die area and more power consumption, two undesirable traits. The die area saved with smaller capacitors could easily be negated by the second amplifier. However, in the common case where K=–1, the second amplifier will be the negative of the filter output, and the SLP topology gives the designer a free differential output which could be used to drive the input of a differential ADC. This feature may be well worth the additional die area and power consumption required by the additional amplifier. In a differential form, as will be shown in Section A.4, the SLP topology does not require the additional amplifier.

[1]e.g. if the previous capacitor ratio was 1000pF:1pF, the new capacitor ratio may be 100pF:1pF

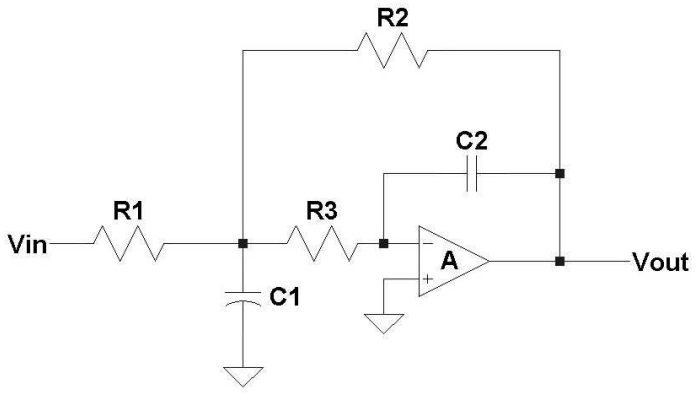

Figure A-2: Multiple Feedback Lowpass Filter Topology.

A.1 Comparison to the Multiple Feedback Topology

The SLP topology offers many benefits over the standard multiple feedback (MF) topology, shown in Figure A-2. Referring to Figure A-1 and Equations A.3 and A.4, it is apparent that the MF topology is simply the SLP topology without the K feedback amplifier (K=0). The characteristics of the multiple-feedback topology are therefore very similar to the SLP topology:

$$H_o = -\frac{R_2}{R_1} \tag{A.5}$$

$$\omega_o = \frac{1}{\sqrt{C_1 C_2 R_2 R_3}} \tag{A.6}$$

$$Q = \frac{R_1\sqrt{R_2 R_3}}{R_1 R_2 + R_1 R_3 + R_2 R_3}\sqrt{\frac{C_1}{C_2}} \tag{A.7}$$

To gain more insight on the effect of removing that K feedback term, we can manipulate Equation A.7 further:

$$\begin{aligned} Q &= \frac{R_1\sqrt{R_2 R_3}}{R_2\left(R_1 + R_3 + \frac{R_1 R_3}{R2}\right)}\sqrt{\frac{C_1}{C_2}} \\ &= \frac{1}{-H_o}\frac{\sqrt{R_2 R_3}}{\left(R_1 + R_3 + \frac{R_3}{-H_o}\right)}\sqrt{\frac{C_1}{C_2}} \end{aligned}$$

As the DC gain H_o increases, $R_3\left(1+\frac{1}{H_o}\right) \approx R_3$:

$$\begin{aligned} Q &\approx \frac{1}{-H_o}\frac{\sqrt{R_2R_3}}{R_1\left(1+\frac{R_3}{R_1}\right)}\sqrt{\frac{C_1}{C_2}} \\ &\approx \frac{1}{-H_o}\sqrt{\frac{R_2}{R_1}}\sqrt{\frac{R_3}{R_1}}\frac{1}{\left(1+\frac{R_3}{R_1}\right)}\sqrt{\frac{C_1}{C_2}} \\ &\approx \sqrt{\frac{1}{-H_o}}\sqrt{\frac{R_3}{R_1}}\frac{1}{\left(1+\frac{R_3}{R_1}\right)}\sqrt{\frac{C_1}{C_2}} \end{aligned} \tag{A.8}$$

The ratio $\frac{R_3}{R_1}$ will not be too large, since R_3 is directly connected to an amplifier input, and therefore directly contributes voltage noise. Looking at Equation A.8, the Q term largely depends on the ratio of capacitors in the topology and the DC gain, H_o. As the gain increases, which may be desirable in a filter application, the ratio of capacitors must also increase the same way to keep Q the same. Since the ratio of R_3 and R_1 should not increase too much due to noise, those terms will not help much.

The problem with this topology is that although the cutoff frequency and DC gain are the same, there is much less control over the quality factor, Q, of the filter once the values of the capacitors have been determined. In order to integrate the multiple feedback filter topology into an IC, the fraction of C_1 and C_2 in Equation A.7 can't be too large—otherwise, too much die space is taken up by the capacitors, and the relative tolerances of the capacitances will not be well-controlled. Therefore, the range of characteristics available is limited—the combined sizes of C_1 and C_2 cannot exceed a certain range if we want the capacitors small enough to fit in an IC. The performance of the multiple feedback filter, therefore, is mostly limited to discrete designs.

A more subtle flaw of the multiple-feedback topology comes when trying to design an actual filter. Due to the limited ranges of Q available for a given DC gain and cutoff frequency (or any other combination of dependent and independent variables), the R and C values in Equations A.5–A.7 do not always converge for a set of desired H_o, ω_o, and Q.

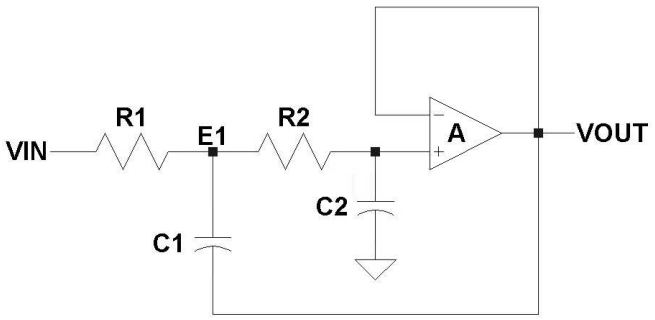

Figure A-3: Sallen-Key Lowpass Filter Topology.

A.2 Comparison to the Sallen-Key Topology

The Sallen-Key topology, another common filter topology, is shown in Figure A-3.

Starting with KCL at node E_1,

$$\frac{V_{IN} - E_1}{R_1} = sC_1(E_1 - V_{OUT}) + \frac{E_1 - V_{OUT}}{R_2}$$

$$\frac{E_1 - V_{OUT}}{R_2} = sC_2V_{OUT}$$

$$E_1 = V_{OUT}(1 + sR_2C_2)$$

Substituting into the first KCL equation,

$$\frac{V_{IN}}{R_1} = E_1\left(\frac{1}{R_1} + \frac{1}{R_2} + sC_1\right) - sC_1V_{OUT} - \frac{V_{OUT}}{R_2}$$

After some algebra, we arrive at the familiar transfer function:

$$\frac{V_{OUT}}{V_{IN}} = \frac{1}{(R_1R_2C_1C_2)s^2 + (R_1C_2 + R_2C_2)s + 1} = \frac{\frac{1}{R_1R_2C_1C_2}}{s^2 + \left(\frac{R_1C_2+R_2C_2}{R_1R_2C_1C_2}\right)s + \frac{1}{R_1R_2C_1C_2}}$$

From here, we can see the characteristics:

$$H_o = 1 \tag{A.9}$$

$$\omega_o = \sqrt{\frac{1}{R_1R_2C_1C_2}} \tag{A.10}$$

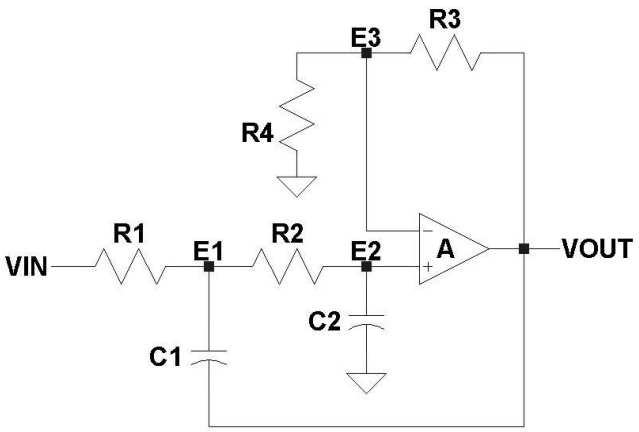

Figure A-4: The non-unity-gain Sallen-Key low-pass filter topology.

$$Q = \frac{\sqrt{R_1 R_2 C_1 C_2}}{R_1 C_2 + R_2 C_2} \tag{A.11}$$

A unique trait of the Sallen-Key topology is that it is non-inverting, whereas the SLP and multiple-feedback topologies are inverting. Notice that the Sallen-Key topology shares many of the flaws of the multiple-feedback topology: once the values of C_1 and C_2 are set, there is very limited independent control over the quality factor and cutoff frequency. To integrate a Sallen-Key filter, the capacitors need to be small, and that limits the range of Q for a given cutoff frequency.

Another disadvantage of the Sallen-Key configuration is the fact that the inputs of the op amp are not at ground (or virtual ground). Since the inputs of the amplifier must have the same voltage swing as the input, the common-mode capabilities of the op amp limit the performance of the Sallen-Key topology. The CMRR and common-mode range come into play: if the CMRR of the op amp is poor, then distortion will occur at the output. Similarly, if the common-mode range is poor, the output voltage will distort and clip if the input signal is too large.

A.3 Sallen-Key Filter with Gain

In most cases, the Sallen-Key filter will be operated in unity-gain, but it is possible to operate this topology with gain, as shown in Figure A-4. Going through the same

math as in the previous section, we arrive at the following transfer function:

$$\frac{V_{OUT}}{V_{IN}} = \frac{G\frac{1}{R_1R_2C_1C_2}}{s^2 + \left[\frac{R_1C_1+R_2C_2+R_1C_2-R_1C_1G}{R_1R_2C_1C_2}\right]s + \frac{1}{R_1R_2C_1C_2}} \tag{A.12}$$

$$G = \frac{R_3 + R_4}{R_4}$$

Note that G is the gain term from the resistors R_3 and R_4, and it appears in the denominator as well as in the numerator. From this, we deduce the main filter characteristics:

$$H_o = G = \frac{R_3 + R_4}{R_4} \tag{A.13}$$

$$\omega_o = \sqrt{\frac{1}{R_1R_2C_1C_2}} \tag{A.14}$$

$$Q = \frac{\sqrt{R_1R_2C_1C_2}}{R_1C_1 + R_1C_2 + R_2C_2 - R_1C_1G} \tag{A.15}$$

From a first look at the filter topology, it might appear that the DC gain G is completely independent of all the other characteristics of the filter. However, Equation A.15 shows that the gain comes in as a reduction term in the denominator of Q. Comparing this to Equation A.3, we see a similar effect: Q now has another degree of variation in comparison to H_o and ω_o. In essence, this is the non-inverting version of the SLP topology. The applied gain to the Sallen-Key topology removes some of the limitations on setting filter characteristics, and may allow for much smaller capacitors and capacitor ratios than in the unity-gain version. However, there are important distinctions that make this topology inferior to the SLP topology.

The benefit of using a non-inverting topology is the input resistance of the Sallen-Key filter. At DC, input variations see the input impedance of the non-inverting terminal of the amplifier. That is a very high imput impedance compared to the SLP topology, where the feedback reduces the input impedance to simply the input source resistance (in Figure A-1, shown as R_4). However, this comes at the cost of increased common-mode distortion in the amplifier. The negative feedback of the SLP topology limits the voltage swing at its input terminals to a fraction of the voltage swing at the

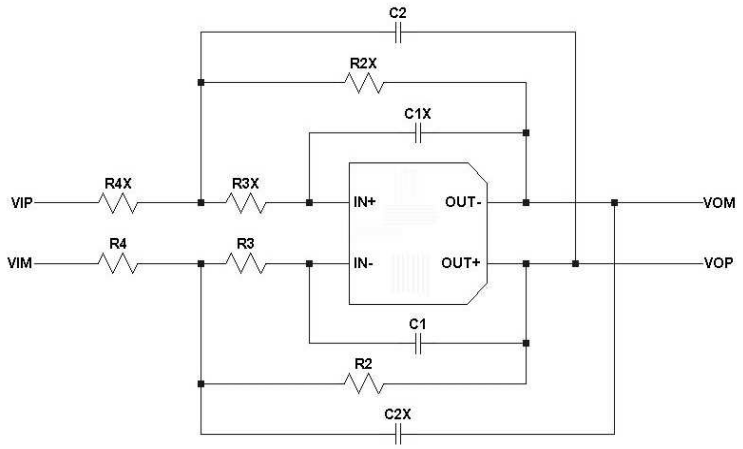

Figure A-5: Differential version of the SLP topology.

input and output of the filter. Therefore, the non-linearities of the amplifier and its common-mode rejection characteristics do not contribute as much to distortion of the output signal. Referring to Figure A-4, we see that at low frequencies, almost all of the voltage swing at V_{IN} appears as a common-mode voltage at the input terminals of the amplifier. This will have two effects: first, the common-mode rejection capabilities of the amplifier come into play. The non-linearities of the input stage coupled with other non-idealities in the design of the amplifier will distort the signal at the output. Secondly, the input voltage swing will be limited by the common-mode range of the amplifier. Comparatively, the SLP topology allows rail-to-rail input swing since the common-mode voltage seen by the inputs of the amplifier are a fraction of the voltage applied to V_{IN} (or, the op amp inputs are at virtual ground).

A.4 Differential Filter Topologies

A final benefit of the SLP topology is just how easily and effectively it can be turned into a differential filter topology. Referring to Figure A-1 and Equation A.3, we have noted that the implemented SLP topology often incorporates K values ranging from –0.5 to –1. Here, we will focus on the value of K being –1.

Figure A-5 shows the differential version of the SLP topology [1]. This topology is simply two identical SLP topologies applied to a differential-in-differential-out am-

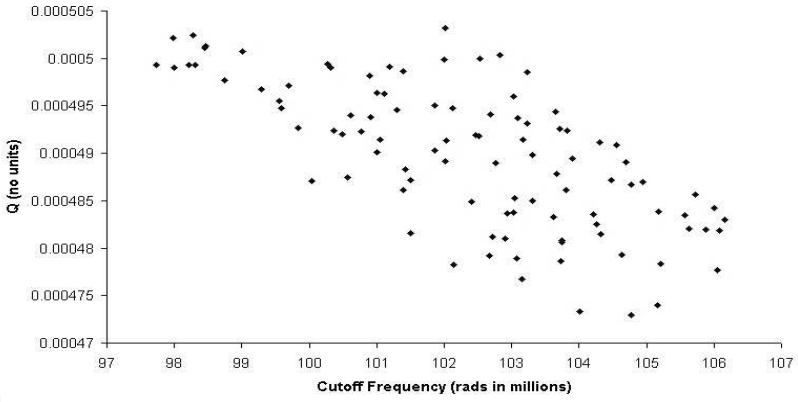

Figure A-6: Variation in ω_o and Q of a discrete multiple-feedback filter.

plifier. Note that the gain block K in Figure A-1 has been instead replaced by a wire tying the feedback capacitor to the opposite amplifier output. In this configuration, the gain block K is built-in to the differential amplifier, since each output is simply the other output inverted (i.e. multiplied by –1). This feature, which is utilized in the LT6600 filter, makes the SLP topology easily integrated in differential form, since no additional components are necessary for creating the positive feedback. However, this simple feedback wire allows the capacitors to be much smaller than in the multiple-feedback topology for the same design constraints.

Referring back to the multiple-feedback topology from above, the differential version will be the same as the differential SLP topology, except without the extra feedback to the capacitor. Does this apply to the Sallen-Key configuration? Looking back at Figures A-3 and A-4, there is no way to implement the Sallen-Key filter in fully differential form.

A.5 Benefits of Integrating Filters

It has already been suggested that an integrated SLP filter design is superior to a discrete topology. In an integrated filter, the designer saves the boards space of all of the individual resistors and capacitors that must go into a discrete design. In addition, there is less need to worry about the tolerances of the components. Figures A-6 and A-7 show the calculated variation in cutoff frequency and Q of a discrete multiple-

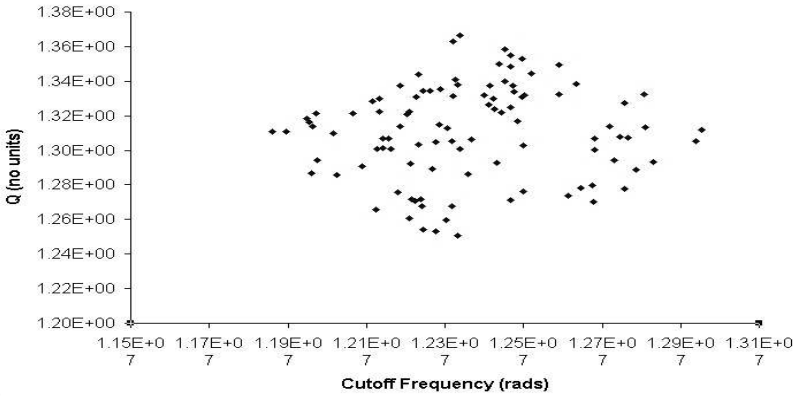

Figure A-7: Variation in ω_o and Q of a discrete Sallen-Key filter.

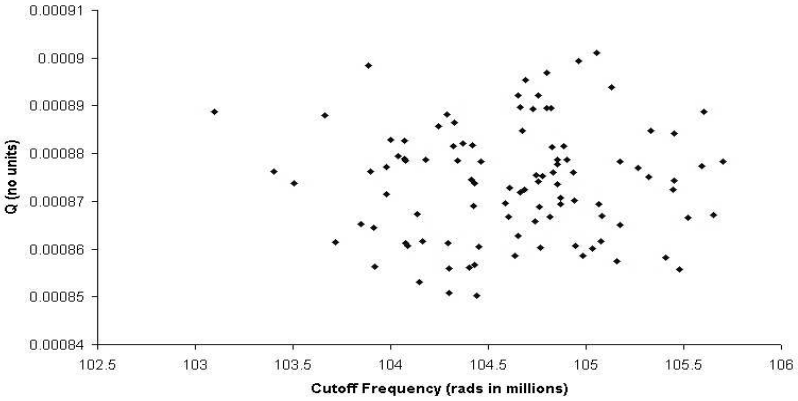

Figure A-8: Variation in ω_o and Q of an integrated SLP filter.

feedback filter and Sallen-Key filter, respectively. The graphs were constructed with a theoretical tolerance of 1% in the resistors, and 5% in the capacitors. These are typical tolerances for off-the-shelf components in mass production. Using these tolerances, Figure A-6 shows that the MF topology exhibits a maximum variation of approximately 4.5% away from the mean for ω_o and 3.4% from the mean for Q, with a standard deviation of around 2%. Figure A-7 shows a maximum variation of 4.5% away from the mean, with a standard deviation of 2% for ω_o and Q. Compare those numbers to Figure A-8 , which shows the same variances for an integrated SLP filter. The integrated filter allows a precise trimming of the resistors and/or capacitors, which allows for tight control of their values. Figure A-8 was created assuming a tolerance of 1% for the resistors, and 1% for the capacitors. These are worst-case values for a well-designed IC. The graph shows a maximum variation from the mean

	R tol.	C tol.	Max ω_o var.	Max Q var.	σ_{ω_o}	σ_Q
MF	1%	5%	4.5%	3.4%	2%	1.5%
Sallen-Key	1%	5%	4.3%	5%	1.8%	2.1%
SLP	1%	1%	1.5%	3%	0.5%	1.35%

Table A.1: Variations in ω_o and Q as a result of component tolerances. σ refers to the standard deviation of ω_o and Q.

of approximately 1.5% and 3% for ω_o and Q, respectively, with a respective standard deviation of 0.5% and 1.35%. The above results are summarized in Table A.5.

There is a more subtle, but very important benefit to integrating filters: Although the SLP topology allows somewhat independent control of Q, the value of Q is still dependent on a ratio of capacitors. For most filters, Q and other key characteristics will depend not only on how close the capacitors are to the ideal values, but also how well-matched they are *to each other*, e.g. Equation A.7. In the case of an integrated filter, since the capacitors are on the same die on the same wafer, their ratio will be well-controlled. That is, if their absolute tolerances are 1%, the tolerance of the *ratio* of two integrated capacitors on the same chip are typically less than 0.5% or even 0.25%. The calculations used in Table A.5 did not take this into account, so on a real IC the statistics could be expected to be even better than what Figure A-8 indicates.

Appendix B

LT6600 Model Netlist

```
* LT6600-10 Macromodel
XA9O N005 N008 OP OM VCC VEE VOCM a9o
XA9I IM IP N001 N002 VCC VEE VMID a9i
D1 IP VCC DESDUP
D2 VEE IP DESDUP
D3 IM VCC DESDUP
D4 VEE IM DESDUP
D5 VMID VCC DESDUP
D6 VEE VMID DESDUP
D7 VOCM VCC DESDUP
D8 VEE VOCM DESDUP
R5XB N001 IM 402
R5B N002 IP 402
C4XB N001 IM 32p
C4B N002 IP 32p
R4X N003 N002 80
R4 N006 N001 80
C3 N003 N006 153p
R1X N004 N003 80
R1 N007 N006 80
R3X N005 N004 40
R3 N008 N007 40
C1X OP N005 109p
C1 OM N008 109p
R2X N004 OP 160
R2 N007 OM 160
C2 OM N004 130.8p
C2X OP N007 130.8p
D9 OP VCC DESDUP
D10 VEE OP DESDUP
D11 OM VCC DESDUP
D12 VEE OM DESDUP

* block symbol definitions
.subckt a9o IN+ IN- OUT- OUT+ VCC VEE VOCM
R3 VA- VCC2 52.4
R4 VA+ VCC2 52.4
R5 N006 N005 1.03
R6 N006 N007 1.03
VOS N015 VIM 89.53
C1 VA+ VA- 1p
ICC N006 VEE2 0.988mA
D1+ VB+ N002 DLIM
D2+ N001 VB+ DLIM
V1+ VCCSIM N002 0.739
V2+ N001 VEESIM 0.739
G1+ VCC2 VB+ VA+ VA- 19.1m
G2+ VEE2 VB+ VA+ VA- 19.1m
R7+ VCC2 VB+ 73.9k
R8+ VB+ VEE2 73.9k
D1- VB- N004 DLIM
D2- N003 VB- DLIM
V1- VCCSIM N004 0.739
V2- N003 VEESIM 0.739
G1- VCC2 VB- VA- VA+ 19.1m
G2- VEE2 VB- VA- VA+ 19.1m
R7- VCC2 VB- 73.9k
R8- VB- VEE2 73.9k
GOSIT N006 VEE2 VA+ VA- 1.0m
D5+ VCC2 N008 DLIM
```

```
D6+ VCC2 N009 DLIM
D7+ VEE2 N008 DZNR
D8+ VEE2 N009 DZNR
G13+ N009 VEE2 VB+ VO- 1m
G14+ N008 VEE2 VO- VB+ 1m
G12+ 0 VO- VB+ VEE2 16m
G11+ VO- 0 VCC2 VB+ 16m
R23+ VCC2 VO- 188
R24+ VO- VEE2 188
D5- VCC2 N010 DLIM
D6- VCC2 N011 DLIM
D7- VEE2 N010 DZNR
D8- VEE2 N011 DZNR
G13- N011 VEE2 VB- VO+ 1m
G14- N010 VEE2 VO+ VB- 1m
G12- 0 VO+ VB- VEE2 16m
G11- VO+ 0 VCC2 VB- 16m
R23- VCC2 VO+ 188
R24- VO+ VEE2 188
GNOISE+ 0 VIP INOI+ 0 1
GNOISE- 0 VIM INOI- 0 1
RN+ 0 N012 0.3
RN- 0 N013 0.3
I2 INOI+ 0 0
I3 INOI- 0 0
R7 OUTCM OUT+ 10k
R8 OUT- OUTCM 10k
GOCM1 0 VB+ VOMID OUTCM 2
GOCM2 0 VB- VOMID OUTCM 2
LOUT- VO- OUT- 1n
LOUT+ VO+ OUT+ 1n
COUT OUT+ N014 3.5n
ROUT N014 OUT- 360
Q1 VA+ VIP N007 0 NPN1
Q2 VA- N015 N005 0 NPN2
VEE2 VEE VEE2 0
VCC2 VCC VCC2 0
ICMBIAS VOCM VEE2 3
C3 VO+ 0 3p
C4 VO- 0 5p
E2 VIM IN- VNOI2 0 1
R11 VNOI2 0 8k
I4 VNOI2 0 0
L1 VNOI2 0 20
R12 PS+ VCC2 15
G3 0 OUT+ PS+ 0 0.01
R13 PS- VEE2 15
G1 0 OUT- PS- 0 0.01
L4 N012 0 1n
L5 N013 0 1n
C7 INOI+ N012 1n
C8 INOI- N013 1n
V1 VOMID N016 12m
RMID VOMID 0 10MEG
I5 PS- 0 0
I6 PS+ 0 0
L6 INOI+ 0 1E20
L7 INOI- 0 1E20
C9 PS+ 0 10p
C10 PS- 0 10p
E3 N016 0 VOCM 0 1
VBUF VIP IN+ 0
DOLIM+ OUT+ N020 DLIM
DOLIM- OUT- N019 DLIM
VOLIM+ N018 OUT- 1.7
VOLIM- N017 OUT+ 1.7
R1 N019 N017 5
R2 N018 N020 5
C2+ VCC2 VB+ 12p
C3+ VB+ VEE2 12p
C2- VCC2 VB- 12p
C3- VB- VEE2 12p
E1 VCCSIM 0 VCC2 0 1
E4 VEESIM 0 VEE2 0 1
GPD1 VCC2 VEE2 VEE2 VCC2 0.0056
IPD VCC2 VEE2 28mA
.ends a9o

.subckt a9i IN+ IN- OUT- OUT+ VCC VEE MID
R3 VA+ VEE1 229
R4 VA- VEE1 229
R5 N008 N007 178
R6 N008 N009 178
VOS N001 N002 109V
C1 VA- VA+ 1p
ICC VCC1 N008 1.088mA
RREF1 VCC1 VH 1k
RREF2 VH VEE1 1k
D1+ OUT- N004 DLIM
D2+ N003 OUT- DLIM
```

```
V1+ VCCSIM N004 0.739
V2+ N003 VEESIM 0.739
G1+ VCC1 OUT- VA+ VA- 10
G2+ VEE1 OUT- VA+ VA- 10
R7+ VCC1 OUT- 188
R8+ OUT- VEE1 188
D1- OUT+ N006 DLIM
D2- N005 OUT+ DLIM
V1- VCCSIM N006 0.739
V2- N005 VEESIM 0.739
G1- VCC1 OUT+ VA- VA+ 10
G2- VEE1 OUT+ VA- VA+ 10
R7- VCC1 OUT+ 188
R8- OUT+ VEE1 188
Q1 VA+ VIP N007 0 PNP1
Q2 VA- N001 N009 0 PNP2
GOSIT VCC1 N008 VA- VA+ 1.5m
E1 VIP IN+ VNOI1 0 1
RVN 0 VNOI1 90k
V1 VIM IN- 0
I1 VNOI1 0 0
R7 OUTCM OUT+ 10k
R8 OUT- OUTCM 10k
GOCM1 0 OUT+ MID OUTCM 8.367
GOCM2 0 OUT- MID OUTCM 8.367
R9 VCC1 VM 11k
R10 VM VEE1 11k
L1 VNOI1 0 0.3m
VSUP+ VCC VCC1 0
VSUP- VEE VEE1 0
E2 N010 0 VM 0 1
R11 N010 0 5.5k
R1 IN+ VICM 100k
R2 VICM IN- 100k
G7 VCC1 VE VICM VH 0.794
G8 VEE1 VE VICM VH 0.794
R19 N011 VE 1000
R20 VE N012 1000
L4 N012 VEE1 159
L3 VCC1 N011 159
ECM N002 VIM VE VH 1
C2 VE 0 200p
R12 MID N010 0.01
G1 VCC1 VEE1 VEE1 VCC1 0.005
E3 VCCSIM 0 VCC1 0 1
E4 VEESIM 0 VEE1 0 1
.ends a9i

* Library File for LT6600 Macromodel

.MODEL DLIM D (IS=1E-12 BV=100 RS=0.1 XTI=1
+ CJO=0 TT=0)
.MODEL DOUT D (IS=1E-12 BV=100 RS=0.1 XTI=1
+ CJO=5p TT=1e-9)
.MODEL DZNR D (IS=0.6E-6 BV=50 RS=1 XTI=1
+ CJO=0 TT=0)
.MODEL PNP1 PNP (IS=9.8047E-16 BF=22.7 RB=0)
.MODEL PNP2 PNP (IS=9.8047E-16 BF=22.7 RB=0)
.MODEL NPN1 NPN (IS=9.8047E-16 BF=55.6 RB=0)
.MODEL NPN2 NPN (IS=9.8047E-16 BF=55.6 RB=0)
.MODEL NPNLIM NPN (IS=1E-12 BF=1000 BR=1000 RB=0)
.MODEL PNPLIM PNP (IS=1E-12 BF=1000 BR=1000 RB=0)
.MODEL NMOSLIM NMOS (VTO=0.5)
.MODEL PMOSLIM PMOS (VTO=-0.5)
.model DESDUP D (IS=1E-12 RS=0.001 CJO=1p VJ=0.3
+ TT=1e-9)

.end
```

Bibliography

[1] N. G. Sevastopoulos and D. A. LaPorte, "Flexible Monolithic Continuous-Time Analog Low-Pass Filter with Minimal Circuitry," U.S. Patent 6,344,773 B1, February 5, 2002.

[2] LT6600 Datasheet, Linear Technology Corporation, Milpitas, California, 2002.

[3] R. Schaumann and M. E. Van Valkenburg, *Design of Analog Filters*, Oxford University Press, New York, 2001.

[4] G. R. Boyle, B. M. Cohn, D. O. Pederson, and J. E. Solomon, "Macromodeling of Integrated Circuit Operational Amplifiers," *IEEE Journal of Solid State Circuits*, Vol. SC-9, No. 6, December, 1974.

[5] M. Alexander and D. F. Bowers, "SPICE-Compatible Op Amp Macro-Models," Analog Devices Application Note AN-138, Norwood, Massachusetts, 1990.

[6] K. H. Lundberg, *Feedback Control Systems for Analog Circuit Design*, Unpublished, 2003.

[7] P. W. Tuinenga, *SPICE: A Guide to Circuit Simulation and Analysis Using PSPICE*, Prentice Hall, New Jersey, 1995, pp. 81-88.

[8] R. D. Middlebrook, "Measurement of Loop Gain in Feedback Systems," International Journal of Electronics, vol. 38, no. 4, 1975, pp. 485-512.

[9] T. M. Frederiksen, *Intuitive Operational Amplifiers: From Basics to Useful Applications*, Revised Edition, McGraw-Hill Inc., New York, 1988, pp. 116-145.

[10] P. R. Gray, P. J. Hurst, S. H. Lewis, and R. G. Meyer, *Analysis and Design of Analog Integrated Circuits*, Fourth Edition, John Wiley and Sons, Inc., New York, 2001, pp.748-803.

[11] W. Jung, *LT1056 Improved JFET Op Amp Macromodel Slews Asymmetrically*, Design Note 43, Linear Technology Corporation, Milpitas, California, 1991.

[12] C. E. Shannon, "A mathematical theory of communication," Bell System Technical Journal, vol. 27, July and October, 1948, pp. 379-423 and 623-656.

[13] A. V. Oppenheim, R. W. Schafer, and J. R. Buck, *Discrete-Time Signal Processing*, Second Edition, Prentice Hall, New Jersey, 1999, Chapter 4.